PHASE I ENGINEERING REPORT

STUDY OF A FLUIDIC ATTITUDE CONTROL SYSTEM FOR A SOLAR PROBE SPACECRAFT

ER 14436

November 1966

Prepared by J. L. Hinson

Approved by P. A. Freeman

Martin-Baltimore
Baltimore, Maryland

TABLE OF CONTENTS

		Page
	Foreword	v
I.	Summary	1
II.	Introduction	2
III.	System Approach	4
	A. Mission Description	5
	B. Vehicle Description	7
	C. Vehicle Control System Requirements	9
	D. Control System Environment	12
	E. Control System Configuration	16
	F. Controls Reliability Requirement	24
IV.	Control System Implementation	27
	A. Sensors	27
	B. Fluidic Power Systems	40
	C. Electric-to-Fluid Conversion	55
	D. Momentum Exchange Actuation	62
	E. Fluid Logic Devices	68
V.	Fluidic Performance Trends Under Solar Environment	73
	A. Introduction	73
	B. Temperature Testing Installation	74
	C. Test Results	75
	D. Summary	80
VI.	Materials Considerations	81
	A. Materials of Construction for Fluidic Control System Components	81
	B. Materials for Special Components	82
	C. Working Media (Fluids)	83
	D. Materials Choice Summary	84
VII.	Reliability Prediction	86
VIII.	Conclusions	91
IX.	References	93

LIST OF TABLES

Table		Page
I	Weight Summary	8
II	Accuracy	11
III	Performance Specification	22
IV	Cumulative Reliability of Attitude Control System	26
V	Solar Probe Attitude Control System Power Requirements	42
VI	General Fluid Amplifier Types	71

LIST OF FIGURES

Figure		Page
1	Solar Probe Experiment Phenomena	96
2	Solar Probe Trajectory Versus Booster Capability . .	97
3	Communication Limits Versus Perihelion	98
4	Solar Probe Vehicle Configuration	99
5	Spacecraft Thermal Profile	100
6	Solar Probe Pitch Control System	101
7	Solar Probe Roll Control System	102
8	Preliminary Logic Diagram Attitude Control and Stabilization--Flywheel Control	103
9	Experimental Fluidic Bolometer	104
10	Pure Fluid Sun Sensor	105
11	Sun Sensor	106
12	Vortex Rate Sensor	107
13	Experimental Fluid Rate Sensor	108
14	Fluidic Element Power Computation	109
15	Brayton Cycle Fluidic Power System	110
16	Reciprocating, Recirculating Power Supply	111
17	Schematic of Adsorption Power Supply	112
18	Concept for Fluidic Momentum Wheel	113
19	Fluidic Element Characteristics	114
20	Temperature Test Set-up	115
21	Experimental Results - Corning Element #190738 . . .	116

LIST OF FIGURES (cont'd)

Figure		Page
22	Pressure-Flow Characteristics - Corning Element #190738	117
23	Experimental Results - Corning Element #190738	118
24	Pressure-Flow Characteristics, Martin Element FLE-101	119
25	Pressure-Flow Characteristics, Martin Element FLE-101	120
26	Experimental Results, Martin Element FLE-101 . .	121
27	Temperature Test of Martin Momentum Exchange Bi-stable Element	122
28	Temperature Test of Martin Momentum Exchange Bi-stable Element	123
29	Control Pressure - Load Characteristics Martin Momentum Exchange Element	124
30	Control-Output Pressure - Temperature Characteristics - Martin Momentum Exchange Element	125
31	Experimental Results - Martin	126

FOREWORD

This document represents the Phase I technical report of a 3-phase study and investigation of a Fluidic Solar Probe Space Vehicle Attitude Control System, performed by the Martin Company, Baltimore, Maryland, for the National Aeronautical and Space Agency, Electronics Research Center, Cambridge, Massachusetts, in response to Item C-2, Page 5, of Contract NAS 12-127.

I. SUMMARY

The Phase I activity of the subject program has consisted of a system requirement study for a fluidic Solar Probe Spacecraft Attitude Control System, and a comprehensive analysis and evaluation of all available fluidic elements, sensors, components, etc., that might be used to implement this attitude control system. The evaluation of fluidic devices has been implemented through a comprehensive industrial and literature survey, and a number of visits to government facilities.

This effort has shown that a fluidic approach for a spacecraft attitude control system is both feasible and promising in terms of eventual reliability and operational lifetime, but that the state of development of certain system components, notably closed-cycle fluidic power supplies, and some sensors, is lagging badly; and that much additional work needs to be done in establishing fluidic device performance at elevated ambient temperatures, and establishing criteria for reliability predictions of fluidic system performance.

II. INTRODUCTION

Fluidic/Flueric technology has recently emerged from the research laboratories as a very promising approach to satisfy a wide variety of control, logic and computational requirements, without special protection, under environments that are currently well beyond the capability of present day conventional electronics. These environments include:

a) Ambient temperature ranges from cryogenic to incondescent;

b) Hard nuclear radiation.

In addition, the minimum of moving parts promises high ultimate reliability of such systems.

In view of these capabilities, the National Aeronautics and Space Agency, Electronics Research Center at Cambridge, Massachusetts, has undertaken to explore the use of fluidics/fluerics for a spacecraft control system, whose mission will generate a wide temperature range, high radiation environment. Such a spacecraft is the unmanned Solar Probe. The Martin Company, at Baltimore, is assisting NASA-ERC in this exploration under the subject contract.

Program

The subject program is being conducted in three phases:

Phase I will include an investigation of available fluidic/flueric devices for general applicability to the subject spacecraft mission, including the materials for constructing the various system elements. System elements to be considered include:

Sensors (Radiation and Inertial)
Power Supplies
Electric/Fluidic Signal Conversion
Momentum Exchange and Actuation Devices
Logic and Circuit Elements

Phase II will consist of the analytical verification synthesis of a suitable control system based on the selection of system elements from Phase I. Performance and energy requirements for the various system elements will be generated as part of this phase.

Phase III will consist of the modification of the current Martin "SOFACS" breadboard fluidic attitude control system to simulate the selected system configuration from Phase II, and the demonstration of its performance on the Martin air-bearing motion simulator.

Report Coverage

This report will cover the results obtained from Phase I of the subject study. Included will be:

a) A description of the Solar Probe Mission and Vehicle (based on a recent study by the Martin Company for NASA's Ames Research Center (see Ref. 1);

b) The vehicle attitude control system evolved during this study;

c) A suggested fluidic/flueric implementation of this control system;

d) A discussion of expected fluidic/flueric elements and materials performance trends under the mission environment, together with a reliability prediction;

e) Conclusions and references.

III. SYSTEM APPROACH

The broad objective of the Solar Probe Mission is to obtain detailed information on fields, particles, radiations, and other solar phenomena in interplanetary space. The present level of knowledge of the sun and its atmosphere is based on the traditional combination of theory and experiment. However, experimental investigations have been limited by the difficulty of simulating the sun and its atmosphere in the laboratory and by the presence of the earth's atmosphere and magnetosphere. In the last decade, studies have been made in experimental investigation by use of rockets, earth-orbiting satellites (e.g., OSO) and the first interplanetary probes (Mariner II and Mariner C). Even with the large accumulation of experimental data since 1950, there is no certainty as to which, if any, of the many concepts of dynamic corona is correct (Ref. 2). To help answer this and other questions, measurements of: the properties of the "solar wind" and magnetic fields, the density and distribution of energetic charged particles of solar and galactic origin, and the concentration and energies of dust and micrometeorites in the interplanetary medium (both in and out of the plane of the ecliptic) would be obtained by use of a Solar Probe Vehicle.

This section of the report discusses the mission characteristics, a description of the vehicle which has been proposed to carry out the scientific objectives of this program, and the attitude control system requirements resulting from the scientific objectives, mission characteristics and anticipated environment.

A. MISSION DESCRIPTION

Consideration of data available on the sun and its atmosphere and the disagreement of basic concepts of the dynamic corona point out the need for additional experimental data. Experiments which will resolve the important unknowns in the structure of the Sun's magnetic field and the mechanisms of the dynamic corona are considered to be of primary importance for the Solar Probe mission. Figure 1 summarizes the phenomena which is of interest, the advantage of using perihelion distances to investigate these phenomena, and the type instruments which would be required.

Figure 1 indicates that the spacecraft must approach as close as 0.4 AU to the Sun for the scientific objectives of a solar probe to be reasonably satisfied. A closer approach is, of course, desirable. It is also desirable to orient the trajectory out of the plane of the ecliptic to broaden the scope of measurements to be made with the scientific payload.

Some of the limitations in trajectory are shown in Fig. 2, which shows perihelion radius for typical spacecraft weights and several possible booster combinations, each with the same solid rocket injection stage. These data, from Ref. 3, indicate that, for flights restricted to the plane of the ecliptic and a perihelion radius of 0.32, payload weights of 250 lb (using Atlas/Agena) or 900 lb (using Titan III-C) can be accommodated. Our studies have shown that the payload capability of these boosters decreases rapidly for out-of-the-ecliptic flights, and with a practical maximum inclination of approximately 25°.

Other considerations important to selection of the exact trajectory to be used for the solar probe mission are the test requirements of the payload experiments, as well as system tradeoffs in the communication and data handling, thermal control, onboard power, and attitude control systems. Typical trajectories, showing the path of the spacecraft relative to a rotating Earth-Sun line, for several perihelion missions, are presented in Fig. 3. The communication blackout regions for the 85-ft and 210-ft DSIF antennas are shown, together with timing marks representing days after launch, demonstrating the relationship between communication distance and capability for monitoring solar flare activity not observable by Earth-orbiting satellites. Note that, as the energy in the trajectory is increased (higher perihelion radius), the spacecraft will spend more time directly behind the Sun, providing a longer period of time for sampling the inner corona. Correspondingly, a lower energy trajectory (lower perihelion radius) results in a shorter orbital period, which in turn reduces the spacecraft equipment (including the attitude control system) lifetime necessary to accomplish a given number of orbits about the Sun.

Based on the above, for the Titan II/Centaur/Solid, 210-ft DSIF antenna and 400 lb payload, the most practical compromise values of perihelion radius, corona sampling time and spacecraft lifetime would be 0.3 AU, 70 days and 1 year, respectively. These figures have served as a basis for defining the lifetime, vehicle inertias, solar radiation and heat environment for which the control system must be designed.

B. VEHICLE DESCRIPTION

While several spacecraft configurations have been proposed for the Solar Probe mission an open compartment configuration, stabilized about three axes and shown in Fig. 4 was selected for the subject study based on the configuration study work done under Ref. 1 . In this configuration the insulated heat shield and all of the spacecraft's systems are attached to the cruciform beams that form the backbone of the spacecraft. Onboard electrical power, necessary for certain experiments and the spacecraft communication system, is supplied by two 35-sq ft solar cell arrays hinged from the aft end of the vehicle. These panels are deployed 42° from the spacecraft centerline following injection, and stepped down to 22° as the Sun is approached. The four-foot parabolic antenna is mounted normal to the ecliptic on a two axis gimbal with 360° azimuth scanning and ± 15° elevation scanning. Omni-antennas are mounted on the solar cell panels.

Experiment sensors such as the plasma probe, neutron phoswich and mass spectrometer are mounted on rotating platforms. Magnetometers are mounted on booms away from the main body of the spacecraft. A breakdown of the weight of the 400-lb spacecraft is given in Table I. Approximately 23% of the spacecraft weight is devoted to the scientific sensors. The particular arrangement of the spacecraft is to compromise between the requirements of static, dynamic, thermal and solar pressure balance.

The antenna, solar arrays and experiment booms are wrapped around the solid rocket injection stage. All of these devices are erected after de-spin, following injection.

TABLE I

Weight Summary

	Lb.
Scientific Instrumentation	93
Structure, Heat Shield and Mechanisms	25
Communication, Data Handling and Monitoring Systems	150
Electrical Power System	96
Stabilization and Control System*	37
Total Spacecraft Weight	401

*Based on a conventional Electronic-E/M control system approach

C. VEHICLE CONTROL SYSTEM REQUIREMENTS

The influence of the experimental payloads on the solar probe mission and onboard subsystems design defines the performance requirements and the anticipated environment in which the subsystems must perform. The perihelion distance influences both temperature and radiation environment and defines (within the confines of available booster capability) the vehicle weight and resulting inertia characteristics. The magnetic field experiment requires the spacecraft to be magnetically clean as possible. Vehicle configurations required to accommodate the experiment package and supporting subsystems play an important role in the magnitude of disturbance for which the attitude control system must compensate.

Several solar probe system studies have been conducted as part of the study contract (Ref. 4) in which the relative advantages of spin versus attitude stabilization concepts were evaluated, all of which recommended the latter approach. In most of these studies the booster configuration has included a solid rocket injection stage using a spinning approach to provide stability during the thrust period. The solar probe vehicle is separated from the injection stage and approximately despun with a "yo-yo" mechanism. The control system for the spacecraft must then:

1) Cancel all residual attitude rates subsequent to the yo-yo despin operation.
2) Maintain the orientation of the heat shield and solar panels with respect to the Sun line during the entire flight.
3) Provide a celestially fixed three-axis attitude reference for use in experiment orientation and data analysis, and orientation

of the high-gain communication antenna toward Earth.

4) Provide auxiliary control functions for positioning antennas, sensors, probes, etc.

A detailed study of the solar probe mission has established that there are no stringent vehicle attitude accuracy requirements imposed by either the experiments or the onboard systems ($\pm 1^{\circ}$ at most, which is required by the communication subsystem).

In sizing any attitude control system, the maximum corrective torque and total impulse requirements must be established. For the solar probe, the maximum torque level will probably be sized, based on either the maximum rate allowable for the solar flare monitoring experiment or the maximum response rate of the system required to counteract meteoroid disturbances within the thermal limits of the vehicle.

The total impulse requirements are usually established by a combination of reorientation maneuvers and cancellation of disturbing torques. The maximum disturbing torque to be encountered during the solar probe mission will result from the error in coincidence between the solar center of pressure and the vehicle c.g. While meteoroid impact and motion of internal equipment must be accounted for, the solar pressure disturbance represents the major impulse requirement of the attitude control system. A summary of the accuracy, response rate and disturbance cancellation requirements for a typical solar probe mission is shown in Table II.

TABLE II

Accuracy

	(deg)
During communication	± 1
Solar flare monitoring	± 1.5
Remaining experiments	± 5
All other systems	± 5

Response Rate

	(rad/sec x 10^{-4})
Maximum limit allowable for solar flare monitoring	± 1.45
Required to counteract meteoroid disturbance within thermal limits of vehicle	± 2.53

Disturbances

	(dyne-cm)
Solar pressure--dish antenna (near earth)	29
Solar pressure--20-cm CP uncertainty (near earth)	100
Magnetic torque (entire vehicle of iron)	10.1
Gravity torque (0.3 AU mission--maximum)	3.46×10^{-3}
	(deg/sec)
Meteoroid impulse (0.01 probability of exceeding this)	0.145
Tape recorder--momentum transfer	1.15×10^{-4}
	(deg)
Solar panel (20-deg motion)	0.745
Yagi antenna (2-deg motion)	0.0139
Dish antenna (2-deg motion)	0.00214

D. CONTROL SYSTEM ENVIRONMENT

Perhaps the most severe design requirement imposed on the attitude control subsystem is that of reliable operation for long time periods under the combined intense temperature and radiation environment. This requirement is even more severe when it is realized that, with the extremely critical payload weight restrictions, a minimum of system redundancy can be allowed. A detailed radiation damage study for a typical solar probe mission (Ref. 1) has indicated the necessity for some shielding of electronic components, along with judicious component selection and subsequent location on the vehicle. The temperature environment expected during the mission may necessitate special design features in many of the control system components. It appears that the Sun sensor, in particular, requires a special housing design to provide radiation cooling, as well as automatic gain control to compensate for the changes in solar intensity during the mission, while the Sun sensor optics require special coatings to avoid darkening. The environment is described in more detail below.

1. Solar Radiation Environment

Components of the extraterrestrial environment which should be included in the design of a space probe are radiation (both electromagnetic and corpuscular), meteoric debris, low pressure and density, gravitation-free fields, and magnetic fields. Detailed data concerning the components of the extraterrestrial environment are available from a variety of sources (Refs. 5 thru 9) and are continually being reviewed. Examples of the data available for radiation and meteorite interaction studies are shown in

Figs. 6, 7 and 8.

An evaluation of the environment and its subsequent effect upon a solar probe type vehicle has indicated that the major external source of consequence will be the solar proton radiation that occurs at the time of a major solar flare, as well as the continuous solar electromagnetic radiation (Ref. 1).

Interactions of radiation with materials and subsequent consequences are dependent upon the energy and the type of the radiation (electromagnetic or corpuscular). Such interactions can manifest themselves in volume effects, surface effects or both, depending upon the energy transfer mechanisms (i.e., ionization, excitation, phonon generation, displacement, etc.).

Continuous solar electromagnetic radiation is of consequence for the solar probe since this field is the major contributor to the thermal environment of the system. The solar constant at 1 AU is calculated to be 1.4 kw/sq cm (443 Btu/sq ft-hr) and is considered to follow the inverse square law to at least 0.2 AU. The majority of the solar energy (91%) lies in wavelengths longer than 0.4μ. In addition to providing the thermal environment, however, the solar spectrum contains an appreciable amount of short wavelength radiation which is easily absorbed and which can give rise to color center generation and photolytic reactions which in turn can manifest themselves as changes in absorption properties of thermal control surfaces and photoconductive materials. Such changes in optical properties can be reflected as uncertainties in the internal thermal environment (Ref. 10). At present there is some controversy as to the importance of the simultaneous interaction of solar electromagnetic radiation and the corpuscular radiation encountered in a solar orbit upon changes in absorption of solar energy. (The effect of the meteoroid environment upon optical properties is considered minuscule by comparison to the effect from solar electromagnetic radiation.)

The requirement which led to concern over solar flare protons was the need that all electronic equipment operate in the natural and induced radiation environment during a 0.3 AU mission (Ref. 1). Since it has been well established that the threshold for the degradation of electronic characteristics--specifically semiconductor devices--is well below that for other damage criteria (Ref. 11), such devices set the radiation shielding requirements. An analysis of the minimum shielding requirements for the protection of the electronic components indicated that a shield of 0.044-in. aluminum was required and that the solar flare proton flux (NASA/Ames Model) was the external source making the major contribution to the acceptable radiation exposure.

2. Solar Heat Environment

The spectral range of the electromagnetic radiation which has a critical influence on the thermal environment of the spacecraft happens to be the most predictable. The average solar thermal flux (approximately 450 Btu/sq ft-hr at the Earth's orbital distance from the Sun) increases by factors of 10 and 25 at 0.3 AU and 0.2 AU, respectively. A thermal profile for a typical spacecraft is presented in Fig. 5 . The discontinuity shown at 0.6 AU corresponds to the programmed shift in solar array orientation. The temperature limits shown indicate that the control system components must be designed for operation in a maximum temperature environment of 1000°F if exposed, or less than 100°F if protected by the heat shield.

The location of the control logic elements is extremely important when implemented electronically since the temperature variation as shown covers a range of approximately 700^{o}F during the course of the mission when directly exposed. If not protected by the thermal control system some components could be required to operate at near zero ^{o}F through the high temperature range. It is desirable that a fluidic control system be as insensitive as possible to these temperature variations.

E. CONTROL SYSTEM CONFIGURATION

During our previous Solar Probe System Study contract the requirements for attitude control and stabilization were considered in detail and various control system approaches were evaluated. These approaches considered alternative references such as Sun, planets and stars and selected the Sun as the basic two axes reference and the Star Canopus for the third reference axis. Canopus was selected because of its location, brightness and availability of star sensors which have been designed specifically to track this star. Various control logic schemes and control torque devices have been studied for application to the solar probe mission and are reported in Ref.1. Trade-offs of system weight, complexity and reliability are presented, and recommendations for the system approach are made. Analog and digital logic approaches are considered in combination with reaction jets, momentum exchange devices and solar pressure torquing techniques. The recommended approach uses momentum wheels for transient disturbances and solar pressure vanes for trimming the vehicle, desaturating the momentum exchange devices and providing damping in the solar pressure control mode. This system selection was based on the following considerations:

1) The flywheel system (except in the roll axis) operates without need for an effluent. Although there has not been agreement on the effects of such effluents as N_2, H_2O, H_2, etc., on the various experiments, it is conceded that these materials may generate a problem. Since the primary purpose of the solar probe is to collect data by means of its experiments, it was decided

that there is a significant advantage to a non-expulsive system, such as the flywheel system, which significantly reduces the potential experiment degradation problem. Using reaction jets and solar pressure for trim and long term damping the average effluent rate is 0.287×10^{-3} lb/hr while the recommended flywheel system with reaction jets for roll control has an average effluent rate of 0.148×10^{-3} lb/hr.

2) The reaction jet system requires lead circuits, rate gyros of an extremely low threshold or psuedo rate switching networks for primary damping. While this is not an insurmountable problem, the advantages in the self-damping characteristics of the velocity controlled flywheel are obvious. The entire damping problem is avoided.

3) The weight of the reaction jet-solar trim system is 8 lbs lighter and includes 2.0 lbs for limit cycle propellant and tankage (based on a specific impulse of 50). The actual calculated limit cycle propellant and tankage, using a timed-pulse jet controller for low level limit cycle control, is 0.68 lb. A safety factor of three was chosen, leading to the 2.0 lb requirement. Earlier scientific satellite control systems, such as that on Mariner, have had factors of up to ten in propellant and tankage. If a safety factor of ten were applued to the calculated limit cycle propellant and tankage for the solar probe jet system, the reaction jet system weight would increase by 4.8 lb narrowing the weight difference between the jet and fly-

wheel systems to 3.2 lb.

4) The limit cycle amplitude in the jet system is heavily dependent on the various sensor gains, being inversely proportional to the sensor gains, and the resulting propellant consumption rate is proportional to the sensor gains. While a gain compensation system is included in the recommended electronic sun sensor design, its failure in a jet system would lead to extremely tight limit cycles near the sun and the propellant margin would be dissipated. On the other hand, a gain compensation failure in the flywheel system would simply lead to lower system damping, which would not prevent successful completion of the mission.

5) Due to the necessity for a timed pulse circuit to determine the limit cycle behavior of the jet system, the circuitry for the jet controller would be somewhat more complex than that for the wheel controller. While this is not an overriding factor, it is certainly a consideration in the system choice.

Even having considered all of these factors the weight advantage of the reaction jet-solar trim system cannot be ignored. While the flywheel system is recommended (as a guideline for the fluidic system implementation), it should be noted that either the reaction jet system with solar pressure or the flywheel system with solar pressure would be a satisfactory choice.

In the recommended system momentum wheels are used for short-term stabilization and control. Long-term stabilization and wheel desaturation are accomplished in pitch and yaw by solar pressure control surfaces, and in roll by nitrogen gas jets. Sun sensors provide a reference to the Sun line in pitch and yaw, and provide the signal to both the momentum wheel torquer and servo-actuators for the control surfaces. A Canopus tracker provides vehicle roll reference and input signals to the roll momentum wheel system. Block diagrams for the pitch and roll control systems are shown in Figs. 6 and 7.

Considering the application of a constant disturbing torque at M_{DT} (Fig. 6), the initial angular acceleration of the vehicle causes a momentum wheel moment to be developed, which cancels the disturbing moment within 60 sec. Were there no trim system, the momentum wheel would ultimately settle to a constant acceleration, requiring a constant vehicle rate to be present and quickly resulting in wheel saturation. The trim system, however, begins to accumulate any required trim moments, driving the attitude error and wheel speed to zero in the steady state. Ultimately, $M_V = M_{DT}$ and $M_W = \sigma = 0$. Without trim, the ultimate result would be $M_W = M_{DT}$ with $\sigma = \sigma_1 + M_W t/J$. The natural static stability of the vehicle (K_S) has no steady-state effect, but is important in achieving adequate dynamic stability. Similar reasoning will show that, where an initial vehicle rate would, without solar torques, result in a steady-state attitude hangoff and constant wheel speed, the basic static stability of the vehicle, with or without the trim system, leads to an ultimate decay in wheel speed and attitude error.

The pitch and yaw momentum wheels are continuously desaturated without an expulsive torque device and continuously operate about stall. Vehicle static stability is achieved by designing the solar panel system and other external appendages to place the center of solar pressure aft of the center of gravity. The trim system in each axis takes the form of two extendable and retractable booms, one on each side of the vehicle. (Thus, there are two yaw trim booms and two pitch trim booms; a total of four.) The booms can be extended (as much as 45 ft) and retracted by motors which operate in parallel with the momentum wheel torquers. When one boom has been fully withdrawn, the logic circuit transfers control to the other boom, which then begins to extend. Thus, a bilateral trimming capability is achieved. The exact mechanization of the trim system can vary; for example, use of trim vanes on the end of solar panels (such as used on Mariner C) could replace the above concept.

The roll control system (Fig. 13) utilizes no solar pressure. Since the steady roll disturbing torques are expected to be some two orders of magnitude less than those in pitch and yaw, no trim system is included in this design. Integral control of the momentum wheel is used to eliminate attitude hangoff which would result from initial vehicle rate about the roll axis. A tachometer, mounted on the torquer wheel shaft, is monitored to determine when to fire desaturation jets. When the wheel speed, as indicated by the tachometer output, reaches a level of 95% of the wheel saturation speed, the appropriate jets fire and remain on until the indicated wheel speed has dropped below a level of 5% of the wheel saturation speed. Again, the principal loop damping is supplied by the torquer's own velocity feedback characteristics.

Results of analog computer studies using this system for a typical solar probe mission are reported in Refs. 1 and 12.

The proposed system requires the following types of components for implementation:

Canopus Tracker
Sun Sensor - Primary and Secondary
Angular Rate Sensor

Flywheel Momentum Storage Device
Reaction Jet System
Boom Actuators
Bi-metallic Vane Actuator
Control and Logic Circuitry - Including various operating modes
Interface Circuitry for Ground Commands and Telemetry.

A typical performance specification is presented in Table III to indicate the requirements which the components must meet in a typical solar probe mission.

TABLE III

Performance Specification

Item	Nominal	Maximum	Minimum
Power requirements	16.3 watts	20 watts	--
Volume	982 cu in.	1100 cu in.	--
Weight	37.0 lb	40.0 lb	--
Canopus tracker field	$4^\circ \times 52^\circ$	$4^\circ \times 56^\circ$	$4^\circ \times 32^\circ$
Canopus tracker linearity	+10%	--	--
Sun sensor field (primary)	$180^\circ \times 180^\circ$	--	--
Sun sensor field (secondary)	$180^\circ \times 180^\circ$	--	--
Ambient temperature requirements*			
Sun sensors	--	$+50^\circ$ C	-10° C
Canopus tracker	--	$+51^\circ$ C	-10° C
Flywheels	--	$+70^\circ$ C	-50° C
Control electronics	--	$+70^\circ$ C	-50° C
Fuel tanks	--	$+80^\circ$ C	$+20^\circ$ C
Rate gyro	--	$+70^\circ$ C	-50° C
Boom actuators	--	$+70^\circ$ C	-50° C
Rate sensor threshold	0.005 deg/sec	0.02 deg/sec	--
Rate sensor linearity	±20%	--	--
Rate sensor limit	5 deg/sec	--	1 deg/sec
Flywheel momentum storage	0.32 ft-lb-sec	0.4 ft-lb-sec	0.3 ft-lb-sec
Flywheel time constant	35.7	50.0	--
Flywheel motor stall torque	2 oz-in.	2.5 oz-in.	1.8 oz-in.
Flywheel power required (stall)	4.6 watts	5.0 watts	--
Flywheel maximum speed	1000 rpm	1250 rpm	940 rpm
Flywheel motor torque-speed linearity	±5%	--	--
Jet system storage pressure	3000 psi	3500 psi	2500 psi
Jet thrust	0.01 lb	0.02 lb	0.005 lb
Jet valve delays	20 ms	40 ms	--
Jet propellant required	2.9 lb	4.0 lb	2.5 lb

*These requirements are based on the use of a passive thermal control system required for electronic subsystems on-board the spacecraft.

TABLE III (cont'd)

Item	Nominal	Maximum	Minimum
Boom actuator voltage	6 v dc	7.5 v dc	5.5 v dc
Boom actuator power	1.5 watts	1.9 watts	--
Boom actuator maximum rate	0.077 fps	--	0.070 fps
System gains			
Boom motor rate gain (K_1)	450 ft/sec/rad	550 ft/sec/rad	45 ft/sec/rad
Flywheel velocity control gain			
Yaw, pitch (K_5)	700 sec^{-1}	1000 sec^{-1}	500 sec^{-1}
Roll (K_4)	256 sec^{-1}	350 sec^{-1}	150 sec^{-1}
Sun sensor--preamp gains (K_D)	-1.0	-0.8	-1.2
Roll integral control gain (K_1)	0.01 sec^{-1}	0.01 sec^{-1}	0.001 sec^{-1}
Roll jet turn-on level (A)	99 rad/sec	131 rad/sec	90 rad/sec
Roll jet turn-off level (b)	5.3 rad/sec	11 rad/sec	0 rad/sec

F. CONTROLS RELIABILITY REQUIREMENT

Extensive reliability studies were performed under our previous Solar Probe study contract. In this study the various configurations of control system implementation used electro-mechanical components (Ref. 1). These studies involved evaluating the mission probability of success based on the reliability, weight and performance capabilities of the vehicle systems and subsystems, along with various equipment operating modes. These studies included:

1) Identification of subsystem functional operations.
2) Identification of failure effects.
3) Establishment of systems logic diagrams for each configuration, showing every possible success mode.
4) Establishment of mathematical models, using information in logic diagrams.
5) Establishment of environmental matrix.
6) Establishment of component reliability estimates for inputs to mathematical models and estimation of the reliability for each system.

The logic diagram for the attitude stabilization and control system, used for the reliability study, is shown in Fig. 8 . The logic diagram shown includes each functional equipment, shows all redundancies and each separate path to success. It was used to establish logic equations for subsystem reliability. The mathematical model was taken directly from the logic diagram to establish an equation for the sum of all the probabilities of each independent path to success.

The environmental matrix showed the expected environments and their estimated distributions from prelaunch through two complete solar probe orbits. The environmental matrix was used to define the probability that the equipment would meet its reliability requirements.

A principal result of these studies is a reliability comparison of reaction jet control system versus a flywheel control system. The flywheel system proved to be lighter and to have a higher reliability. This comparison as a function of mission time is shown in Table IV. Since these studies were conducted for electro-mechanical implementation of the control system the resulting reliability of a fluidic implementation would have to better or equal that obtained with electronics, in order to justify the fluidic approach. The expected reliability of the fluidic approach will be discussed later in the report.

TABLE IV

Cumulative Reliability of Attitude Control System

Basic Subsystem Reliability	3 months	6 months	9 months	12 months	Mission
Jets	0.946239	0.892478	0.838716	0.784955	0.775527
Flywheels	0.950618	0.901236	0.851854	0.802472	0.793812

IV. CONTROL SYSTEM IMPLEMENTATION

A. SENSORS

To provide the long term stabilization of a deep space probe to facilitate the scientific sensors and the communication system, a reference system based on radiation from celestial objects is the only practicable approach. Radiation type sensors have been used on Surveyor, Lunar Orbiter, and the Mariner series as well as a large number of earth satellite programs. The most convenient and largest source of radiation is the sun and as a consequence this source of reference has been used on almost all space programs. Planet sensors have been used when the trajectory of the space vehicle is such that a large percentage of the mission is spent near the planet, i.e., horizon scanners in earth orbit. Stars provide another source of radiation although their intensity is several orders of magnitude less than the earth, moon, or sun. Star sensors have been used on Mariner Mars and Lunar Orbit.

Inertial type sensors are useful for short duration attitude changes required for maneuvering the spacecraft or pointing the scientific sensors.

For the Solar Probe Vehicle attitude control requirement some sensors will be needed for pitch and yaw stabilization and a stellar reference for roll control. Based on previous studies under NASA contract in the Solar Probe Vehicle (Ref. 1), the Star Canopus offers the best roll reference for the planned mission. Inertial sensors are required for initial vehicle stabilization following injection and to maintain attitude following a loss of the celestial reference due to a disturbance. Based on these requirements our survey of fluidic sensors has been primarily aimed at work which has been accomplished on fluidic sun, star and inertial rate sensors.

1. Solar

A fluidic solar radiation sensor must respond to the anticipated irradiation levels, of 0.13 watt/sq cm at 1 AU and 1.2 watts/sq cm at 0.3 AU, with an adequately strong fluidic signal and an acceptable response time. Two categories of solar radiation sensors have been investigated by the Martin Company. These are:

(1) Direct fluidic radiation sensors in which the radiation acts immediately on a fluidic element and gives a fluidic output signal resulting from a change in its operating condition.

(2) Indirect radiation sensors in which a primary sensor gives a non-fluidic output signal which is then introduced into the fluidic control system with the aid of a suitable transfer.

Direct fluidic radiation sensors will always convert impingent radiation energy into heat by absorption and use this heat addition for changing the fluid flow passing through them. In other words, these sensors are essentially fluidic thermometers. The best known and most widely used fluidic thermometer is a gas-operated fluid oscillator which is a bistable element with a feedback loop between its two control ports. Its frequency is clearly determined by the travel time of a pulse through the feedback path, which changes with the sound velocity (c) in the gas and therefore with the gas temperature (T), since c is proportional to $\sqrt{T}$. The output of this fluidic temperature sensor is therefore a variable frequency of the oscillation, and one can obtain the fluid temperature by comparison with a standard frequency from an unheated oscillator (i.e., by counting beats). To use this element as a radiation sensor, the feedback path is exposed to the radiation, resulting in a frequency change as an output signal.

There are a number of problems to be solved in order to obtain a sufficiently fast response from this sensor. The worst of them is that the small mass of the gas in the feedback loop (in comparison with that of its walls) makes it necessary to use a very thin wall of a material with good heat conductivity, low specific heat (per unit volume, not per unit mass) and adequate mechanical strength. In this respect, pure silver with an outer coating of platinum black for absorption may be superior to both gold and platinum which are both too heavy and have a lower heat conductivity. Another problem with this type of radiation sensor is that of getting rid of the relatively substantial amount of absorbed heat in the wall as fast as possible after it has served its purpose of indicating the presence of radiation by a frequency change. This seems to require a forced cooling which could (for instance) be provided by an arrangement where the frequency change would also trigger a short injection of cold gas into the feedback path to remove the excess of stored heat in the sensor wall. On the basis of our preliminary examination of this radiation sensor concept, we believe that it can be developed into a practical device, although it will have to be complex in order to meet all requirements for its use in an attitude control system.

A second typical example for a direct fluidic radiation sensor and, in fact, for a sensor of great simplicity, is obtained by "translating" the well-known electrical "bolometer" into the system of fluidics. An electrical radiation sensor of the bolometer type is simply a thin blackened platinum strip whose temperature, and therefore whose electrical resistance, changes by absorption of energy from a radiation field. The corresponding "fluidic bolometer" is a thin-walled metal capillary with a blackened surface, conveniently coiled up into a flat spiral and positioned at the focus of an optical system, whose "flow resistance" for laminar flow is changed by radiative heating, since the viscosity coefficient of a gas increases with its temperature. The output signal from this simple radiation sensor is an increase of the pressure difference between its two ends under irradiation, and a pressure signal of this type is easy to utilize in a fluidic control system where it can (for example) trigger the switching of a bistable element to initiate a control action. Since the continuous gas flow through the sensor provides internal cooling of the element, there is no need to provide extra cooling to improve response characteristics. Experiments with this sensor have been performed in our laboratory and have demonstrated that it works well in radiation fields with a minimum intensity of around 1 watt/sq cm up to rather high intensity levels. We believe, therefore, that the fluidic bolometer concept may be well suited for the present application. The experimental unit is shown in Fig. 9.

In the state-of-the-art survey conducted as part of the subject contract, we found one reference which discussed radiation type sensors. Garner and Tuller in Ref. 13 discussed two types of sensors, one each of categories (1) and (2). The first involved a "green-house" concept in which the suns energy raised the temperature of the working fluid housed in a radiation detector thus changing its specific volume and flow characteristics. This sensor is similar to the Martin "bolometer" approach, but would appear to be less sensitive since the Martin approach depends primarily on changes in viscosity with temperature and not on pressure-volume relationships. Garner stated that laboratory test using this sensor have been conducted at NASA-Langley to demonstrate its feasibility, and while no attempt was made to optimize the configuration, sensitivity was low. Figure 10 is taken from Ref. 13 and illustrates the working principals of the device. The differential pressure signal of the two radiation detectors is used for the control ports of a proportional amplifier, similar to the configuration of photocells in conventional electronic sun sensors. The second sensor investigated by Garner and Tuller utilized the difference in thermal expansion of a sandwich construction to cause a "flexible-leaf" motion to drive a conventional pneumatic pick-off. The sandwich consists of high coefficient of expansion metal outer layers and a thermal insulator for the middle layer. The front-to-back temperature gradient introduces a bending moment and the resulting motion of a flexible leaf is used as a fluidic control source. A schematic of this sensor is shown in Fig. 11 taken from Ref. 13. The time-lag in this system can be used in a phase stabilizing mode of attitude control.

The "flexible leaf" sensor is a category (2) type and one can generate a large number of concepts which fall into this category. Two examples under investigation at Martin are:

(1) The primary radiation sensor is a shadowed bimetallic strip whose bending under radiative heating gives an output in the form of a mechanical displacement. This type of actuator has been used on Mariner Mars for moving auxiliary panels which provided vehicle stabilization. The mechanical motion could be used in a number of ways to provide a fluidic signal. For instance, the displacement can be used to insert a knife edge into a jet and cause it to be deflected from the axis of a jet splitter configuration or a simple jet collector inlet, or it can be used to produce a

lateral displacement of the nozzle of a power jet relative to a jet splitter. This concept is much like that of Garner's "flexible leaf" in Ref. 13. We have examined the use of the bimetallic strip and found that there will be a need for providing forced cooling of the strip in order to remove the absorbed heat as fast as possible after it has served its purpose. This will increase the complexity of this otherwise simple and rugged device.

(2) The primary sensor for radiation would be electrical such as a thermoelectric device which gives a low-level d-c signal as its output. This signal could drive an audio-frequency generator (e.g. 2 to 6 x 10^3 cps), and its output could be converted into sound in a piezo-electric or other sound generator which is placed in the vicinity of the exit nozzle of a turbulence amplifier. It takes very little sound energy to upset the balance of a laminar jet and cause it to become turbulent, and we believe that it will be possible to obtain this energy from a series of metal thermocouples. The inherent advantage of such a "local electric loop" in the radiation detection part of a fluidic solar attitude control system is its very fast response (of the order of a few milliseconds and essentially only the travel time of the jet from the nozzle of the collector). We believe that its main difficulty, reliable operation in an environment of elevated temperature, can be overcome if there is a real need for a faster response than can be obtained with

non-electric devices, but we prefer the latter ones because of their greater simplicity.

As a result of our fluidic survey and our in-house studies of solar radiation sensors we can see no limiting problems with the development of a fluidic solar sensor. The response time needed of such a sensor in the Solar Probe application is not expected to exceed that which can be obtained with pure fluidics. The Martin fluidic bolometer concept has been demonstrated in the laboratory and adequate sensitivity obtained. While further development is required to obtain a proven sensor design, the feasibility of such fluidic solar sensing concepts has been established.

2. Star

Stabilization about the vehicle axis pointing to the sun must be provided by a star reference. Pure fluidic star sensors are beyond-the-state-of-the-art and perhaps are not feasible technically. Garner in Ref. 13 discusses the possible application of the Golay cell which is thought to be the most sensitive fluidic sensor available to date. A telescope aperture of about ten miles would be required to obtain a signal-to-noise of one from Canopus. The sensitivity would have to be increased by two orders of magnitude for practical applications and considerable development work would be required to provide a fluidic pick-off system.

The most promising approach at present for the Solar Probe Attitude Control System is to use one of the developed canopus trackers, with slight modifications, and incorporate one of the electrical to fluidic conversion devices under development. This approach provides a ready interface with the ground command and control system which would be necessary for proper mission control in any case. Due to the difficulty in providing automatic lock-on of Canopus (or any star) the procedure which has been used in Mariner requires the output of the Canopus tracker during a search mode to be transmitted to ground. Those outputs are observed and evaluated to determine which output represents Canopus. The ground observer then commands the vehicle to initiate lock-on when the Star Canopus is being approached during the search. In addition, the tracker has upper and lower control gates to prevent transmission of all the stars in the search field and to protect against saturation from too bright a signal. Since the process of star reference lock-on (and re-lock-on should the reference be losed following initial acquisition) is difficult and requires interface with ground command and control, the use of an electronic stellar reference is accommodated.

3. Inertial

Inertial reference sensors will be required on the Solar Probe Spacecraft to provide efficient initial damping of residual rates following injection and to provide a secondary reference in case of temporary loss of the celestial reference particularly about the vehicle axis which is aligned to the sun. An inertial rate sensor is also required to provide a such mode for inertial acquisition.

Fortunately more development work has been conducted throughout the country on inertial fludiic rate sensors than either the fluidic sun or star sensors. Because of the mode of operation of the inertial sensors for Solar Probe (that is to provide rate information and only temporary attitude hold) , they are not required to have excessively low drift rates. The fluidic gyros of the gas lubricated bearing type have been under development for some time and have been applied in flight vehicles. Garner in Ref. 13 points out that at least one of these has proven its long life and reliability in a standby operation. A recent paper by Straut, Ref. 14 describes a two-axis pneumatic pick-off (TAPP) gas bearing gyro which has been flight tested. This unit incorporates a gas supply bottle for the spin-up bearing and pick-off power supply. A two-axis jet-pipe pick-off is used in conjunction with a flueric summary module. Although no detailed performance information is available and operation in a closed loop (power recovery) is not discussed, the TAPP should be considered for Solar Probe.

Garner also discusses a two-axis gyro in which a single externally pressurized spherical gas bearing serves for both gimbal and spin bearings. The unit uses fluidic torquers and pick-offs. A rate gyro under development by Eclipse-Pioneer Division of Bendix, Ref. 15 consists of a simple turbine wheel rotating on gas bearings. A jet-pipe pick-off is used to measure gimbal displacement between two orifices. The gyro has the following characteristics:

Size	2.0" x 3"
Weight	2.75 lb
Maximum rate	40°/sec
Resolution	0.05°/sec
Threshold	0.1°/sec
Natural frequency	15 cps
Damping ratio	0.5 + 0.2
Hysteresis	1% full scale max.
Linearity	1% full scale max.
Maximum flow	.25 lb/hr

Although the threshold characteristics do not meet the state requirements for the Solar Probe Attitude Control System given in Table II, this unit was considered for the inertial rate sensor requirement. Bendix is investigating this unit under Air Force contract for possible application in a flueric control system capable of operating in a 1400°F environment.

Conventionally in Mariner and Surveyor Spacecraft, rate integrating gyros are operated in the rate and rate integrating modes to provide the necessary attitude reference. In Lunar Orbiter the gyro is switched to its rate mode for vehicle re-orientation and a vehicle rate commanded for a specified time to accomplish the desired re-orientation. After re-orientation, the gyro is switched back to the integrating mode.

At present there is no known development program, (and for that matter no identified conceptual approach) for a flueric angular displacement sensor. Consequently, we must depend on operating the inertial rate instruments in an integrating mode. The use of flueric integrations along with their inherent inaccuracies needs to be further explored.

Another candidate for the inertial sensors for the subject study is the vortex rate sensor. Versions of this unit have been studied, built and tested by HDL, Bowles Engineering and Honeywell. Honeywell has demonstrated their vortex rate sensor in aircraft and missiles performing an attitude stabilization function. This sensor consist basically of an ideal sink flow between two coaxial dishes and a vortex created by the rotation of the unit about its axis of symmetry. Hellbaum of NASA-Langley in Ref. 16 has conducted a study of a vortex rate device to evaluate the effects of various geometrical design patterns (flow rate, coupling element diameter, exhaust orifice diametry and cylinder height). Figure 12 presents a schematic of a vortex rate sensor. Hellbaum has found that an increase in ratio of tangential component to radial component of velocity occurs for a decrease flow rate and that optimum radius to height ratios may exist for various flow rates. The exact configuration of these sensors and a detailed description of their pick-off techniques are not available in the open literature.

A recent paper by Hall, Lindahl and Ostlund, Ref. 17 does give performance characteristics of a vortex rate sensor used in a test of a fluidic attitude control system in the F-101B. This sensor had the following characteristics:

Threshold	-	0.05°/sec
Range		$\pm 10^{\circ}$/sec
Linearity		$\mp$5% full scale
Scale Factor	-	0.06 in $H_2O/^{\circ}$/sec
Transport Delay	-	0.015 seconds

A transfer function $e^{-0.0255}$ is used in the analysis of the system for the rate sensor which represents the lumped transport lags of the rate sensor and amplifier cascade. A high pass filter was used on the output $\left(\frac{T_3 S}{1 + T_3 S}\right)$ in which $T_3 = 4$ seconds to prevent null shifts from affecting the system. In an earlier paper by Reilly of Honeywell (Ref. 18), a description of the performance of three experimental fluid flight control systems is given and includes a discussion of the sensor used on the F-101B tests. The unit had a 6-inch diameter coupling element and an outlet sink of 0.070 inches. Differential pressure output of the sensor is amplified 100 times by a 5-stage fluid amplifier cascade. The operating characteristics given for this unit meet the Solar Probe requirements listed in Table II with the exception of the threshold. Studies by Lock and Gee of NASA-Langley reported in Ref. 19 have shown that threshold decreases with larger diameters at the expense of increased time lags. Power supply pressure and ambient pressure determine the scale factor which sets the loop pressure gain.

Reilly (Ref. 18) also describes the use of a vortex rate sensor in an attitude hold mode much like that which will be required on Solar Probe. This system was flight tested on the roll axis of the Army's Test Instrumentation Missile (TIM). Output signals from the vortex rate sensor were amplified and separated into two outputs. One signal was fed through a fluid network having a 10-second time constant and then mixed with the pure rate signal. The fluid network essentially integrated the rate signal to provide attitude information. In the presence of a disturbing torque the TIM fluidic attitude control system successfully flight demonstrated a $\pm .5^{\circ}$ limit cycle hold capability. Several variations of the vortex rate sensor configuration have been discussed in the literature. A unit investigated by T. Sarpkaya of the University of Nebraska and reported in Ref. 20 had two sink tubes, top and bottom, and it was found that the output for a given angular rate dropped sharply when one tube was closed. Based on his investigation he recommends that a symmetrical sensor be used. Another form of vortex sensor reported in Ref. 22 used separate pressure controlled oscillators on each of the output ports and a difference counter to perform the integration. This difference count is then converted to an analog signal which provides differential pressure on flow rate which is proportional to angular rate.

Angular rate sensors which use a high density-low viscosity fluid have also been proposed and are under development. A unit under development at Martin employs jets to spin fluid in a practically enclosed cavity serving as a momentum trap. The cavity is spring-retained and the angular displacement can be picked off by a low torque fluidic displacement sensor (e.g., a jet interrupter). The hydraulic version of such a device is shown in Fig. 13. In a similar version reported in Ref. 22 by Mott and Diamond, the momentum of the fluid causes it to maintain a fixed orientation in space when the cavity is moved and causes a small angle to develop between the area of rotation of the fluid and the axis of rotation of the cavity. This displacement causes an unsymmetrical pressure distribution about the spin axis which can be sensed. A unit described by Rae and Ostrander of Development Laboratories Inc., Ref. 23 and 24, describes a modified vortex sensor which determines angular rate by direct measurement of angular velocities in the fluid. This unit is described as follows: a flatten vessel, filled with hydrocarbon fluid, having a dividing wall with a hole in the center so that the fluid can circulate radially inward on one side of the passage, radially outward on the other side. Pumps are placed in return passages, a porous plug is used to straighten the flow and impact an angular velocity to the working fluid. The added spatial rotation is measured by heating elements in the stream with sensing electrodes slightly downstream. The arrival of hot molecules at the sensing electrode provide velocity information.

The operation of the vortex rate system and its associated pick-offs and amplification stages under changing elevated temperature environments has not been explored. One indication of this performance was obtained from Ref. 25 written by Clayton and Posengies. In this case a vortex rate sensor was being operated from a N_2 "blow-down" system with supply pressure changing from 3300 psia to 330 psia during the mission. This change in supply pressure caused a change in temperature of 130°F in the working fluid and resulted in a null shift of several degrees/second.

After a review of the current status of inertial rate sensors and the Solar Probe Attitude Control Requirements it appears that there will be little problem in finding an acceptable sensor. The vortex type rate sensor can be used and its performance has been demonstrated in flight tests under similar performance application. The subject of effect of temperature on the sensor and its output amplification needs further study, however.

B. FLUIDIC POWER SYSTEMS

1. Problem Description

One of the most difficult aspects of implementing a fluidic spacecraft control system is the generation of fluid power. The present approach to spacecraft fluid power systems, as exemplified on Mariner, Surveyor, Gemini, and others, is the stored, pressurized gas vessel, or open-loop "blowdown" system, usually supplemented with such accessories as regulators, shutoff valves, relief valves, etc. Such systems are relatively light, simple, and to date have been fairly reliable. The control systems powered with such open-loop power systems require flow only on an intermittent basis, and are implemented with conventional pneumatic or hydraulic components involving moving parts, seals and general complexity. These components are unfortunately subject to leakage, wear, contamination and generally degraded reliability problems, as compared to the flueric elements contemplated for the subject spacecraft control system.

On the other hand, the intrinsic operating advantages of the flueric elements are offset by the requirement for continuous flow in order to retain operating memory necessary for control functions. The continuous flow requirement unfortunately is incompatible with the nature of the open-loop power system, particularly for long duration missions, since the total weight of stored pressurized fluid and container can become grossly excessive.

This dilemma gives credence to the concept of a closed-loop, or continuously recirculating fluid power supply, where fluid weight is traded off against the weight of pressurizing and recirculating equipment. Such systems require the application and removal of external energy for operation. However, it appears that such energy is available, either from the Sun, or a nuclear radioisotope-thermoelectric-generator (RTG); and that the removal of energy through a deep space radiator appears practical through the operation of the spacecraft attitude control system, which keeps the vehicle constantly oriented with respect to the Sun, so that the radiator can be constantly pointed away from the Sun.

The closed-loop power system approach is, in operating principle, more compatible with the low pressure, steady flow demands of flueric logic elements on extended time missions. However, such systems may show weight disadvantages in order to handle the large transient flow demands made by miscellaneous actuators, and momentum exchange devices that are required in order that the control system can perform its various functions. Thus, it appears that the optimal fluid power supply for a fluidic spacecraft control system will probably contain both open and a closed-loop functions, since neither appears capable of doing the whole job.

In the discussion following, emphasis will be given primarily to the closed-loop power supply concept, since the open-loop approach is well covered in the existing literature, both in terms of theory and practice, while there is a disturbing scarcity of coverage on the closed-loop approach of either theory or practice. A discussion of probable control system fluid power requirements will be followed by a discussion of general operational principles of closed-loop systems and several possible specific approaches.

2. System Power Requirements

The power requirements of a fluidic solar probe attitude control system have been formulated (Table V) based on known fluidic element performance with

TABLE V

Solar Probe Attitude Control System Power Requirements

Subsystem or Component	No. Req'd.	Operating Pressure Differential (psig)	Flow Per Unit Syst. (lb/sec)	Total Sub-System Flow (lb/sec)	Power (Milli-watts)
Momentum wheel bearing	3	3 psig	$.53 \times 10^{-4}$	1.59×10^{-4}	500
Momentum wheel (jet driver)	3	7 psig	22.1×10^{-4}	66.3×10^{-4}	66400
Boom actuator	4	7 psig	5.5×10^{-4}	22×10^{-4}	22000
Hysterisis switch	6	2 psig	$.253 \times 10^{-4}$	1.518×10^{-4}	300
Inverter	6	2 psig	$.25 \times 10^{-4}$	1.52×10^{-4}	300
Amp (binary)	6	7 psig	$.8 \times 10^{-4}$	4.8×10^{-4}	4800
Primary bol. amp	6	7	$.8 \times 10^{-4}$	4.8×10^{-4}	4800
Sec. bol. amp	6	7	$.8 \times 10^{-4}$	4.8×10^{-4}	4800
Boom logic	8	2 psig	$.266 \times 10^{-4}$	2.13×10^{-4}	6000
E-F conv.	3	2 psig	$.3 \times 10^{-4}$	$.9 \times 10^{-4}$	180

Total flow required by fluid logic and amp — 18.3×10^{-4} lb/sec

Total flow required by actuators and momentum wheel jets system — 107.4×10^{-4} lb/sec

The total power required is $\approx$ 120 watts air and the required circuit element quantities based on experience with the SOFACS program (Ref. 26). Recent Martin experiments have shown that fluidic elements of the momentum exchange type can work at extremely low Reynolds numbers (about 10) corresponding to nozzle pressures as low as .25 inches of water. However, pressures in the 2 psi range have been selected to be conservative. Further orifice sizes (.005" - .008") were selected larger than the smallest state-of-the-art laboratory elements to minimize filtration problems and also tending to make the power estimates conservative. In addition, the preliminary design of actuator and momentum wheel drive have not been optimized with respect to low power consumption.

The power for each nozzle was taken from the curve (Fig. 14) for air. The curve gives the number of watts per square mil of orifice area vs. the pressure drop across the nozzle. P_1 is the downstream pressure in psia and P_s is the supply pressure in psia. An orifice coefficient of .76 was assumed. Note that the power consumption is somewhat dependent on the downstream or back pressure P_1. Values for sonic flow were used in the estimate, which represents maximum flow at any particular pressure P_s. This is also very conservative.

Inspection of Table V shows that the power requirements can be divided into distinctive high and low power groups. The actuators and momentum wheel drivers form the high power group and the fluid logic and amplification comprise the low power group. The high power group requires almost five times the power of the low power group.

In addition to the requirement information given in Table V, it is estimated that the required storage weight of fuel for jet reaction system (in place of momentum wheels) is 3-4 lbs.

3. Closed Loop Power Systems

Closed-cycle fluidic power systems involve a thermodynamic cycle with the usual requirements of:

A working substance

An energy source or hot body

A receiver or cold body

A heat pump where the fluid can do work or have work done on it.

For a solar probe, energy sources are the Sun itself, electrical resistance heaters, RTG waste heat or component electrical heat equivalent heat dissipation. Only the Sun and RTG (radiosotope-thermoelectric-generator) waste heat appear to be practical energy sources for a long-term mission. Space serves as a near-perfect radiant heat sink for absorbing unavailable energy. The solar heat source is variable and a function of the solar distance. RTG waste heat offers the advantage of a nearly constant heat source. In addition, it would simplify the power system design and dynamic response analyses, since temperature transients would be at a minimum.

The well known difference between the available and unavailable energy in a thermodynamic cycle is considered work, or its best equivalent, leaving the system. In a closed fluidic attitude control system, the only work leaving the system appears as heat due to flow friction, friction in moving parts and any venting required to desaturate the momentum wheel. The enclosed area on a PV or TS diagram of the fluidic power cycle would be necessarily small in comparison to a regular heat engine. The temperature differences between the hot and cold bodies of the cycle need not be large to keep the energy source and sink heat exchanger sizes small.

Temperature Ranges - It is worthwhile to mention the temperature levels that can be expected of the hot body when exposed to a solar or RTG heat source. In space applications, the cold junction temperature of current and contemplated RTG units falls around 700°R to 800°R for radiator area minimization purposes. RTG units are currently about 5% efficient (or slightly better). An RTG unit required to supply 100 watts of electrical power would dissipate about 1900 watts as waste heat, which is nominally 2.5 horsepower. Only a very small fraction of this power would be needed in any contemplated fluidic attitude control system, since the thermodynamic cycle can be made essentially reversible except for heat and friction losses. It is expected that acceptable fluid flow rates can be obtained by temperature differences of about 100°F between the hot and cold bodies.

A solar absorber hot body can have a wide range of equilibrium temperatures. Solar orbital distance would be sufficiently gradual to permit assumption of steady-state conditions in the absorber at any trajectory point after Earth escape. The absorber temperature (T) would be that value defined by the thermal balance between the solar heat absorbed and the heat reradiated to space plus that absorbed in the flowing fluid:

$$T = \left[\frac{1}{\sigma \epsilon} \quad \frac{\alpha_s Q_s}{(AU)^2} - Q_A \right]^{1/4}$$

where

σ = Stefan-Boltzmann constant

ϵ = emissivity of the surface

α_s = solar absorptivity of the surface

Q_s = solar constant at 1.0 AU

AU = ratio of probes to earth's solar distances

Q_A = heat added to the fluid in the absorber

For a given fluidic system design using a solar energy source and passive absorber, Q_A, the heat rejected, would be a dependent variable of T; (itself a function of the solar orbital distance). Therefore, the fluidic system temperature excursion for a solar probe using a solar heat source will be much larger than for a system using RTG waste heat. In the solar probe study (Ref. 2), the first heat shield of titanium, having an α_s = 0.6 and ϵ = 0.4, acquired equilibrium temperatures of approximately 680^{o}R at 1.0 AU, 1200^{o}R at 0.3 AU, and 1800^{o}R at 0.1 AU. Assuming material temperature compatibility with high temperature in the fluidic system, a design for the 1.0 AU condition would be overdesigned at 0.1 AU because of the much higher energy absorptions. From a practical design standpoint, it may be better to go to a semipassive system which regulates, by an iris or louvers, the amount of solar heat flux falling on the absorber surface.

4. Possible Closed Loop Power System Approaches

Brayton Cycle - An example of what could be used to power a fluidic system is the gas turbine operating on the Brayton (or Joule) cycle. The principle of operation of the Brayton cycle can be explained by referring to the PV, TS and block diagrams in Fig. 15. The enclosed area within the thermodynamic processes represents the network extracted from the cycle. Since, in a fluidic attitude control system, the only net work extracted is in the form of heat due to frictional losses and that required to cause momentum change in the attitude stabilization spinning disc, the enclosed area will be rather small.

The disadvantage of the turbine-compressor fluidic power system is the devices themselves. The relatively low values of fluid flow rates and work extraction indicate extremely small size turbines and compressors. The necessarily high rotational speeds associated with miniature turbines and compressors, coupled with the long operational period, pose a reliability problem. Also, the angular momentum of such devices is, in itself, objectionable in a space vehicle. Miniature turbine-compressor components have been under development at the Martin Company for a number of years for closed cycle cooling systems for cryogenic applications to IR detectors, semiconductor circuitry, etc.

A reciprocating device could substitute for the rotational prime movers to enhance reliability. A simple pressure intensifier would serve as the expander and compressor. Valving is required in any reciprocating device to regulate the flow of the working substance in the proper sequence of cycle events. A diagram of one concept of a reciprocating fluidic power source which utilizes an area difference bellows type of intensifier, check valves, fluidic flow control valves, pressure surge chamber or plenum, solar absorber and space radiator is shown in Fig. 16. Thermodynamically, the cycle is similar to the nearly reversible Brayton cycle described previously. Instead of continuous flow, there is a rapid series of compressions, nearly constant pressure heat addition, expansion through the fluidic logic and attitude control loop, rapid switching by pressure pulse to pressurize the expander bellows and constant pressure cooling in the space radiator.

<u>Capillary or Heat Pipe Power Supply</u> - A dual phase power system which is currently being studied by JPL and others is the heat pipe or capillary system.

The principle of operation is shown in the schematic diagram below:

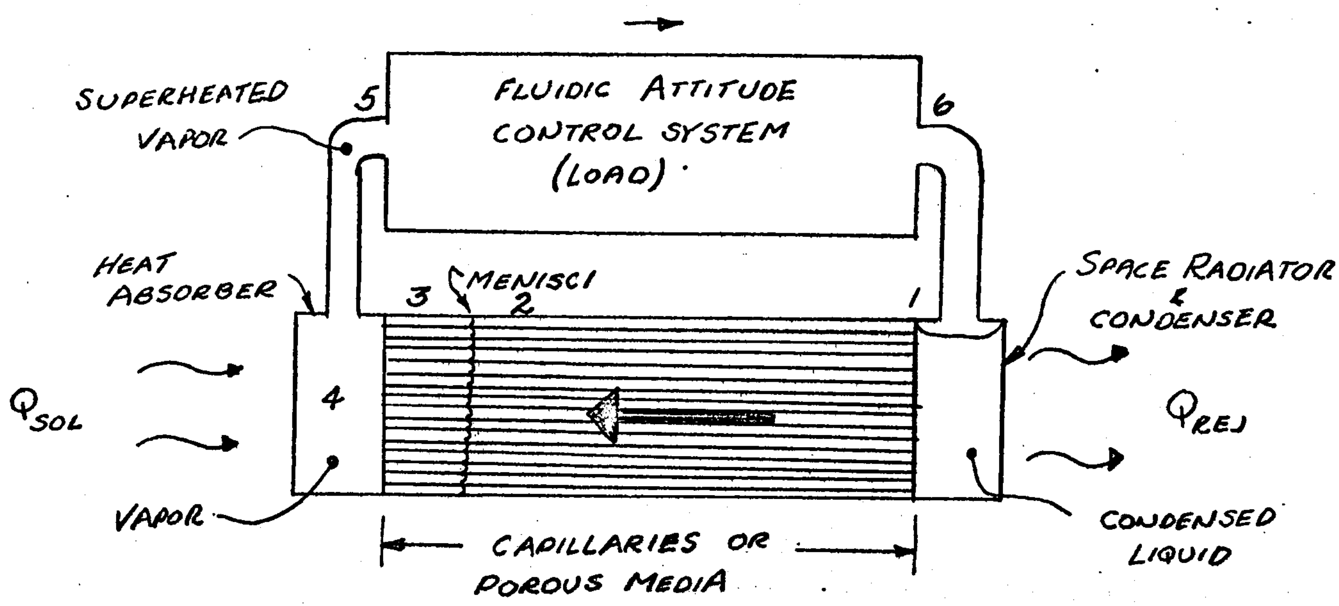

The system is charged with a fluid such as freon. The freon condenses as a liquid at the cold junction 1 and passes to the capillaries or porous media. The capillary action produces a pressure rise due to the surface tension phenomena of the liquid providing the required pumping. Near the end of the capillary section, the liquid is vaporized and superheated before it passes through the fluidic control system and returns to the condenser.

The cycle may be described on a P-T diagram as shown below.

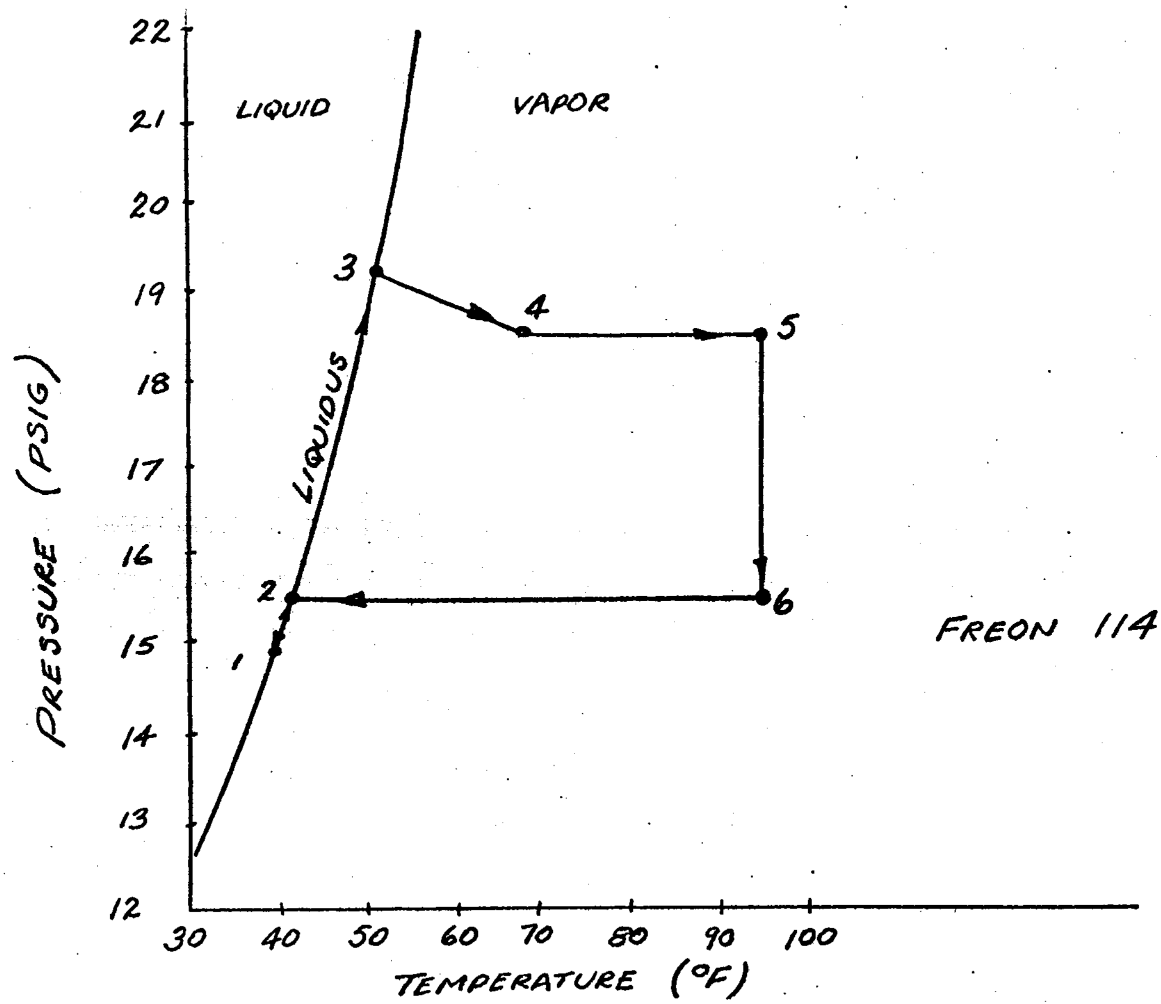

2-1 Viscous drop through liquids capillary
1-3 Capillary pressure rise
3-4 Viscous drop of vapor through rest of capillary
4-5 Superheat at heat absorber
5-6 Pressure drop through fluidic load
6-2 Condensation at space radiator

The system has no moving parts, will operate in a zero g environment and does not necessarily require large temperature differentials to operate effectively. The range of differential pressures produced by capillaries of diameter range of 10^{-4} to 10^{-3} inches is from 3 to .4 psi at temperature differentials less than $100^{\circ}F$.

JPL experiments have shown it is possible to stage the capillary sections to gain increased pressure and power, operating between the same temperature differential. (See Ref. 27.)

The required pressure differentials of fluid logic elements to perform in the attitude system are in the same pressure range as produced by capillary action (see Table V).

Using the results of JPL's analysis of this type of supply it appears that 5 stages would produce a pressure differential across the load of 2 psi while delivering a flow rate of 2.6×10^{-3} lb/sec. Each stage consists of 2×10^{6} capillaries of 6×10^{-4} inch diameter and are .3 inches long. The void area in each stage would be .72 in^{2}. Assuming a 5% void area as in a porous media, this means that each stage would occupy an area of 14 sq in. or an equivalent diameter of 4.3 inches.

This system would require development to be practical but it appears from the experience of JPL that it is feasible and would suffice as a closed loop power supply for running the fluidic logic in an attitude system using fluidically driven jet reactors where the power required is relatively low for the recirculating loop. But the system would become too large if used in addition to drive momentum wheels and boom actuators which require five times the power of the basic fluidic logic. (See section on System Power Requirements.)

The system is very attractive, of course, because of the fact it requires no moving parts and would enhance the attitude system reliability.

Adsorption Cycle Power Supply - The process of adorption of gas and vapors on a fine porous material of large topographical surface area such as silica gel, alumina, metal oxide, etc., is called physical adsorption as distinguished from chemisorption as in the case of water adsorbing ammonia.

Heat is liberated in the process of a sorption for it amounts to the restriction of the number of degrees of freedom of the movement of the gas molecules. At first when few gas molecules are at the adsorber's surface, the heat evolved per unit mass of vapor is quite high, but as the process continues it becomes essentially identical thermodynamically with condensation of the gas to its liquid phase. Mechanically the liquid is, of course, restricted in motion by the solid matrid holding it. The process is therefore controlled entirely by the topographical surface temperature of the adsorber or adsorbent. A possible arrangement of this device is shown schematically in Fig. 17. Six cells containing adsorbing material rotate about a fixed valve stem. The cell configuration is rotary-stepped by a fluidic drive-motor-and-control (not shown in schematic) when pressure in cell position 3 exceeds by a predetermined amount the pressure in cell positions 1 and 2. Note that cells at positions 1 and 2 are interconnected through the superheater and fluidic load to cells at positions 4 and 5. The operation begins as cells 1 and 2 are fully heated, causing evaporation of the liquid freon adsorbed in the cell material. The vapor passes through the superheater then through the load and at low pressure is adsorbed in the cooled cells 4 and 5. When the pressure in cells 1 or 2 drop below the pressure in cell 3 (which has been cooling) an actuator steps the cell configuration clockwise one step and the process begins again. Silica gel may be a very attractive adsorbant, but the thermal conductivity of the adsorber must be relatively good in order to rapidly adsorb and dissipate heat in the heating and cooling phases of the cycle. The choice of adsorbent probably also is influenced by the affinity of the gas for its surface as well, and is certainly influenced by the mass of adsorbent and size of cell required to handle the flow and energy rates. A considerable amount of research and some experiment is indicated to arrive at an optimal choice of materials. The adsorber cells should present a reasonable surface for radiation, be relatively thin so that thermal path lengths are small, and confine the adsorbent so that it does not "pack down". The technique of chem-milling and resistance welding stainless steel used for micrometeoroid impact sensing suggests itself as a convenient structure.

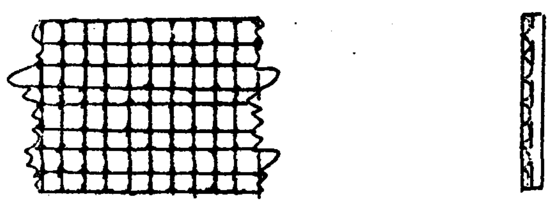

It may be that iron oxide (rouge) would be a fair adsorber and have relatively high thermal conductivity as compared to silica gel. The area of cell vs. volume of adsorber will greatly influence the weight of the device as well as the cycle time.

The superheater is required to add sufficient energy to the gas to avoid condensation in the fluid processes of the load, and to improve cycle efficiency. Aside from the fact that the heat input to it must be controlled approximately constant at various distances from the Sun, no unusual problems are involved in its design. The superheater shutter could easily be controlled by a thermostatic bimetal arrangement sensing gas output temperature.

Osmotic Power Supply - A second two-phase power supply concept, which develops much larger pressures in a single stage of liquid pumping utilizes the principle of osmosis. Here a solvent is in contact with a strong solution of a solute through a "semipermeable membrane" through which the solvent may pass but not vice versa. The result is that the thermal energy of the solvent's molecules allows them to pass through the membrane (but the solutes molecules cannot diffuse in the opposite direction) until a pressure in the solution is reached which is equivalent to that which would exist if the solute existed as a gas at the temperature in question and occupied a volume equivalent to that of the solution. It is evident that quite large pressures (many atmospheres) are available by this means, and pumping rates would be limited only by the membrane area and diffusion-rate of solvent away from the membrane.

It is not known what combinations of solvent (working fluid), solute and membranes could ultimately prove most useful. A large amount of both theoretical and experimental work would need to be done to establish this. It is known, however, that water (superheated steam) as the solvent (working fluid) and sucrose as the solute with a membrane of copper ferrocyamide precipitated in the pores of a ceramic matrix ("Pfeffer Pot") can be highly satisfactory in many respects. Perhaps the greatest disadvantage would be the large heat of vaporization of water, but this need only be supplied once. Also, some scheme for controlling free surfaces in the boiler would need to be evolved as well as a scheme for preventing any transport of the solute out of the boiler by entrainment with steam.

This set of problems leaves many questions unanswered at this time, but it seems fairly certain that an entirely satisfactory set of materials and equipment can be developed for the intended purpose.

5. Choice of Power System Approaches

It appears from this study that the power system which is most applicable to the solar probe problem is a combination of open and closed loop systems.

A capillary-type closed-loop system having no moving parts is the preferred choice for delivering power to the fluid logic which requires a low level, continuous power source.

The larger power requirements of the jet reactors and boom actuators are best met with a gas-storage, open-loop system. This system is lighter and smaller in size than the closed-loop counterpart but does require moving-part type valves to completely shut-off gas when not demanded. This tends to lower its reliability, but this type system has been successfully demonstrated many times in space probe applications.

C. ELECTRIC-TO-FLUID CONVERSION

Any practical fluidic attitude control system for a space vehicle will necessarily need a capability to "communicate" with the electrical system of the spacecraft and, through it, with a command and control station on Earth. This will require a two-way link between the electric and the fluidic system, since the fluidic system has to be able to accept electrical commands for its action and also must be able to report its actions and operating condition back to the electrical system. The following survey discusses a number of typical electric-to-fluidic and fluidic-to-electric transducers which can be used for solving this double interface problem.

1. Electric-to-Fluidic Transducers

A very simple and rugged E-F purely flueric transducer, suitable for both analog and low bit-rate digital signals, is a small length of thin-walled metal capillary whose wall is electrically heated. The heat transfer to the gas flow through the capillary changes the viscosity of the gas and also its volume. The end result is an increase of the pressure drop in the gas flow across the capillary. This pressure change, the output of the transducer, can be used, after suitable fluidic amplification, for introducing an electrical signal into a fluidic system. The attractive features of this transducer are its great simplicity and reliability. Disadvantages are a relatively substantial electrical power consumption and a relatively slow response, due to the thermal inertia of the capillary wall.

We have accomplished some work on this concept in our laboratory, and believe that it will be suitable for the present application, where there is no real need for fast response (of the order of milliseconds) but there is a strong incentive to aim for simplicity and reliability.

In its physical principle, this transducer is closely related to the fluidic bolometer mentioned as a promising sensor for solar radiation. The remarks in the section on radiation sensors concerning the possibilities of decereasing the responde time by a suitable selection of the wall material (low specific heat per unit volume and adequate mechanical strength) and by providing forced cooling immediately after input of a digital electrical signal will also apply to the present case. Contrary to the bolometer, however, silver will not be a suitable material for the capillary (since its electrical resistance is too low), and use will be made of alloys such as constantan which have a higher specific electrical resistance.

An E-F transducer for digital signals of moderately fast bit-rates (up to around 50/sec) can be obtained by placing an electric sound generator (e.g., a piezoelectric element with a frequency typically between 2000 and 6000 cps) in the vicinity of the exit nozzle of the laminar jet of a turbulence amplifier. It takes very little sound energy to make the jet turbulent, resulting in a loss of pressure in the collector of the amplifier.

The attractive features of this transducer are its fast response (essentially only the travel time of the jet between the nozzle and the collector, which may only be a few milliseconds in a smaller-than-conventional configuration) and its very low consumption of electric power. Its disadvantage is mainly the restriction to digital inputs; this will not be serious in the present case. The practicality of this concept for an E-F transducer was recently demonstrated with a working model in the Orlando Division of the Martin Company, and we believe that this concept will also be adaptable for the purposes of the proposed study.

HDL has been working on Coanda type elements triggered by acoustic signals. In addition, the Martin Company has done limited laboratory experiments with low-powered momentum exchange fluidic elements wherein they have been triggered acoustically. The element supply pressures in these experiments were considerably lower than 1" of H_2O.

Another E-F transducer which could probably be used in the present application is a simple electromechanical device which produces a displacement which can then be used to modify flow conditions in a fluidic system. For instance, a relay-type electromagnetic positioner can push a knife-edge into a free jet and cause it to be deflected, or it can even turn a valve off and on. (There are a number of ways in which this general idea can be put to use in the present application.)

In principle, this approach to the E-F interface problem is quite straightforward. However, since it operates with moving parts, there may be some question about long-term reliability of operation in the elevated temperature environment of a solar probe. This will have to be investigated very carefully before recommending a practical use.

A number of other concepts for solving the E-F interface problem have been proposed and, to some extent, investigated in the literature. For instance, it has been suggested to trigger a fluidic flip-flop by the pressure wave from an electric spark discharge, although work conducted at MIT indicates that this approach will probably not prove fruitful. It has also been suggested to condition the flow by an ionization of the gas so that it can be influenced by electrical fields (e.g., with the concept of the "ion-drag pump"). In this respect, we have some doubts about any approaches which will require use of high voltages and high power, such as the spark discharge method and probably also the conditioning of the working fluid by ionization; the mounting insulation difficulties at elevated temperatures are more than likely to have adverse effects on the reliability of the transducer.

2. Fluidic-to-Electric Transducers

The preceding examples of E-F transducers can, at least as concepts although not as actual devices, be converted into F-E transducers for the inverse problem of a fluidic-to-electric interface. Therefore, we will consider these three concepts in the same order.

The best-known way to obtain an electrical signal from a flow signal is probably the hot-wire anemometer, where the cooling of an electrically heated resistance wire by heat transfer to a gas (or even liquid) flow changes its electrical resistance, and where the corresponding change of the voltage between the ends of the wire or of the current through it under a constant voltage constitutes the electrical output signal from the transducer. It is well-known that this transducer, with a sufficiently fine wire, can be both very sensitive and fast responding. In fact, hot wire techniques are being used extensively in experimental research on turbulence frequency spectra in both subsonic and supersonic boundary layers and it is no great problem to obtain time resolutions of the order of 10^{-3} sec or less. Thus, the hot wire technique appears quite attractive as a solution to the F-E interface problem.

Customarily, a hot wire probe is oriented in a direction normal to the flow and has a very small diameter (e.g., platinum a few millimeters long and a few microns thick). The wire is electrically heated by direct current to a temperature of around 700° to 800°K. Such a rather delicate probe, while best in the aerodynamic laboratory, may be too fragile for reliable use in a space probe. A thicker wire, of a more rugged design, will be correspondingly slower but could still have an acceptable response time.

In a similar manner, the above-described concept of the E-F transducer in the form of a heated capillary can be almost directly used for the inverse task of an F-E transducer. In fact, this simple and potentially rugged element will not only change its flow resistance by electric heating, but its wall will also change its electrical resistance, if the voltage is kept constant and it is being cooled internally by varying flow rates. The only practical difference between the designs of this element for the two applications is that one would probably want to make the capillary wall in the first case from a material which changes its electrical resistance relatively little with temperature (constantan or other resistance wire alloys), whereas one would like a strong change of the electrical resistance in an F-E transducer and would therefore prefer a pure metal (platinum, nickel, soft iron, etc.) for this application.

The inversion of the acoustic E-F transducer concept of a turbulence amplifier connected with an electrical sound generator to a corresponding F-E transducer concept leads quite naturally to consideration of a combination of a fluidic sound generator (fluid oscillator, reed oscillator, etc.) with a microphone as an electrical pickup. This combination can be used for both analog and digital fluidic signals. In certain cases, it can also be used to extract more than one type of information from the fluidic system. If, for instance, a conventional fluid oscillator is formed using a flip-flop with a feedback path, the oscillator frequency will change with the gas temperature in the feedback loop, because the sound velocity is a function of the gas temperature. Simultaneously, the microphone can pick up the intensity of the sound, which is a function of the supply pressure of the element. This may be an analog signal for a certain physical quantity which is being used in the control system or it may be an indication that the control system is or is not operating with adequate power from its power supply. In addition, the fluidic system may operate in a digital mode (with a bit rate substantially lower than the carrier frequency of the oscillator), and the microphone will extract this digital information from the fluidic system and communicate it to the electrical system and, if necessary, to Earth.

Another typical example of an E-F transducer concept (that of an electromagnetic positioner in combination with a fluidic displacement sensor) also has an obvious counterpart in the line of possible F-E transducers. This is simply a pressure-sensitive electric switch, and various designs for such a device are commerically available. While most of these will probably not be directly usable in a solar probe, we believe that there is a strong possibility of obtaining practical solutions for the F-E interface problem of a solar probe attitude control system on the basis of this concept, at least for digital signals--and probably even for analog signals.

Of the E-F transducers considered, the heated capillary and the acoustically triggered fluidic element are the most rugged and simple. Neither contain moving parts.

The heated capillary could be used where high speed response is of no consequence. The acoustic transducer is better suited to applications requiring higher response.

For F-E transduction, the hot-wire anemometer and acoustic detector (microphone) fluid oscillator approaches appear the most promising.

D. MOMENTUM EXCHANGE ACTUATION

The base line Solar Probe Attitude Control System as described in Chapter III, Section E of this report requires a number of fluidic torque producing devices. The flywheel used in pitch, yaw and roll for cancellation of transient disturbances, the reaction jets used in roll for desaturation of the roll flywheel, and the boom actuators used for providing solar pressure vehicle trim and wheel damping in pitch and yaw represent three types of required fluidic actuation devices. During Phase I of the current study the state-of-the-art survey has established that considerable work is being accomplished on fluidic servo actuators; some work has been accomplished on fluidic-mechanical servo valves capable of operating the roll reaction jets; and there has been no reported work on the fluidic momentum exchange device equivalent to the electronic flywheel control. Work on associated momentum storage devices such as air bearing gyros has been reported.

1. Servo Actuators

The requirements of the servo actuators for solar pressure control panel extension and retraction can easily be met with current state-of-the-art in pneumatic mechanical servo systems. The torque requirements, frequency response and temperature environmental requirements are all exceeded by a surface controller developed by the Bendix Corporation under Air Force contract (Ref. 15). The reported characteristics of this servo are:

Operating Pressure	180 ± 18 psig
Maximum Flow Required	0.085 lb/sec
Horsepower	1.5
No Load Speed	100 rpm
Stall Torque	500 in. lb.
Frequency Response	10 cps

This unit consists of a two-stage servo valve operating a reversible expansion type vane motor. Transmission used in the surface servo was a 75:1 ratio harmonic drive. This particular servo has been operated successfully at 1400°F.

The Bendix Corporation has also developed a Pneumatic Nutator Actuator Motor under contract to NASA Lewis Research Center (Ref. 28). This unit is a low speed high torque motor consisting of a pair of bevel gears with an unequal number of teeth. Rotational output is obtained from nutational motion of the input gear driven by pressurized bellows located around its periphery. The flow control to the bellows is controlled by fluidic logic circuits. Under another contract to NASA Lewis Research Center, Bendix has conducted design and analysis of an all pneumatic servo actuator which would have performance equal to an electro-pneumatic unit (Ref. 29). The servo consists of a piston-cylinder with rack and pinion that produces 180 degrees rotary output. The system was designed to have 6 cps bandwidth, 0.2 degrees resolution and 300 in/lb stall torque.

Several non-industrial organizations are engaged in the development of fluidic actuators. MIT has reported on the development of a pneumatic stepping motor in Ref. 30. The actuator is based on the wobble plate or nutating gear principle powered by bellows or pistons. Reference 31 reports on work accomplished at MIT on a pulse-length modulated pneumatic servo with flapper disk switching. The floating flapper disk is an on-off switching valve that controls fluid flow to a ram, rotary motor or other actuator. This unit consists of a thin circular disk and a series of concentric sealing lands. The advantages of the use of the pulse modulation and flapper disk are given as power efficiency, low quiescent power consumption, high reliability and low cost. Switching times using this valve are quoted as 1 ms. Pennsylvania State University Systems and Controls Laboratory has had a hydraulic stepping motor under design for some time (Refs. 32 and 33).

After a review of the literature and based on our discussions with NASA Lewis Research Center personnel, we have concluded that fluidic servo actuators can be developed for the Solar Probe requirements. While a specific unit which meets these requirements is not developed, the basic technology required has been, and is being explored for actuators with more stringent specifications than those required for the Solar Probe Spacecraft.

2. Fluidic Valves for Reaction Jets

Diaphragm actuated switches and valves are under investigation by, and in some cases commercially available from several industrial organizations. The Martin Company has built several prototype reaction jet pneumatically driven valves. The Howie Corporation has investigated several different designs and has commercially available hardware.

The floating flapper disk valve under development by MIT and described in the previous section of this report would also be used for controlling reaction jets. The switching time for the valve is quoted as 1 millisecond, which is better than that normally available in electromechanical servo valves.

No moving part fluidic valves, which could provide economical reaction jet switching, have not been found in our survey. Work has been reported on such valves in a specific application of thrust vector control by secondary injection. In this case the valve is flowing continuously and is diverted to provide boundary layer control of the thrusting engine when a control moment is required. In the presence of zero control requirement the valve flows in the same direction as the thrusting engine. Using this approach only a minimum loss in efficiency occurs for a no moving parts fluidic valve. With the exception of this type of application no moving part fluidic valves which are used for intermittent control requirements are far too inefficient for long term applications. A valve based on the vortex amplifier approach would be the most promising of the flueric systems because of its potential low quiescent flow.

Other fluidic valves have been proposed which use pills or balls to move in slots and provide a reasonable seal under the condition of zero·flow requirement.

If one accepts the need for a good seal for long term application of a control valve under an intermittent requirement and thereby accepts a moving part device, then there appears to be no new technology development required to meet the valve requirements on the Solar Probe Spacecraft Fluidic Attitude Control System.

3. Momentum Exchange Devices

There are four basic design requirements which must be met if a fluidic flywheel is to be developed for spacecraft attitude control. These are: an efficient gas bearing capable of supporting the required mass, a closed cycle power supply system capable of recovering the flow used in the bearing support and wheel torquing, a wheel torquing system which can provide linear acceleration of the wheel, and a fluidic pick-off capable of providing information on wheel velocity. Although we found no information on fluidic momentum exchange devices in our state-of-the-art survey, the four design requirements have been explored in detail by Martin and others for similar applications.

Based on the required angular momentum storage of the momentum exchange device the use of a rotating gas column does not appear feasible. Liquid flywheels have been under investigation for several years, the most commonly used liquid being Mercury. The most promising approach at this time for the Solar Probe application appears to be a solid wheel suspended on gas bearings.

Gas bearing designs have been developed for gyros and for other inertial measuring devices such as the Martin developed distance meter, velocimeter and the stable platform. The need for gas bearings in these applications has resulted in extensive gas bearing studies by Martin. This work initiated in 1960 and continuing through the present has included design, construction, laboratory testing, and computer programming for theoretical investigations (Ref. 34). As a result of these investigations it was found that standard air bearings had serious limitations. Porous air bearings, on the other hand, have been shown to provide about 200 times more support per unit flow than standard bearings. Design curves have been developed which provides rapid high accuracy gas-bearing performance prediction. This background of data on gas bearings substantiates our conclusion that an efficient gas bearing design can be developed which would provide the support the required momentum wheel.

The acceleration of an air bearing suspended mass by jet torquing has been demonstrated at Martin. The solid wheels may be torqued by jets impinging directly on the rim of the wheel, on vanes or impulse beckets. Relatively large torques may be generated in a small size.

The use of jet pipe and boundary layer pick-offs for determining the velocity of a rotating mass has also been demonstrated by Martin in a distance meter and velocimeter development program. The pressure pick-off velocity could be used for providing stabilization in the flywheel acceleration control loop and by use of a threshold could be used for initiating the solar pressure booms or reaction jets for flywheel desaturation.

A conceptual design of a momentum wheel incorporating some of the design features which have been developed for other sensor applications, is shown in Fig. 18. We feel this concept is technically sound and that previous experience provides the necessary background for implementing this concept in a workable design.

E. FLUID LOGIC DEVICES

Most of the information obtained in our fluidic state-of-the-art survey pertained to basic fluidic amplifier element development status and performance characteristics. Virtually every industrial or non-profit organization involved in fluidics have developed their unique bi-stable or analog amplifier. Unfortunately, there is very little uniformity of technique in testing to establish the performance characteristics or in stating the performance characteristics in the literature. As an example, some bi-stable coanda type elements measure performance with one control port open to atmosphere while others quote operational characteristics determined with one control port sealed. Pressure and flow gains are often quoted at different operating points. In general the testing techniques used in evaluating the element is not presented with the quoted performance.

Basic fluid amplification devices can be divided into two classes: 1) discrete, and 2) proportional. Both types are required to implement a Solar Probe Spacecraft Attitude Control System. A volume of data is available in the open literature describing the effect of geometrical changes in the various devices on their performance characteristics. Static performance data for these devices is more prevalent than dynamic and is usually presented in the form shown in Fig. 19a through 19e. Sometimes normalized control pressure is cross ploted on Fig. 19a and the fan-out, or number of additional similar elements which can be driven is determined by area calculations. Curves such as Fig. 19e gives a great deal of information and are again an attempt to provide the circuit designer with normalized information. Output and input impedance of the element is often taken as the slope of the curves shown in Figs. 19a and 19c, respectively.

Considerable attention is also given, in the literature, to the evaluation of power consumption in the elements. W. E. Gray , in Ref. 28 has given a very useful relationship of power as a function of pressure drop across the supply nozzle. Figure 19f is a reproduction of this relationship from Ref. 28. It should be noted that the power decreases as a log function with decreasing supply pressure and only directly with the nozzle area. Therefore, it could be desirable to use elements which are capable of working at lower supply pressures even at a penalty of increasing the nozzle area. Using this relationship, several Martin developed bi-stable elements are compared with a Corning element in the table below.

Martin Elements	Orifice Size-Mils^2	Min. Ps	Minimum Power-Milli-watts
FLE-101	50 x 5 = 250	0.75	50
Momentum Exchange Type a	50 x 10 = 500	0.10	9
Momentum Exchange Type b	15 x 5 = 75	0.25	7.5
Corning Element			
#190738	40 x 10 = 400	1.0	120

The momentum exchange type of bi-stable device appears to offer significant power savings when compared to the Coanda type of elements.

The bi-stable amplifier can be used in the implementation of a great many functions. NOR, OR and AND gates can be developed to perform logic functions necessary for programming or performing digital computations.

Pulse converters, oscillators, counters and analog to digital conversion can be implemented using modified bi-stable amplifiers in series or parallel arrangements. Proportional amplifiers can be used in many circuit applications ranging from filtering to drive amplifiers. Proportional devices are more sensitive to temperature change, noise and downstream conditions.

The frequency response of fluidic elements is limited theoretically by the speed of sound and practically by the manufacturing technique and in some elements by the change in flow characteristics as size is decreased. This last factor is of importance since theoretically the speed of response can approach the speed of electronic elements if the paths through which the fluidic signals must pass could approach zero length. Using photo etching techniques and careful process control, elements having packaging densities of several thousand logic devices per cubic inch can be visualized even with required interconnects. For this case signal transmission paths could be approximately 100 mils which results in a theoretical upper limit of 100 kilocycles using conventional fluids at standard temperatures. For the Solar Probe Attitude Control System frequency response of the elements is not critical and present packaging densities are sufficient to provide competitive weight and volume comparison with equivalent electronic circuits.

Types of amplifiers and their most significant characteristic and application is shown in Table VI.

After a review of the state-of-the-art in fluidic amplification devices, the available data on circuit application of these devices in computer, missile control, aircraft control and of the functional circuit

TABLE VI

General Fluid Amplifier Types

Type	Characteristic	Applications	Pioneer Developer
Wall attachment	Versatility, resonable performance	Switch, oscillation, logic	HDL
Turbulence	Digital operation	Logic, sensing, counting	R. Auger
Axis symmetric focus jet	Fast, large power flow required	Power switching	Sperry-Utah
Jet deflection	High speed	Analog amplifier	HDL
Vortex device	Best suited for flow control (nearly stops flow)	Amplifiers, restrictors, diodes	Bendix
Double leg elbow	High flow amplification	Low frequency amplifier	Giannini Controls Co.
Impact modulator	High pressure gain	Operational support	Johnson Service Corp.
Moving part devices	Reduces power consumption	Logic, operational support	Kearfott, Martin, IBM, et al

requirements of the Solar Probe Attitude Control System, it is concluded that the present developmental status of these elements is sufficient to implement the control intelligence functions necessary. The system operation in the anticipated environment particularly the temperature range of interest is still subject to question, since there is virtually no elevated temperature operating data on many of these devices in the available literature. This subject is treated in greater detail in Chapter V.

A Solar Probe Attitude Control System could be implemented with a combination of all type devices shown in Table VI. However, after consideration of their characteristics, development status and available data; two types have been selected for further study in Phase II. The wall attachment devices (or possibly the Martin momentum exchange type) will be used to implement the majority of the circuit functions required for the Solar Probe Attitude Control System. The Vortex amplifier, because of its low quiescent (zero signal) power consumption operating capability, will be considered for the primary jet operation used for torquing the momentum wheels which are present in the proposed control system.

V. FLUIDIC PERFORMANCE TRENDS UNDER SOLAR ENVIRONMENT

A. INTRODUCTION

High temperature and slowly changing but wide variation in temperature are the most significant environmental factors of the Solar Probe mission. While some specialized high temperature (1500°F) fluidic systems have been tested, data on the effect of temperature variation even on basic elements is not available. System temperature test data would be more meaningful but less general in application than basic element test. Because of the complete lack of existing data in this critical environmental area, the Martin Company during Phase I decided to conduct some basic temperature test of elements in order to establish the gross effect of temperature on their basic operating characteristics. Conducting tests of this nature are costly and time consuming; therefore, under the confines of the present study only a limited test could be conducted. Three bi-stable fluidic elements were subjected to the temperature test; Corning element #190738, Martin element FLE-101, and a Martin momentum exchange element.

While it is difficult to draw general conclusions from the limited amount of temperature test data obtained and the lack of theoretical explanation of the elements changing characteristics with temperature, the following comments are offered:

- Temperature variation causes changes in the single element operating characteristics.
- Unvented elements will be more seriously effected than vented ones.

- While R_e number effects are suspected as the cause of operating characteristic variations no definite trend as a function of R_e number change with temperature could be established.
- The variation of operating characteristics with temperature seem to be grossly effected by the output load, particularly in the momentum exchange device.
- For a selected output load the Martin momentum exchange element had much better operating characteristics than the Corning or Martin FLE-101 devices.
- This area requires further investigation to establish the requirement for temperature compensation in a Solar Probe Fluidic Attitude Control System.
- Total system effects are still unknown and system temperature tests are strongly recommended.

B. TEMPERATURE TESTING INSTALLATION

The temperature test set-up is shown in Fig. 20. The installation consisted of: a temperature controlled oven capable of greater than 2000°F; a pre-heater with separate temperature control capable of continuously preheating the control and supply flow to the oven temperature; pressure and flow measurement instrumentation for supply, control and output ports of the element; thermocouple installations for measuring the supply and control flow temperatures, balanced bridge potentiometer and thermocouple selector for reading the various thermocouples; external control valves for setting output load, supply pressure and control pressure.

In order to expedite the conduction of the test all pressure and flow measurements were made external to the oven. The supply and control pressure and flow measurements are made just prior to the flow entering the pre-heater. The output pressure and flow measurements are made approximately 2 ft downstream from the oven exits at which point the flow is essentially at room temperature. The variable orifice which is used to establish the loading on the element for the test series is located at this point also. It would have been more desirable to have had the output load control orifice within the temperature environment of the oven but time and cost of the testing program did not permit. For any future testing this change is recommended.

The basic test procedure used after calibration of the test set-up was to establish the element characteristics at room temperature for a given supply pressure and output load. The supply pressure was then held constant as temperature was increased and the loading orifice remained at its initial setting. The switching pressure was established at various temperatures and the supply flow, output flow, output pressure, and control flow data taken. For the FLE-101 two different elements were used and tests were conducted to establish the variability between elements as well as to establish the repeatability of the test data. For the momentum exchange element several tests were conducted in which output load was varied to establish pressure-flow relationships as a function of temperature.

C. TEST RESULTS

The three basic elements tested were all bi-stable types and two were of the vented design. Measurements of the operating characteristics of these elements at room temperature were made prior to the temperature test. The elements tested were: Corning element #190738 (vented design); Martin element FLE-101 (closed design); Martin momentum exchange element (vented design).

1. Corning Element

The Corning element was adapted to the test set-up using a stainless steel tubing interconnection to the standard Corning brass fittings sealed with epoxy. It was anticipated and later demonstrated by test that the Corning epoxy, which provided with their standard brass fitting seals, would fail at a lower temperature than that used by Martin. All tests, both at elevated and room temperatures, were made using the modified element and the test set-up shown in Fig. 20.

Corning performance data, at room temperature, were reproduced using a supply pressure of 1.5 psig. The Corning switching data was obtained with the inactive control port dead-ended and with specified and equal loading on the output ports. A check of the operation of the device as a function of supply pressure or R_e number was made and the results are shown in Fig. 21. The element ceased to function as a flip-flop at supply pressures less than about 1.0 psig corresponding to a R_e number of about 800. Additional room temperature tests were conducted to establish the pressure-flow relationships of the element under various loads. A normalized plot of output pressure as a function of output flow for two different supply pressures is shown in Fig. 22. The output impedance of the element obtained is 1.33 psig/in^3/sec at 1.5 psig supply pressure and 1.21 psig/in^3/sec at 3.0 psig supply pressure. The input impedance was determined as 0.47 psig/in^3/sec at the operating point of 1.5 psig supply.

Temperature tests were conducted on the Corning element using a constant supply pressure of 1.5 psig and with the inactive control port dead-ended. The element and its supply and control flow was heated to various temperatures and its switching and output characteristics measured. Fig. 23 presents a plot of the control pressure, output pressure, control flow, supply flow, and output flow as a function of temperature. At about 350°F the element ceased to function as a flip-flop. Examination of the element indicated the epoxy developed blow holes at this point in the output interconnections forcing testing to be limited to this temperature. The characteristics of the element in this limited temperature range were relatively constant. Pressure gain changed from about 1.95 to 1.75 while switching pressure held constant at 3.0 in. of water.

2. Martin FLE-101

The FLE-101 is an unvented fluid amplifier and the input, control and output ports are normal to the channel flow. Room temperature tests of this element were conducted to establish input and output impedance. The output pressure-flow characteristics for two different supply pressures are shown in Fig. 24. The output impedance determined from this data is 0.194 $\frac{\text{psig}}{\text{in}^3/\text{sec}}$ at 5 psig supply pressure and 2.64 $\frac{\text{psig}}{\text{in}^3/\text{sec}}$ at 10 psig supply pressure. This data was obtained by monitoring constant supply pressure and varying the load. Output impedance is often obtained by maintaining a constant load and varying the supply pressure. Output pressure-flow relationships for the FLE-101 under this condition is shown in Fig. 25. The output impedance determined in this manner is 0.094 $\frac{\text{psig}}{\text{in}^3/\text{sec}}$ at 4 psig supply and 0.112 $\frac{\text{psig}}{\text{in}^3/\text{sec}}$ at 3.0 psig supply. Control and supply input impedance were determined in a similar manner and are shown in the table below.

FLE-101 Impedances

Supply Pressure	4 psi	5 psi
Supply Input Impedance	1.48 psig/in^3/sec	1.56 psig/in^3/sec
Control Input Impedance	0.88	0.137
Output-Input Impedance	0.094	0.112

Temperature tests were conducted on the FLE-101 using a constant supply pressure of 5 psig and with the inactive control port open to atmosphere. The element and its supply and control flow was heated to various temperatures and its switching and output characteristics measured. Figure 26 presents the experimental results obtained for switching pressure, control flow, pressure gain and flow recovery. Performance characteristics fluctuate significantly with temperature particularly above 400°F. Flow recovery is near 75 percent at room temperature and decreases with increasing temperature. The temperature tests were repeated with the same element to establish the repeatability of the data and were conducted using a second element to establish variability from element to element. Figure 26 shows a band about the switching pressure data indicating the uncertainty in these results.

An analytical procedure for predicting or explaining the effects of temperature on this element has not been developed. There are three possible explanations of the differences obtained with the Corning element and the Martin FLE-101. First, the Corning element is vented and previous experience has shown the vented elements in general are less sensitive to variations in all parameters than the unvented elements. Second, the temperature tests on the Corning element were limited to 350°F, and the FLE-101 held relatively constant through this range but showed marked changes at higher temperatures. Third, the FLE-101 may exhibit more sensitivity to temperature due to the configuration of input and output ports which are normal to the channel flow.

3. Martin Momentum Exchange Element

The momentum exchange element, developed by Martin, does not make use of the wall-attachment, (Coanda) effect in its operation; consequently, it was hoped that the lowering of power nozzle R_e number, inherent with elevated temperature operation, would not seriously affect this type of element. This element was tested at room temperature to establish output pressure-flow relationships, at constant supply pressure, under varying load. These tests were repeated at elevated temperatures to establish the effect of varying temperature on the output characteristics. Figures 27 and 28 show the output pressure-output flow characteristics, and the output pressure-pressure gain characteristics, respectively. The switching pressure as a function of output load (or output pressure) at room temperature is shown in Fig. 29 . While conducting the temperature tests on this element it was observed that the performance characteristics (pressure gain, switching pressure) as a function of temperature were sensitive to the initial load. In general, the changing temperature appeared to follow the pattern of a changing load insofar as switching pressure and pressure gains are concerned. Figure 30 is a plot of the switching pressure required for various output pressures as the temperature is increased. Two plots are shown for two different initial load conditions. Comparison of Figs. 29 and 30 indicates that increasing temperature effects pressure gain and switching pressure is much the same way that decreasing load effects these parameters at room temperature. The curve has been changed in shape and position but the trend is apparent. The numbers along each plot on Fig. 30 refers to the sequence of increasing temperature for the two different tests conducted. In most cases, the curve follows the sequence of increase and is probably within the accuracy of reading the data in those few cases which are exceptions. This data again illustrates the importance of having the loading orifice within the temperature environment of the element. Had the test been conducted in this manner the observed variation in operating characteristics would have been decreased. In order to compare the characteristics of this element, under changing temperature, with the Corning and FLE-101 elements, Fig. 31 presents the switching pressure, pressure gain, flow recovery and control flow as a function of temperature. The variation in control flow and flow recovery is limited, while the pressure gain and switching pressure vary rather drastically with temperature.

D. SUMMARY

The temperature tests conducted during Phase I of the subject contract although limited in nature have established that while elements can work well at elevated temperature their characteristics can vary drastically over a wide change in temperature. The most significant result of these tests is the identification of a possible problem area and the conclusion that careful testing of both fluidic elements and systems under temperature variation must be conducted.

VI. MATERIALS CONSIDERATIONS

A. MATERIALS OF CONSTRUCTION FOR FLUIDIC CONTROL SYSTEM COMPONENTS

The environment exposes the materials of the exposed portion of the system to a variety of electromagnetic radiation as well as particles ranging from micrometeoroids through electrons and protons at high energies to cosmic radiation. Little need be said of the effects of particles other than that micrometeoroid damage (which has low estimated probability of occurrence) would probably be crippling, and that so long as metals form the basis of the exposed components, proton and electron effects should be essentially negligible, as should the effects of the neutron flux. The principal environmental hazard is, of course, the thermal flux. This requires that temperatures from 1400°R to 1600°R in fully exposed components must be easily tolerable, and partly shielded or cooled elements should tolerate temperatures of 700 to 1000°R. Because eventualities could produce rapid changes of temperature across several hundred degrees, materials must not respond adversely to thermal shocks of that order.

There seems to be no argument which can hold non-metals as more useful than refractory metals for this purpose. We have satisfactorily tested "Photoceram" fluidic elements at elevated temperatures. Fundamentally, the material is satisfactory for such use, but connections pose severe problems. The material is strong, but brittle and undoubtedly somewhat notch sensitive. Special nickel iron alloys, such as those produced by Carpenter Steel ("Glass Sealing 42" and "Vacumet Micoseal") can furnish thermal expansion coefficients which can match the expansion of borosilicate glasses quite well up to about

600° to 800°F. Beyond this range, risk of fracture exists because of the increased expansion rate of the metals and the brittleness of the Photoceram. Metals, conversely, can be welded or diffusion-bonded into essentially integral systems exhibiting a high degree of ruggedness, toughness, and ductility in the range of temperatures required. A variety of stainless steels and Inconels have been used by us for diffusion-bonded and brazed fluidic assemblies. Tests at high temperature have revealed that as long as chemical effects between the working fluid and metals can be prevented, entirely satisfactory performance can be expected.

Depending upon the nature of the working fluid, some testing for chemical effects at high temperature is in order, but the problem should be a minor one. Specifically, oxygen or other highly active working fluids must be avoided to prevent scaling and deformation or fouling of the fluidic system.

B. MATERIALS FOR SPECIAL COMPONENTS

1. Lenses for Optics

The effects of heat and electromagnetic and nuclear particle radiation on normal optical materials can be expected to produce damage and severe darkening of ordinary glasses. This should be avoidable by the use of fused quartz optics. The optical quality required in terms of correction of alterations is not a problem, for precision imaging is not required.

2. Materials for Porous Bearings

In the event inertia wheels are utilized, they should be supported in gas bearings. We have found that the porous source-surface type is far superior for such applications, because the flow rates (and hence damping) are lower by an order of magnitude than for other types.

Bearings thus far have been constructed of porous metals. For a variety of reasons having to do with control of surface porosity, porous metals are difficult to work satisfactorily for this purpose. Either porous graphite or alumina ceramic (Al Si Mag) appear to be superior for this purpose, and experimental work is under way at Martin to evolve an optimal material and process specification for such bearings.

The temperature effect on neither of these materials can be expected to pose a problem, but neutron or proton fluxes may produce some effects and an experimental check is in order prior to definitive design of a system.

C. WORKING MEDIA (FLUIDS)

1. Single Phase (Gaseous) Systems

In the event that a single phase system is adopted (disadvantages are mechanical pump and valve actions), gas is pumped at low temperature to a higher pressure, heated, circulated through the fluidic load and returned at low pressure to the cool side for recirculation. A simple, chemically inactive gas is desirable which has density and viscosity such as to give proper Reynolds numbers across the range of values in the system requirements. It appears likely that nitrogen will be utilized for attitude control or desaturation of inertia wheels. This would be an entirely satisfactory choice for the fluidic control system working medium, and a common source (with redundancy) for makeup of accidental loss of gas in either system is an obvious advantage.

2. Two-Phase (Liquid/Vapor) Systems

There are schemes for systems which employ non-mechanical pumping of a relatively small volume of liquid from a lower pressure and temperature to the highest system pressure, vaporizing and superheating the vapor by introduction of solar heat (to avoid condensation in the functioning systems), condensing to liquid at the lower pressure and temperature, and again pumping the liquid to the higher pressure. The first such scheme is to utilize the pressure available at the liquid-gas menisci in a finely divided porous matrix (capillary approach). This pressure is produced by the surface tension in the menisci which develop when the medium wets the matrix and is heated therein to produce the vapor. In order for such a scheme to develop useable pressures, several such meniscus cells must be used in series with interstage condensation. This system has the disadvantage that the heat of vaporization must be supplied and rejected several times, but has the advantage of great mechanical simplicity. Free surfaces may possibly be avoided entirely by keeping all liquid entirely within the porous matrices.

For this scheme, Freon 114 appears to have a nearly ideal range of temperatures and pressures, and subject to material compatibility tests is to be highly recommended. It should be borne in mind that superheating of the vapor after the last cell is important to avoid condensation.

D. MATERIALS CHOICE SUMMARY

From the work conducted in Phase I on materials, it appears that quite satisfactory materials and fabrication techniques are available for the construction of a fluidic Solar Probe Attitude Control System that does not require thermal or radiation shielding or environment control. Fluidic elements, sensors, interconnections and plumbing would be made from diffusion bonded refractory metals such as the inconel and stainless groups, with a minimum of mechanical joints; the working fluid would depend on the power system approach chosen; but N_2 appears a workable choice for single phase systems, and Freon 114 or water appear workable for two-phase systems. Other specialty materials are available for sensor optics (fuzed quartz) or E-F conversion devices, (Piezo-electric crystals).

VII. RELIABILITY PREDICTION

Predicting the reliability of fluidic and flueric components at this point in the development of the fluidic field is of necessity qualitative and subjective at best. The application of these predictions to a total system estimate further opens the question as to the validity of the reliability evaluation. The lack of available experimental and application data on failure rates of fluidic components and the desire to obtain a feel for the anticipated reliability, however, requires one to make an attempt to perform the reliability analysis.

In this section an approach will be outlined, based primarily on the techniques presented in Ref. 37 , which will be applied to the Fluidic Attitude Control System during Phase II of the subject contract. While this approach leaves much to be desired it represents the only technique which has been published in the open literature on performing reliability comparisons between the implementation of a system with fluidics and electronics. The key factor in the comparison is the effect on failure rate of the two approaches subject to environments of vibration, temperature, and radiation.

Mr. Fox, in Ref. 37, has used basic failure rate data for electronic components from Earles and Eddins "Reliability Engineering Data Series - Failure Rates". The increase in failure rates caused by operating in other than laboratory environments is also based on the data compiled by Earles and Eddins. The following failure rates were used as optimistic values for electronic components:

	Failure Rates (per 10^6 hrs)
Transistors, silicon	0.01
Diodes	0.001
Resistors	0.005
Connections, per pin or per joint	0.0001

The increase in failure rates of these components when subjected to types of environment characteristic of a solar probe is shown in the table below.

	Factor
Temperature 150°C	10
50°C	5
Missile Vibration	900
Solar Flare (Cislunar Space)	10
Cislunar Space	2

For the solar probe vehicle the radiation intensity levels are anticipated to be an order of magnitude more severe than that for Cislunar space and the respective factors shown above could be expected to increase accordingly. Comparison of the failure rate data given by Mr. Fox with that given in MIC-HDBK-217A, 1 December 1965, supports that the data is optimistic. With the advent of microelectronics and integrated circuits (even though failure rate data is scarce) the basic component failure rates for transistors and diodes need no longer be used. Connections are greatly reduced and the subsequent reliability of a system improved. This updating of the reliability estimates of Ref. 37 will be conducted in Phase II when evaluating the relative reliability of the electronic and fluidic attitude control system.

While the sources of electronic component failure rate data are sufficient for the purposes of the subject contract the fluidic component failure rate data is non-existent. The approach of Ref. 37 given below will be used in the study.

The modes of failure which were assumed are:

1) The failure of connectors between sheets of components. Failure rate data is available for such connectors.
2) If the fluid contains particles which are large enough to obstruct a duct, orifice, or component, failure will probably occur.
3) If the material in which the components are formed separates, cracks, ruptures, peels, fragments, creeps, flows, disintegrates, warps, or twists beyond certain limits, then failure will occur.

After making a number of specially stated assumptions related to the fabrication and testing techniques, Fox proceeds to derive failure rates for the three failure modes. This is accomplished by using experience in other devices which have similar failure modes. For failure mode 3, experience with leakage failures of valves and various type seals is used as a guide to the failure rate to be used for fluidic components. Also previous experience has shown that the failure rate for fracturing or cracking is less than that for sealing and a factor of 10 was used for modifying the sealing failure rate data. The total failure rate used for improperly ducting the fluid (or failure mode 3) was 0.11 per 10^6 hrs. Similar arguments (based on contamination failure experience in carburetors and fuel injectors) were used, assuming state-of-the-art filtering, to establish the failure rate of 1.0 per 10^6 hrs for failure mode 2. Fortunately, failure rate data is given by Earles and Eddins for failure of pneumatic joints as 0.02 per 10^6 hrs (failure mode 1). Using this failure rate data, reliability estimates can be made for various fluidic components which can then be compared to the equivalent electronic circuit. Due to the nature of fluidics and its capability to exist in high temperature, radiation and vibration environment, the correction factors to be applied to the failure rate data for this environment are far less than those of electronic components. Table II indicates these factors given by Fox for typical pure fluid devices.

Table II

Temperature	Factor
+ 150°C	2
- 50°C	2
+ 250°C	3
Missile Vibration	10
Solar Flare (Cislunar Space)	2
Cislunar Space	1

In Ref. 37 the described approach was applied to a fire control computer implemented using both electronic components and using pure fluid components. The electronic version showed 20 to 1 less failures than the fluidic counterpart in a laboratory environment, primarily because it was assumed that a far greater number of fluidic elements would be required to implement the computer than electronic elements. (Note: This may be a poor assumption, since each fluid element is the equivalent of approximately 10 electronic components.) After application of the factors predicted for the effect of environment the picture changed significantly with fluidics showing a resultant ratio of failures to electronics of 1:5. Most significant gains were achieved in the areas of vibration and temperature.

While the above approach is subject to verification through a practical demonstration, it does offer a means of arriving at the relative comparison of reliability. The fluidic components necessary to implement a Solar Probe Spacecraft Attitude Control System will be defined during Phase II and estimates made, using the above described approach.

VIII. CONCLUSIONS

The conclusions reached during Phase I of the subject Spacecraft Fluidic Attitude Control System study are as follows:

General Feasibility - The application of Fluidic/Flueric technology to the Solar Probe (and other spacecraft) Attitude Control requirement is basically both feasible and promising. It appears that significant improvement in reliability and operating life can be made over conventional electronic/electromechanical approaches which should be of significant value for long duration space missions. It is significant that no fundamental "holes" were found in the technology that would preclude its application to the subject problem.

Technology Development Status - The current state of development of the Fluidic/Flueric Arts, as applied to the subject system, has several areas of weakness. These include in order of severity:

Closed Cycle (recirculating) Power Supply Systems
Solar Sensors
Inertial Sensors (angular displacement)
E-F, F-E Signal Conversion Devices

On the other hand, the availability of fluidic/flueric logic elements, angular rate sensors and momentum exchange devices is quite satisfactory.

There is an urgent requirement for much more extensive performance testing of all fluidic devices and complete systems at elevated ambient temperatures, since limited element tests conducted on this program indicate that significant performance variations can and do occur.

There is a need to establish basic reliability performance indices (failure rates, environmental degradation factors) for fluidic systems in order to effectively analyze their overall performance potential, in competition with existing electronic, electromechanical and mechanical system approaches.

The availability of suitable materials for constructing fluidic systems in spacecraft does not appear to be a major problem.

IX. REFERENCES

1. "Solar Probe Study Final Report," Vols. I through V, Martin-Baltimore ER 13110, August 1963.

2. Martin, J. P., "Scientific Objectives and Instrumentation for a Solar Probe," Paper VII-1, delivered at the Symposium on Unmanned Exploration of the Solar System, the American Astronautical Society, Denver, Colorado, 8 to 10 February 1965.

3. de Moraes, C. A., and Gage, D. D., "Mission Objectives and Design Considerations for a Scientific Solar Probe," presented at the AIAA Unmanned Spacecraft Meeting, Los Angeles, California, March 1 to 3, 1965.

4. Mathews, H. F., and Erickson, M. D., "The NASA Advanced Pioneer Mission," presented at the National, SAE-ASME Meeting of April 1964.

5. Leach, E., Fairand, B., and Bettenhausen, L., "The Space Radiation Environment and Its Interactions with Matter," REIC Report No. 37, Battelle Memorial Institute, Columbus, Ohio, January 1965.

6. "Solar Electromagnetic Radiation," NASA SP-8005, NASA Space Vehicle Design Criteria, June 1965.

7. Christensen, D., "The Space Environment," NASA CR-294, Aerojet General Corporation, Azusa, California, September 1965.

8. Thekaekara, M., "Survey of the Literature on the Solar Constant and the Spectral Distribution of Solar Radiant Flux," NASA SP-74, GSFC, 1965.

9. Saylor, W. P., et al, "Space Radiation Guide," ANRL-TDR-62-86, American Machine and Foundry Company, R&D Division, Alexandria, Virginia, August 1962.

10. Van Vliet, R. M., "Passive Temperature Control in the Space Environment," Macmillan, 1965.

11. "Space Radiation Damage to Electronic Components and Materials." REIC Report No. 32, Battelle Memorial Institute, Columbus, Ohio, September 1963.

13. Garner, H. D., and Fuller, H. V., "A Survey of Potential Applications of Fluidics to Spacecraft Attitude Control," presented at the SAE Committee A-6 Symposium on Fluidics, San Francisco, California, 21 October 1966.

14. Straut, H. J., "Hybrid Fluidic Sensors and Their Application to Fluidic Missile Control Systems," presented at the SAE Committee A-6 Symposium on Fluidics, San Francisco, California, 21 October 1966.

REFERENCES (cont'd)

15. WADC TR-60-449, Part I, Vols. I and II, September 1960, Part III and Part IV, February 1964, "Research and Development of a Hot Gas Flight Stabilization System."

16. Hellbaum, R. F., "Flow Studies in a Vortex Rate Sensor," HDL Proceedings of the Fluid Amplifier Symposium, Vol. II, 1965.

17. Hall, J. F., Lindahl, J. H., and Ostlund, O. E., "A Fluidic Flight Control System," presented at the SAE Committee A-6 Symposium on Fluidics, San Francisco, California, 21 October 1966.

18. Reilly, R. J., "Description of Performance of Three Experimental Fluid Flight Control Systems," MIT Summer Course on Fluid Power Control, July 1966.

19. Lock, W. P., and Gee, S. W., "Design, Development, and Flight Testing of a Pure Fluid Autopilot," presented at the SAE Committee A-6 Symposium on Fluidics, San Francisco, California, 21 October 1966.

20. Sarpkaza, T., "Theoretical and Experimental Investigation of the Vortex-Sink Angular Rate Sensor," HDL Proceedings of the Fluid Amplifier Symposium, Vol. II, 1965.

21. X-66-15187, "Pure Fluid Missile Guidance System," Bowles Engineering Corporation, October 1965.

22. Mott, J. R., and Diamond, H. B., "New Fluid Rotor Inertial Sensor," Proceedings of the First Symposium on Unconventional Inertial Sensors, December 1962.

23. Rae, R. S., and Ostrander, M. C., "An Angular Rate Indicator Based on Direct Measurement of Angular Velocities," Proceedings of the First Symposium on Unconventional Inertial Sensors, December 1962.

24. Rae, R. S., and Ostrander, M. C., "Status Report on the Research Work Carried Out by the Development Laboratories, Inc., for the Bureau of Naval Weapons on Angular Rate and Position Indicator Based on Fluid Vortices," Proceedings of the 1964 Symposium on Unconventional Inertial Sensors.

25. Clayton, B. J., and Posingies, "The Development and Flight Test of a Pure Fluid Missile Control System."

26. ER 13963, Martin-Baltimore, August 1965, "Phase I - Sun Referenced Fluidic Attitude Control System."

REFERENCES (cont'd)

27. JPL Research Summary 36-1, 36-2, 36-4, 36-7, 36-9 and 36-10, "Capillary Pumping for Closed-Cycle Gas Systems," Guidance and Controls Research, Guidance and Controls Division.

28. Howland, G. R., "Pneumatic Nutator Actuator Motor (Final Report)," NASA-CR-54788, October 1965.

29. NASA-CR-54758, "Replacement of Electronics with Fluid Interaction Devices," August 1965.

30. Blaiklock, P., and Sidell, R., "Development of a Pneumatic Stepping Motor System," MIT Summer Session, July 1966.

31. Goldstein, S. R., and Richardson, H. H., "A Differential Pulse-Length Modulated Pneumatic Servo Utilizing Floating Flapper Disk Switching Valves," MIT Summer Course on Fluid Power Control, July 1965.

32. Ruppert, D. L., "Simulated Response of a Hydraulic Stepping Motor," A Thesis in Mechanical Engineering, Pennsylvania State University, Graduate School Department of Mechanical Engineering, June 1965.

33. Schiller, R. W., "Hydraulic Stepping Motor," Systems and Controls Laboratory, the Pennsylvania State University, College of Engineering, Research Report No. 3, April 1966.

34. ER 14386, Martin-Baltimore, October 1966, "Final Engineering Report Gas Bearing Design Study."

35. Gray, W. E., and Stern, H., "Fluid Amplifier Capabilities and Application," Control Engineering.

36. Fox, H. L., "A Comparison of the Reliability of Electronic Components and Pure Fluid Amplifiers," HDL Proceedings of the Fluid Amplification Symposium, Vol. I, October 1962.

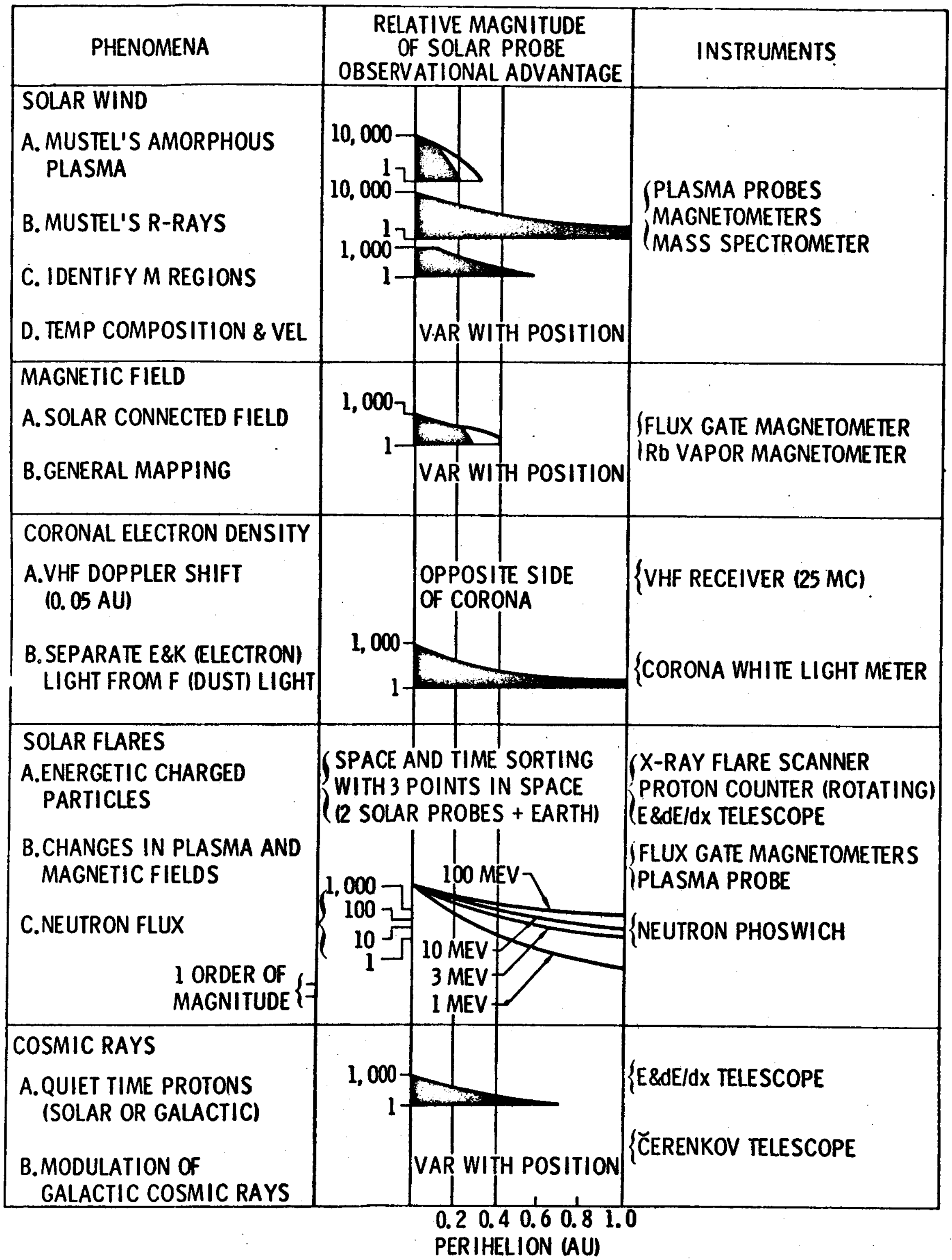

Fig. 1. Solar Probe Experiment Phenomena

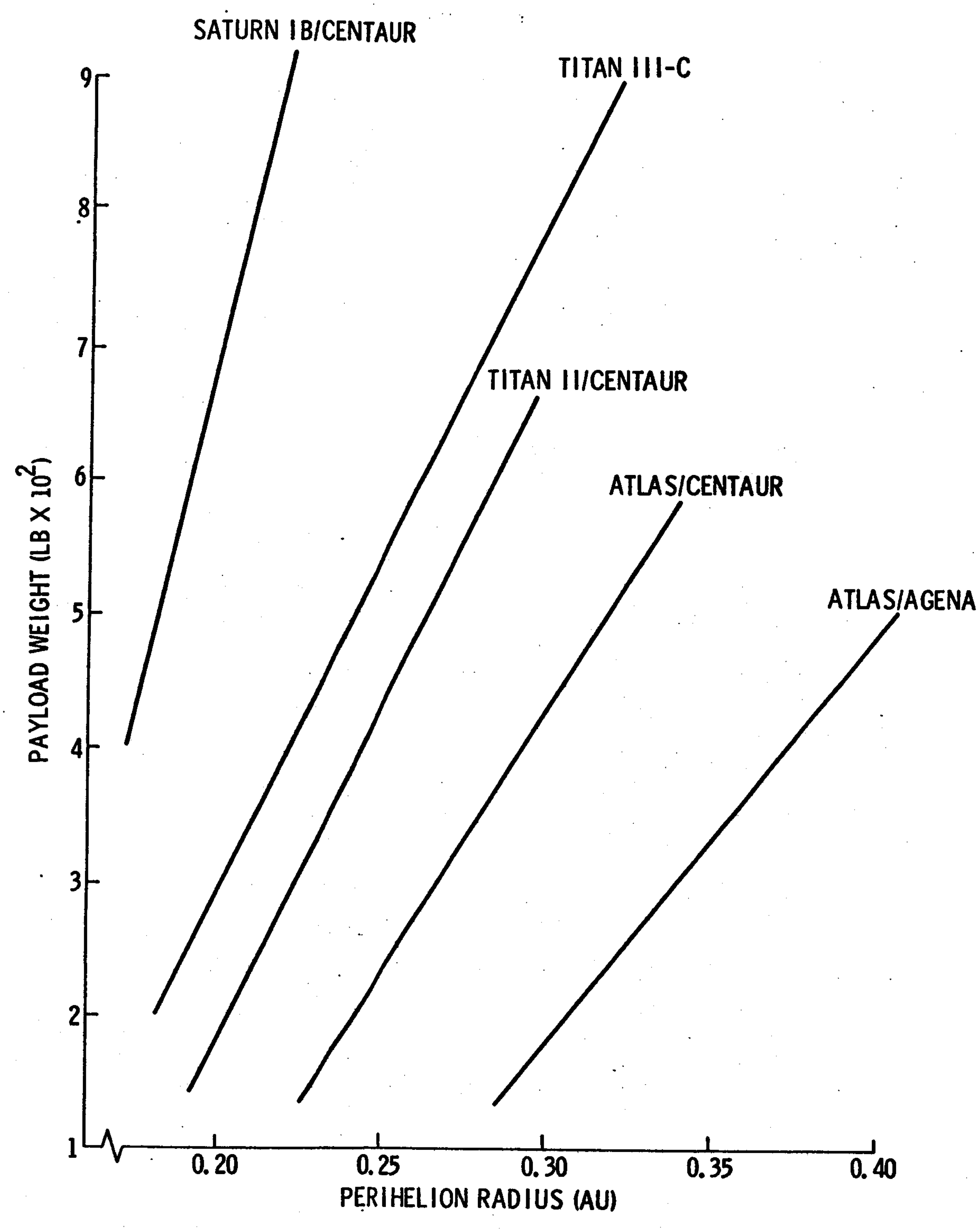

Fig. 2. Solar Probe Trajectory Versus Booster Capability

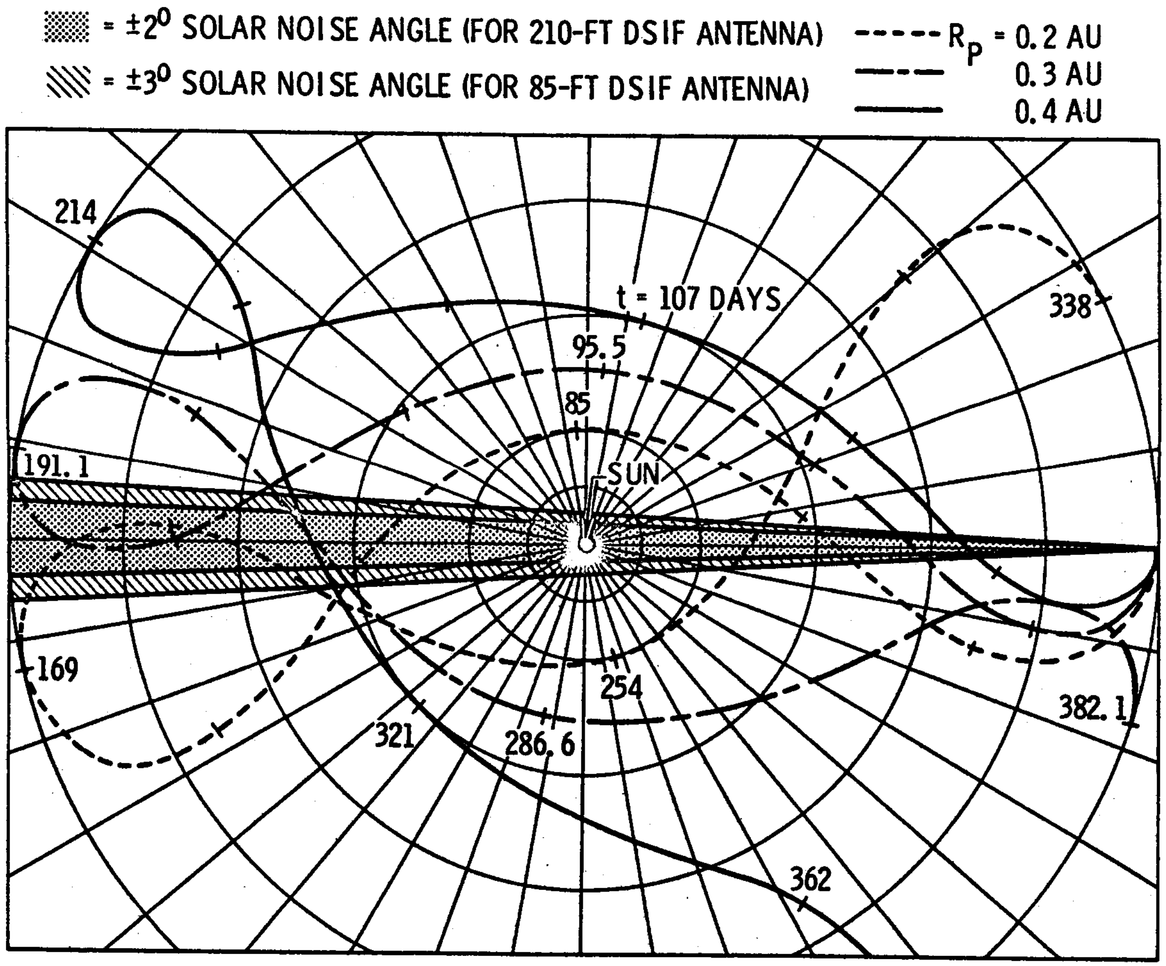

Fig. 3. Communication Limits Versus Perihelion

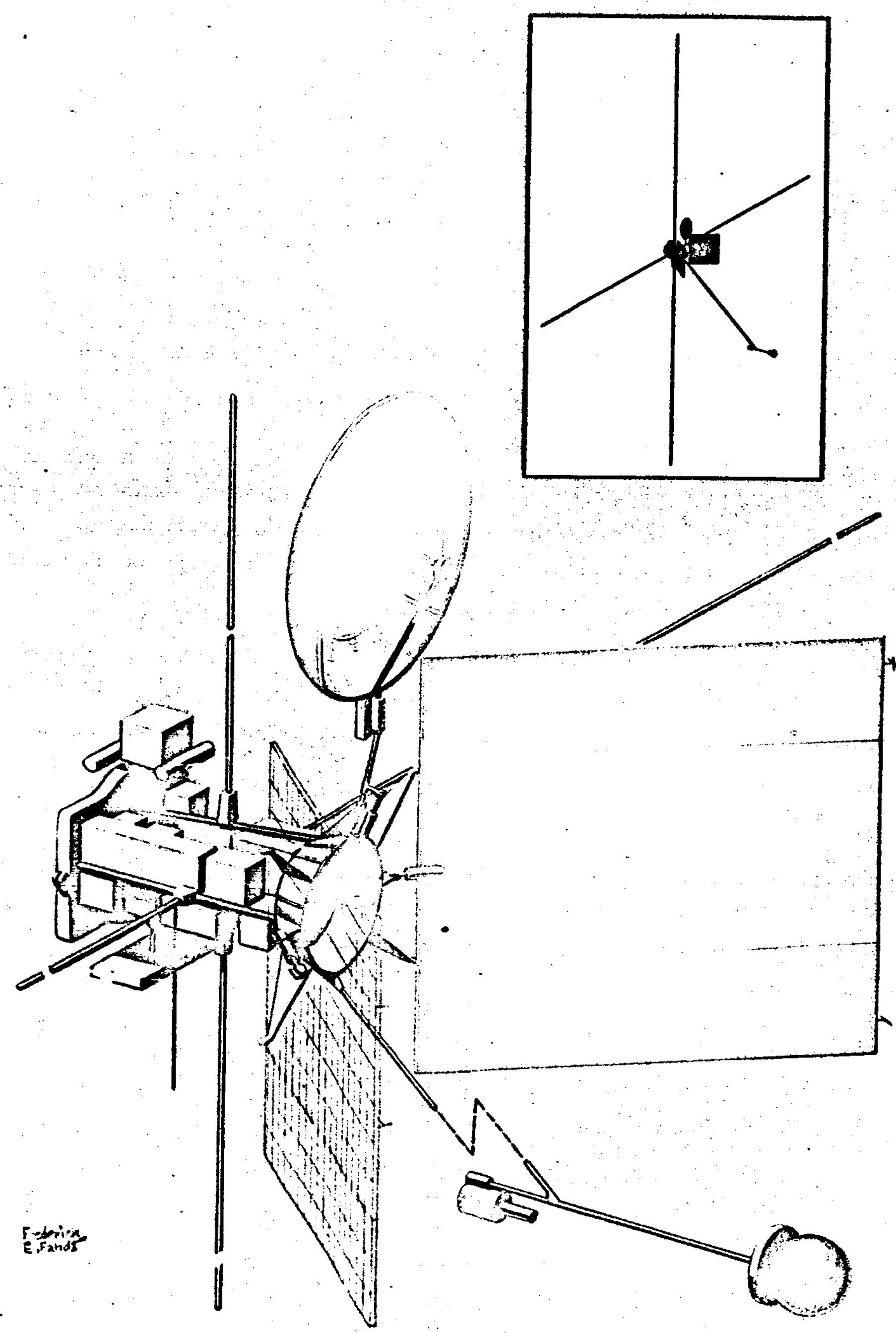

Fig. 4. Solar Probe Vehicle Configuration

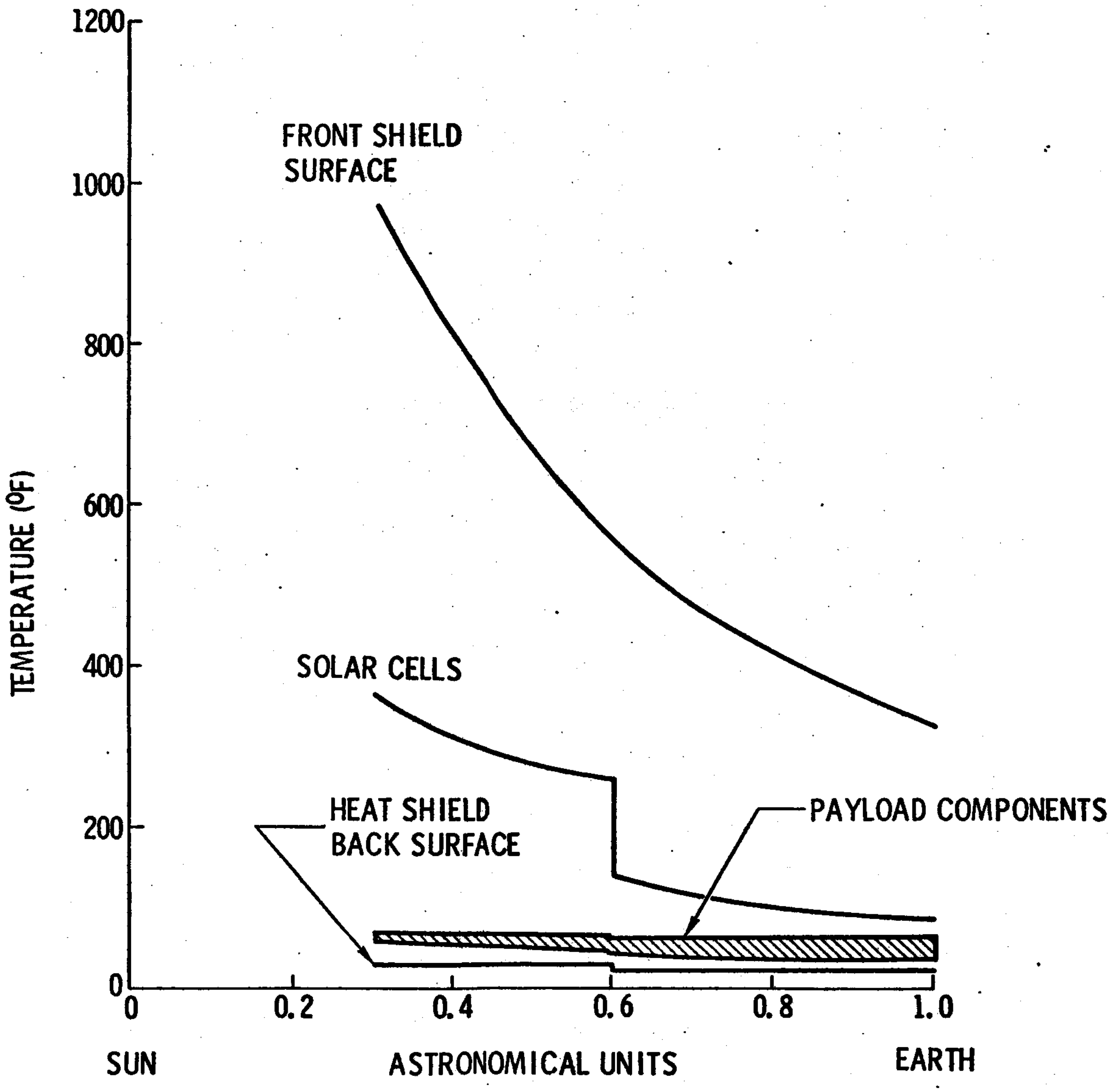

Fig. 5. Spacecraft Thermal Profile

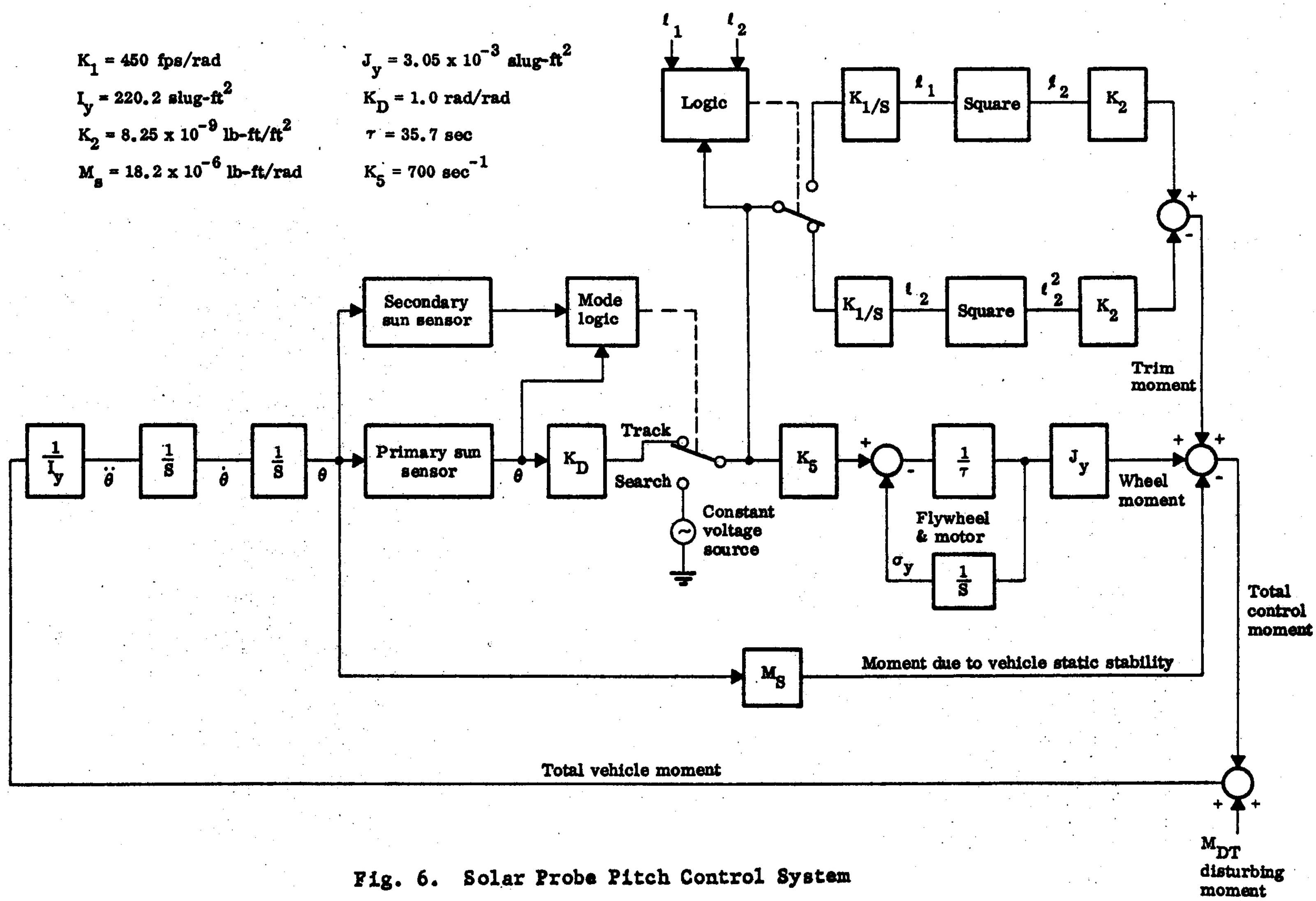

Fig. 6. Solar Probe Pitch Control System

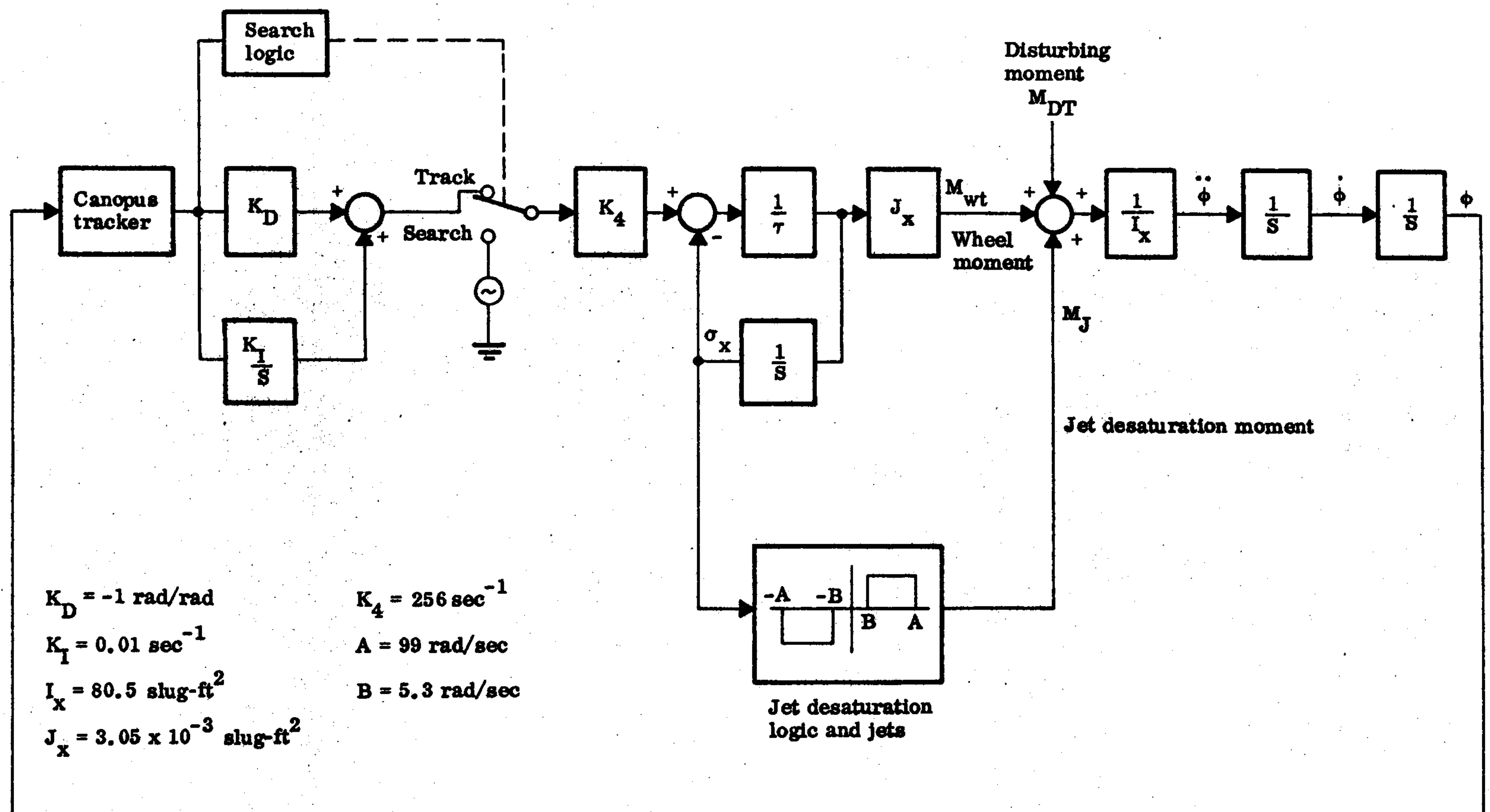

Fig. 7. Solar Probe Roll Control System

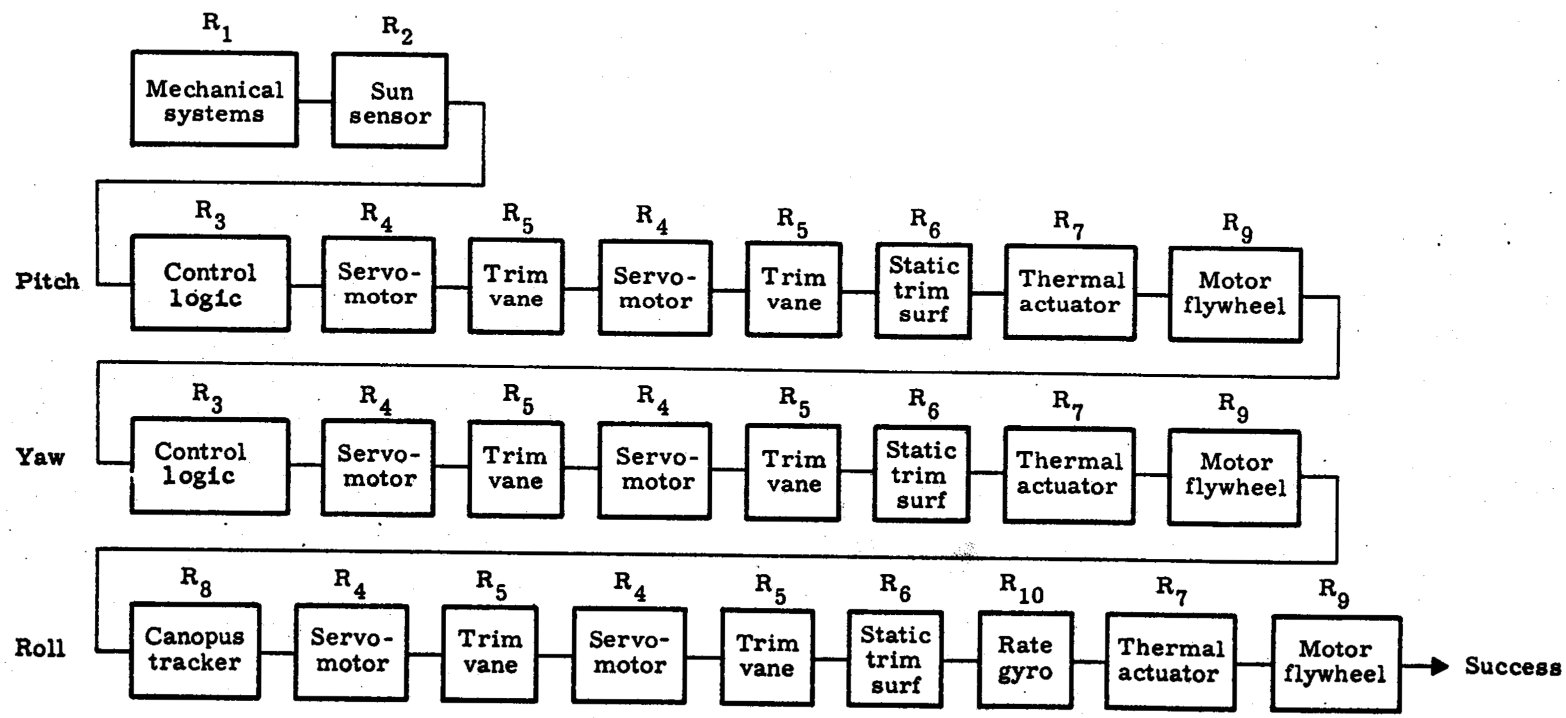

$$R_S = R_1 \times R_2 \times R_3 \times R_4 \times R_5 \times R_4 \times R_5 \times R_6 \times R_7 \times R_9 \times R_3 \times R_4 \times R_5 \times R_4 \times R_5 \times R_6 \times R_7$$
$$\times R_9 \times R_8 \times R_4 \times R_5 \times R_4 \times R_5 \times R_6 \times R_{10} \times R_7 \times R_9$$

Fig. 8. Preliminary Logic Diagram Attitude Control and Stabilization--Flywheel Control

Fig. 9. Experimental Fluidic Bolometer

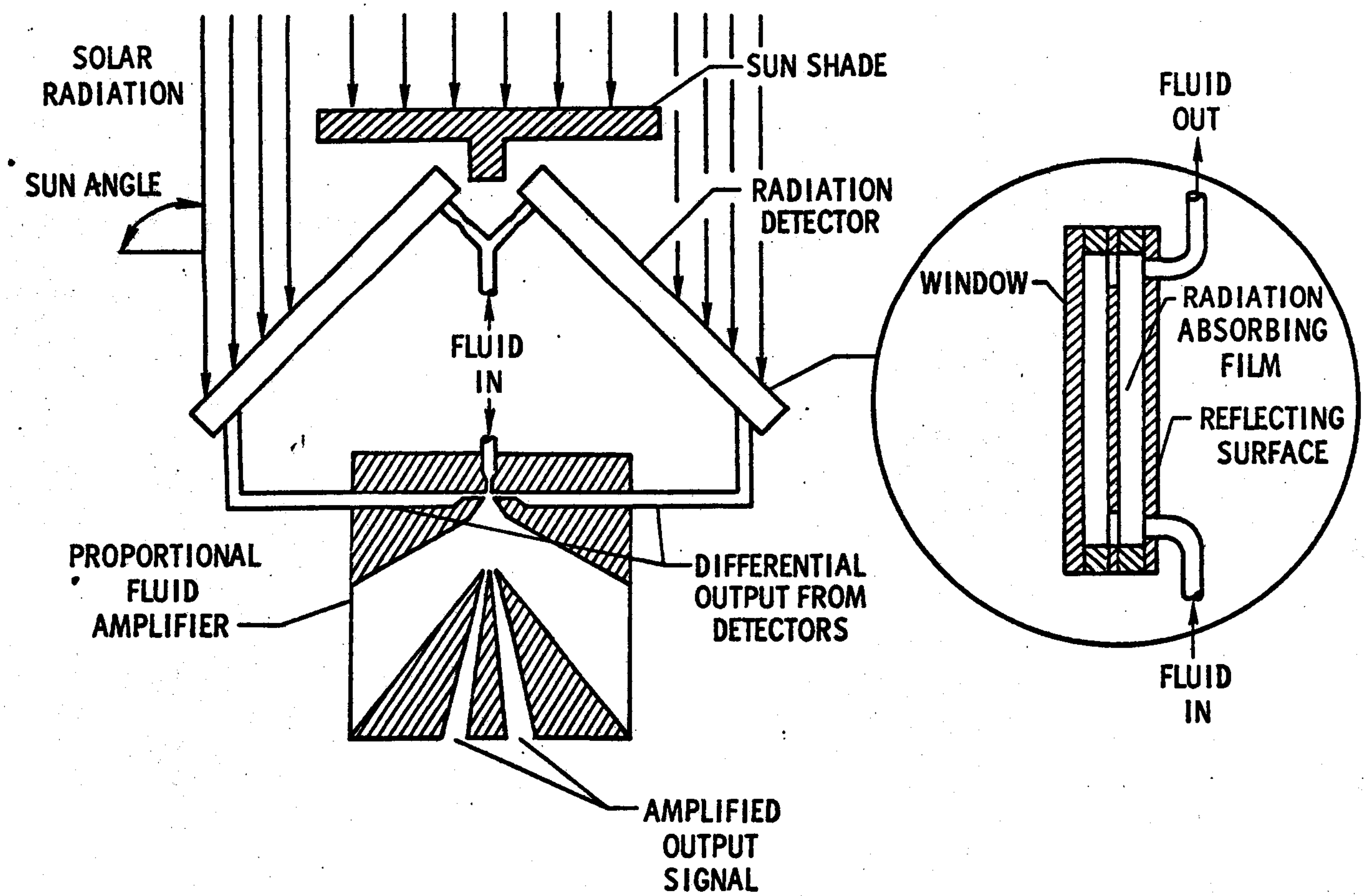

Fig. 10. Pure fluid sun sensor.

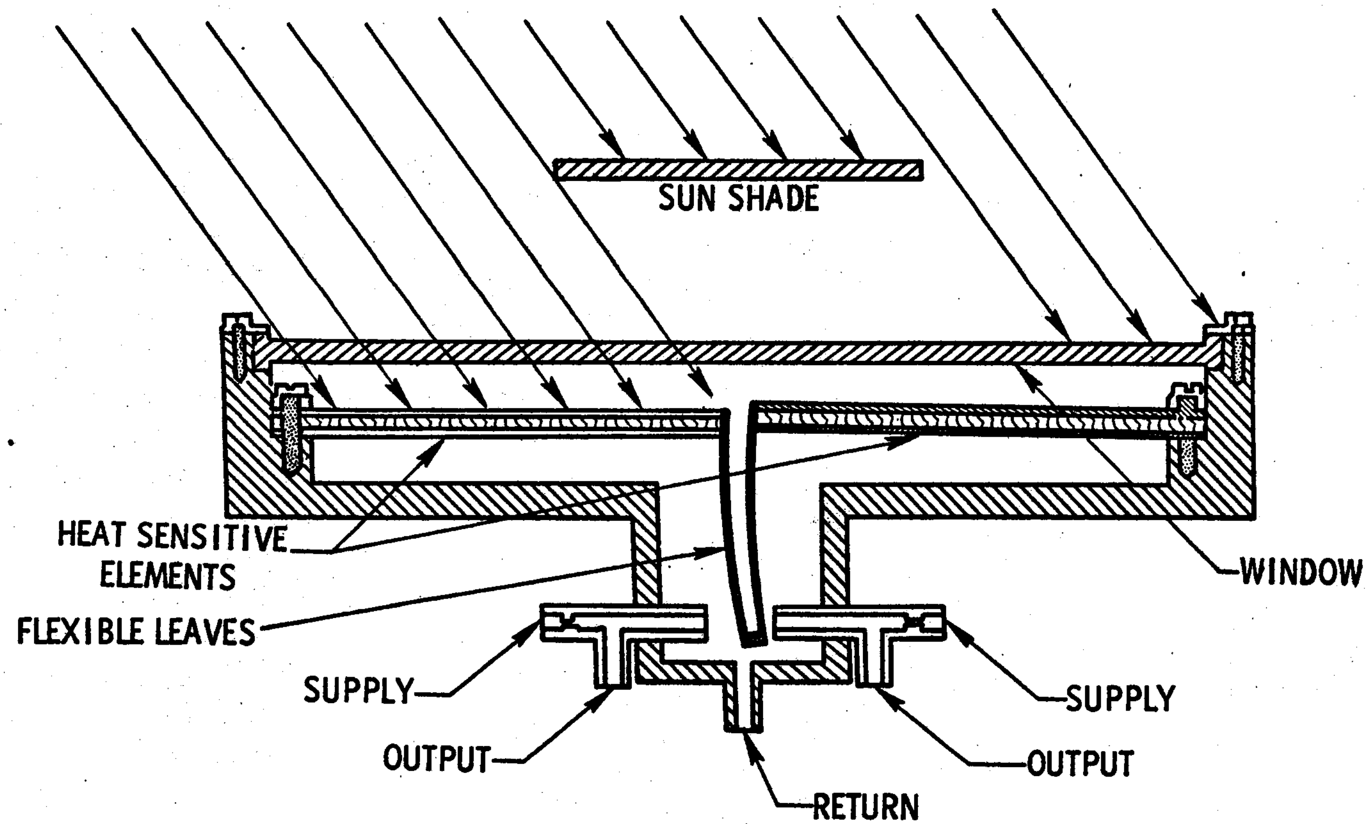

Fig. 11. Sun sensor.

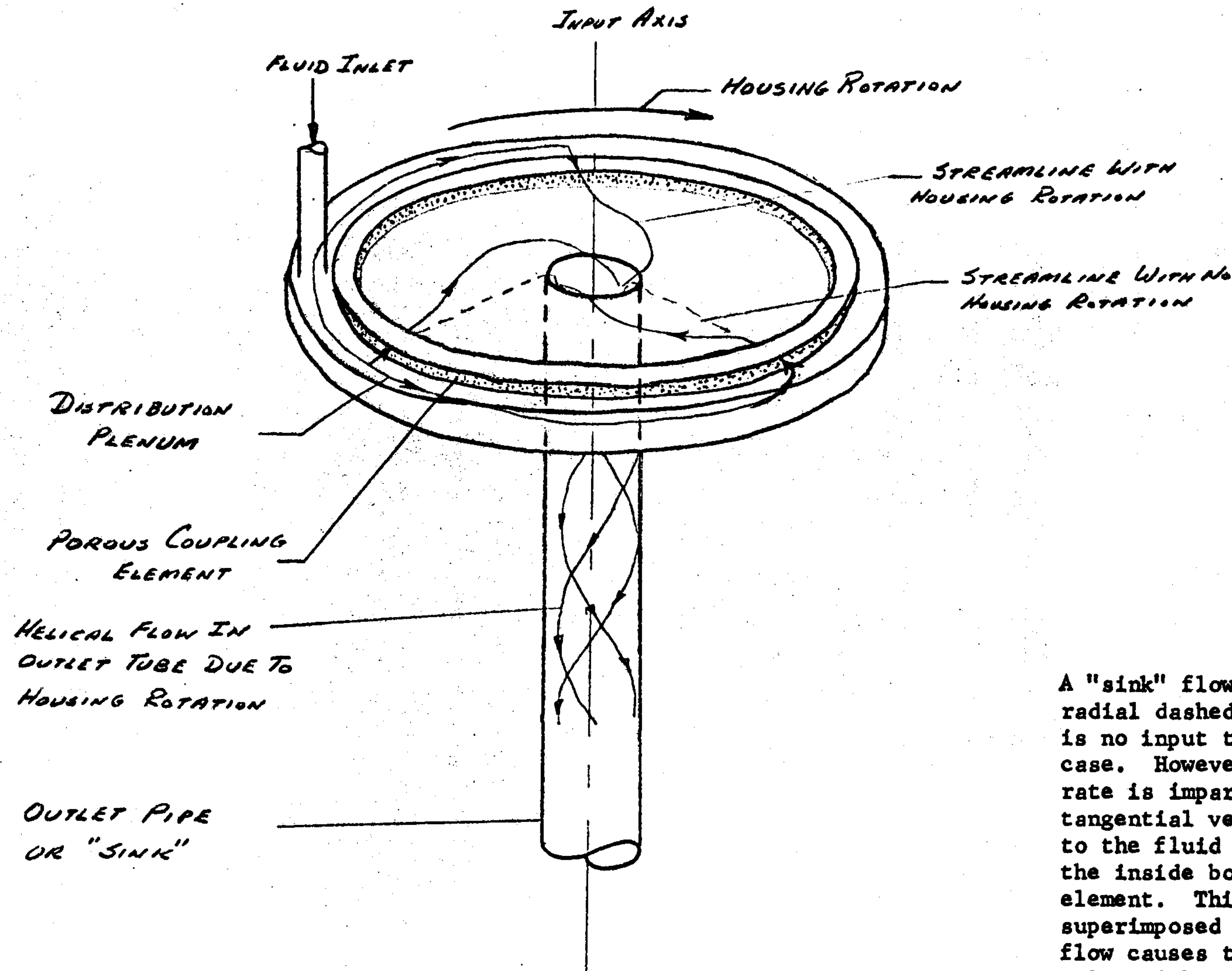

A "sink" flow field, as shown by the radial dashed lines, exists when there is no input turning rate applied to the case. However, when an input turning rate is imparted to the case, its tangential velocity is in turn imparted to the fluid particles as they leave the inside boundary of the coupling element. This tangential velocity superimposed upon the existing radial flow causes the streamlines to assume a logarithmic spiral.

Fig. 12. Vortex Rate Sensor

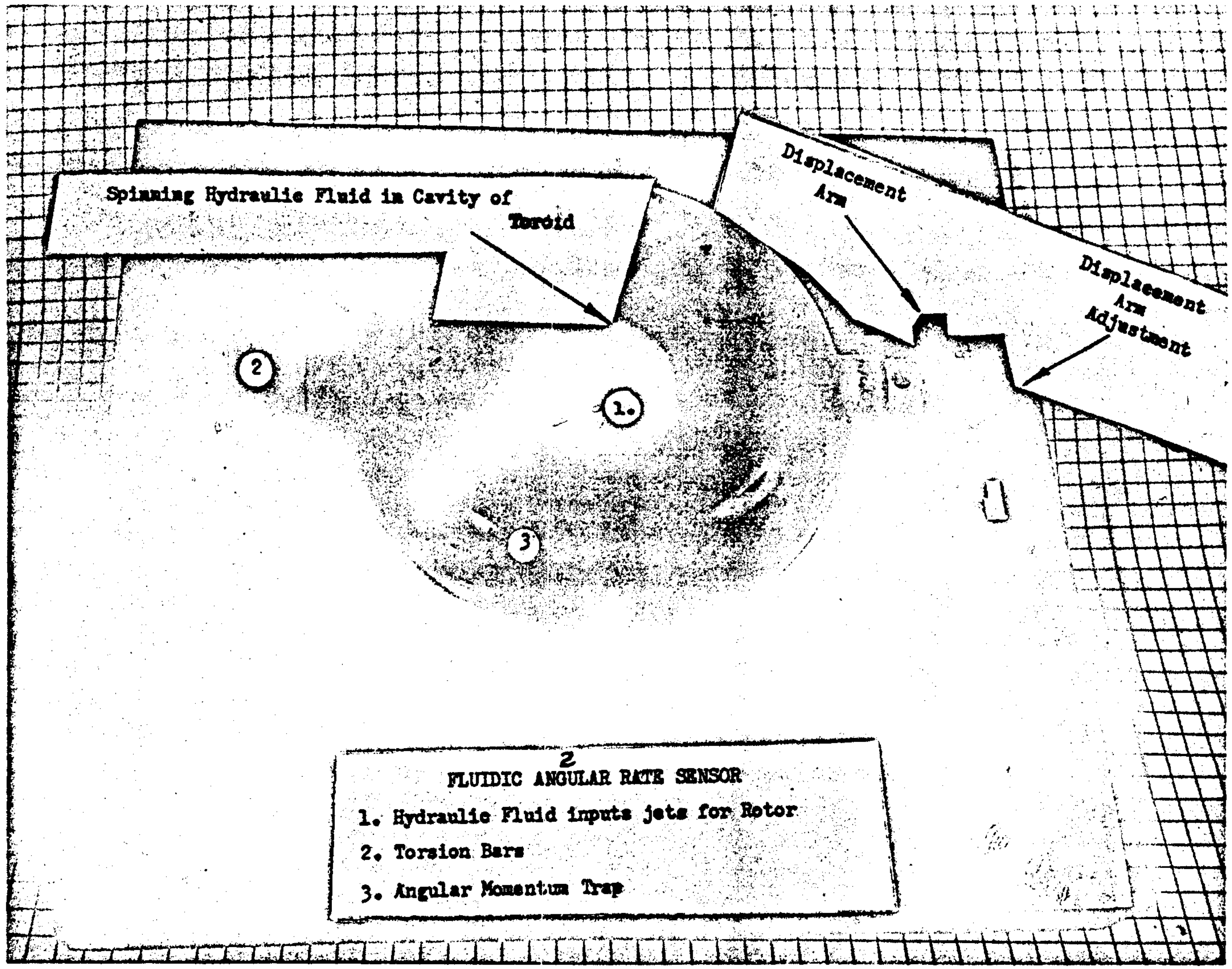

Fig. 13. Experimental Fluid Rate Sensor

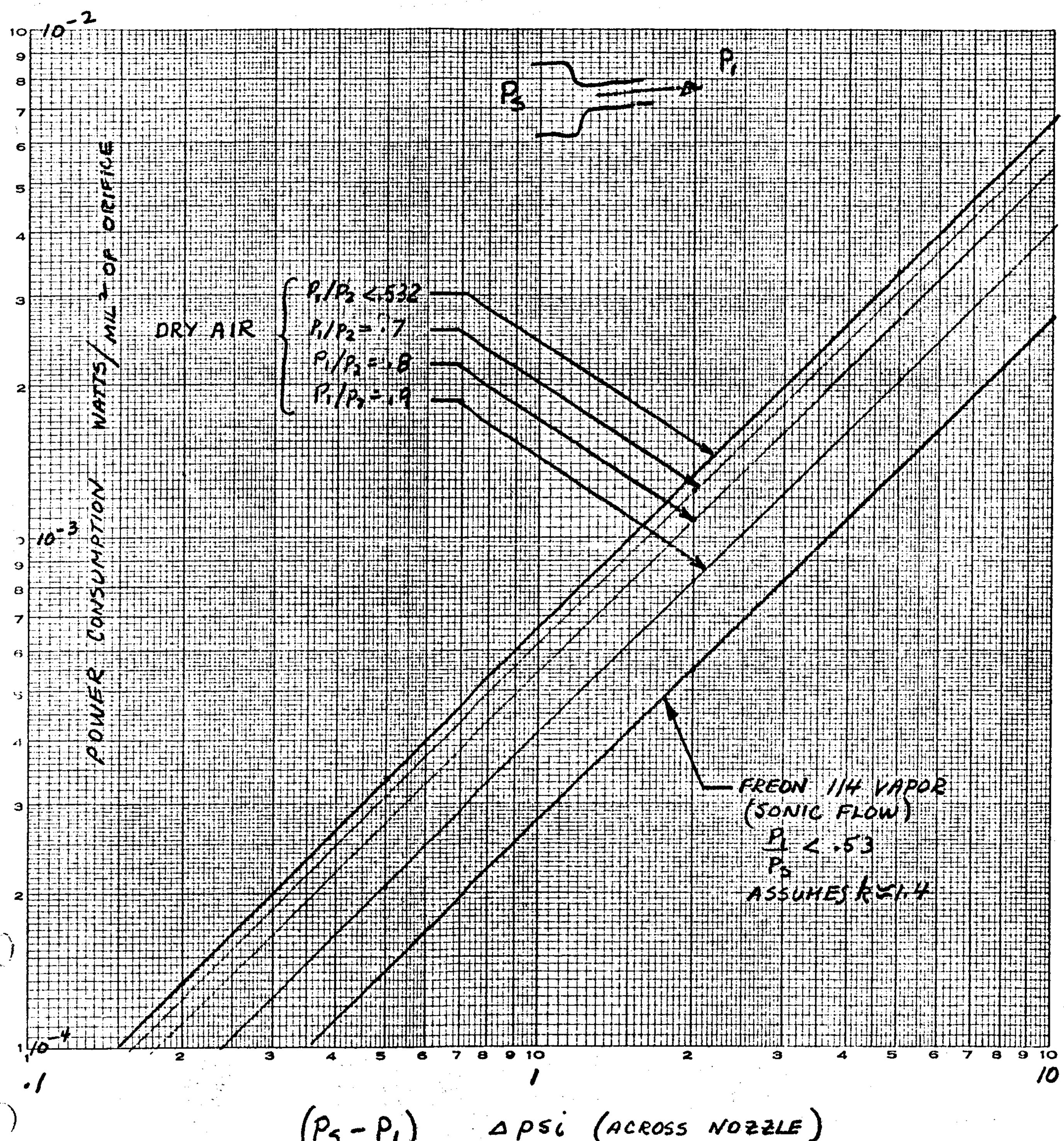

FIG 14. FLUIDIC ELEMENT POWER COMPUTATION

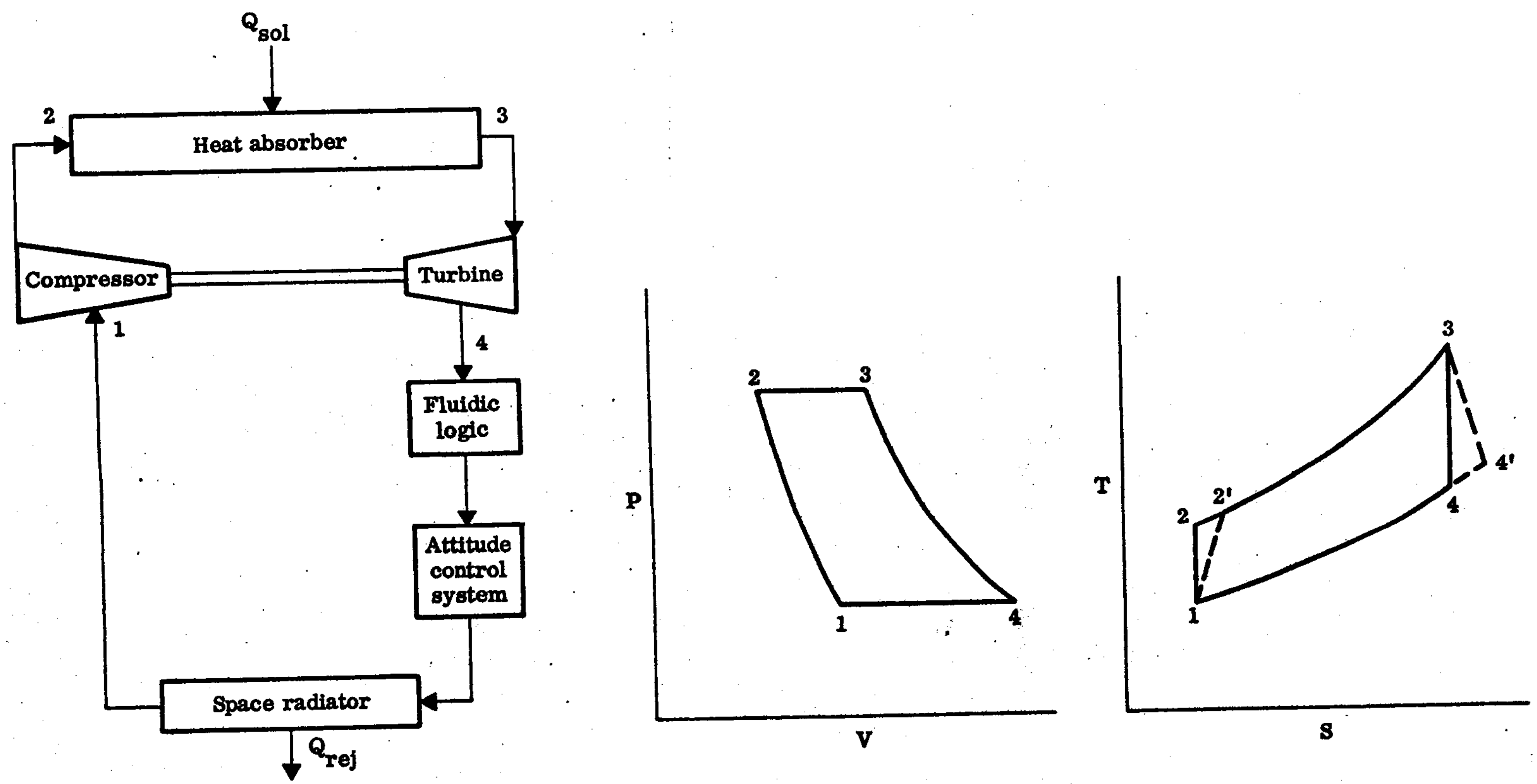

P = Pressure, V = volume, T = temperature, S = entropy

1-2	Adiabatic compression	(1-2') actual compression
2-3	Constant P heat addition	
3-4	Adiabatic expansion	(3-4') actual expansion
4-1	Constant P heat rejection	

Network = $W\,C_p\,(T_3 - T'_4 - T'_2 + T_1)$

Fig. 15. Brayton Cycle Fluidic Power System

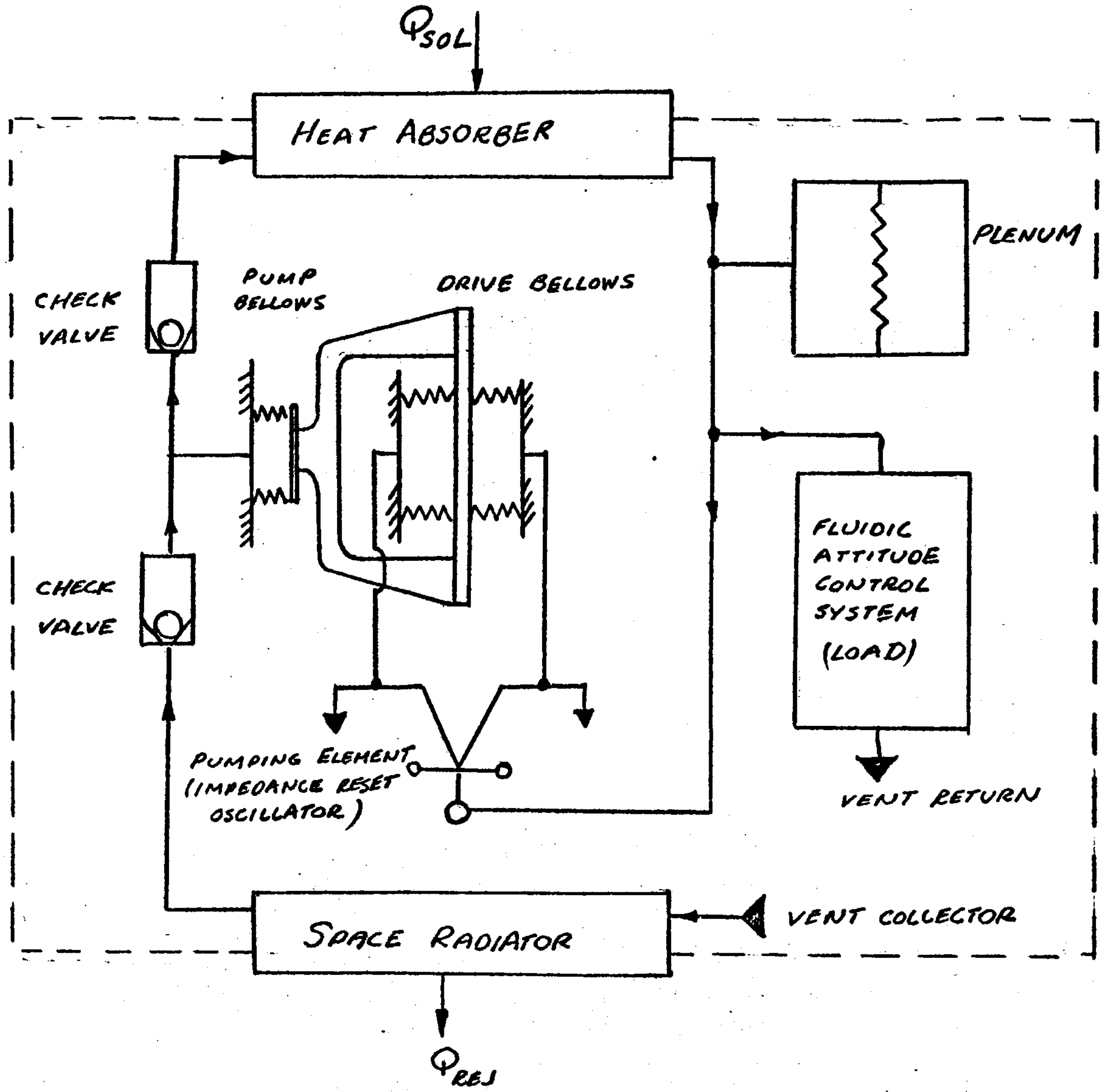

Fig. 16. Reciprocating, Recirculating Power Supply

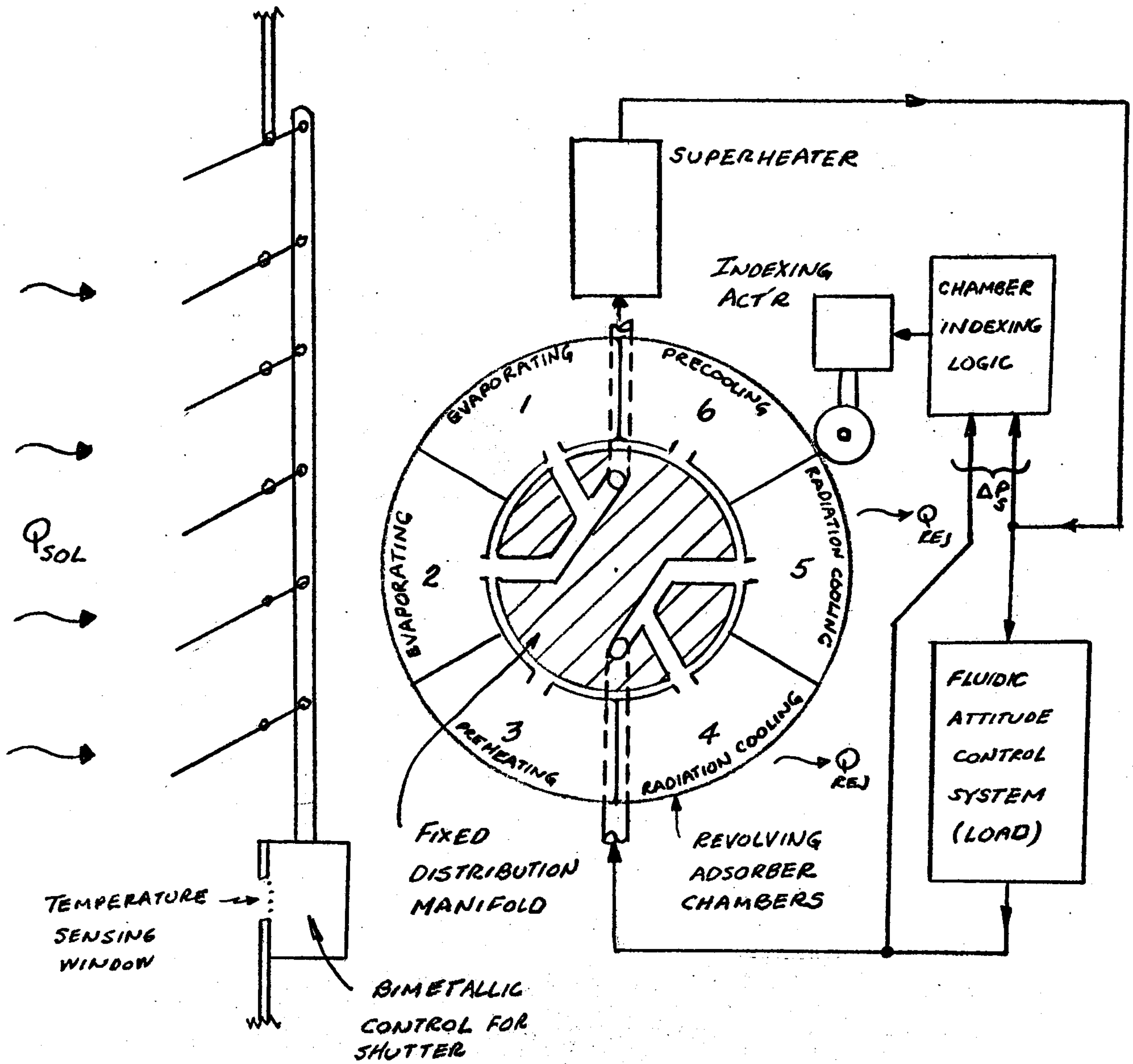

Fig. 17. Schematic of Adsorption Power Supply

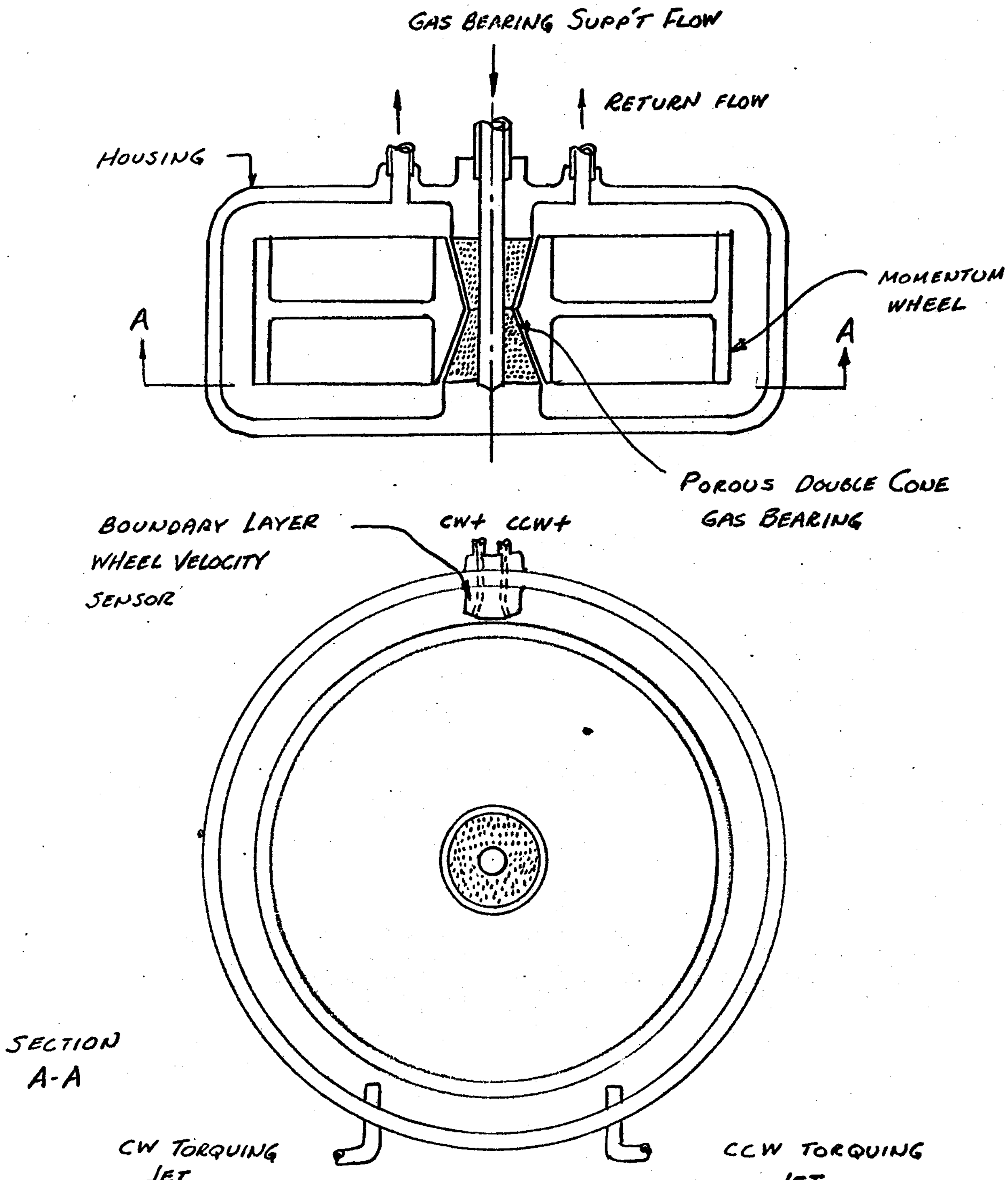

Fig. 18. Concept for Fluidic Momentum Wheel

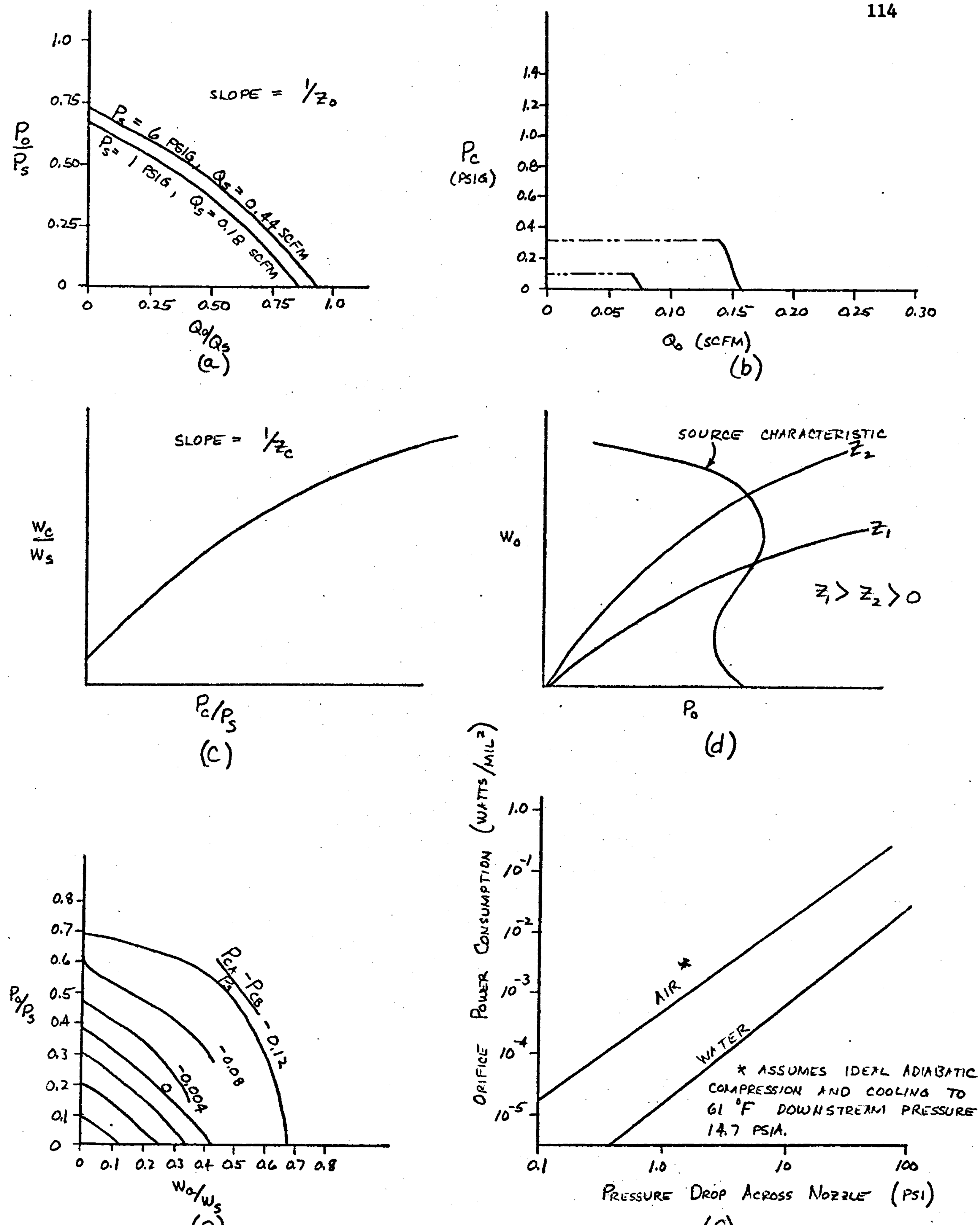

FIG. 19. FLUIDIC ELEMENT CHARACTERISTICS

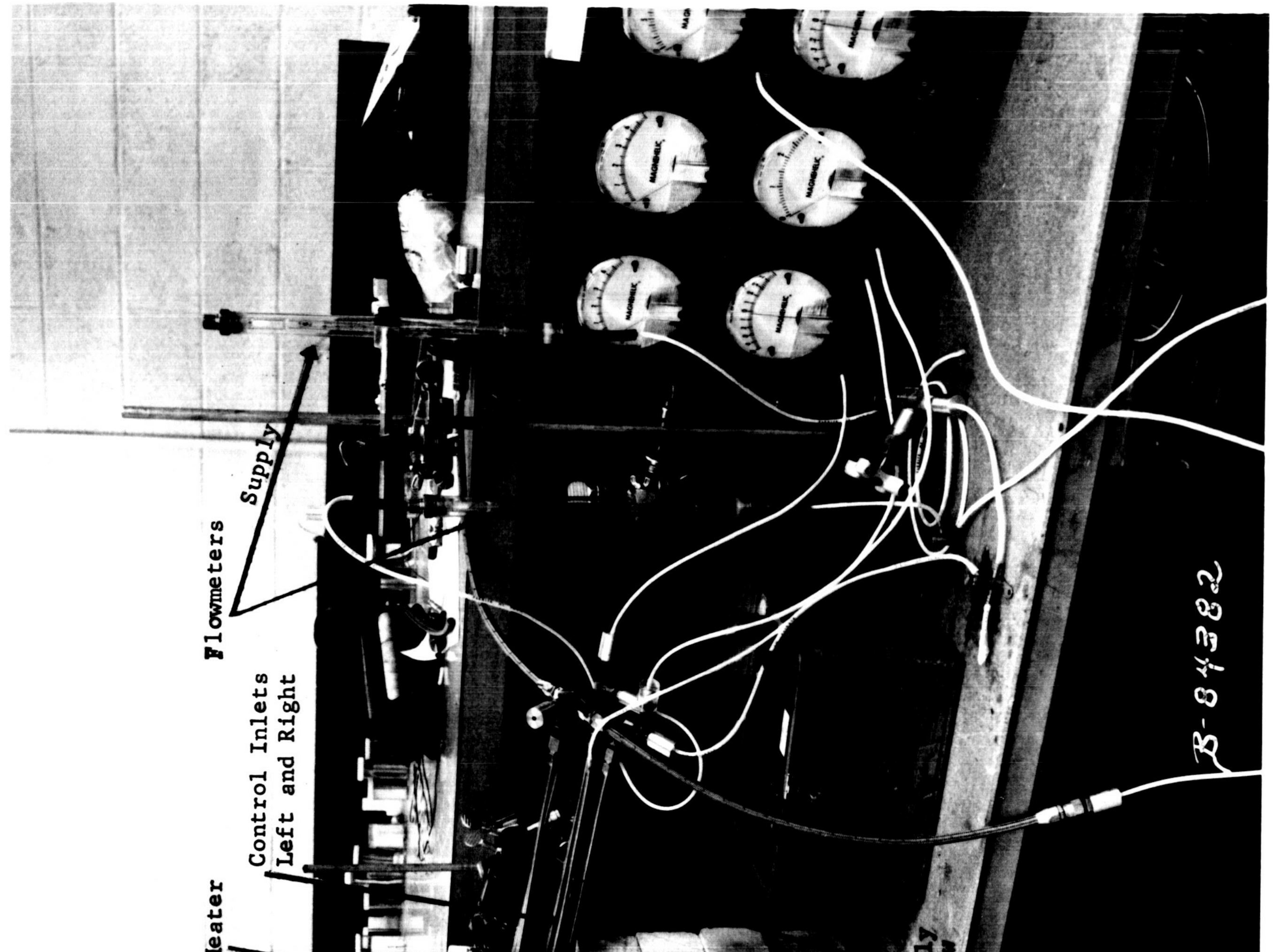

Fig. 10. Temperature Test Set-up

FIG 21

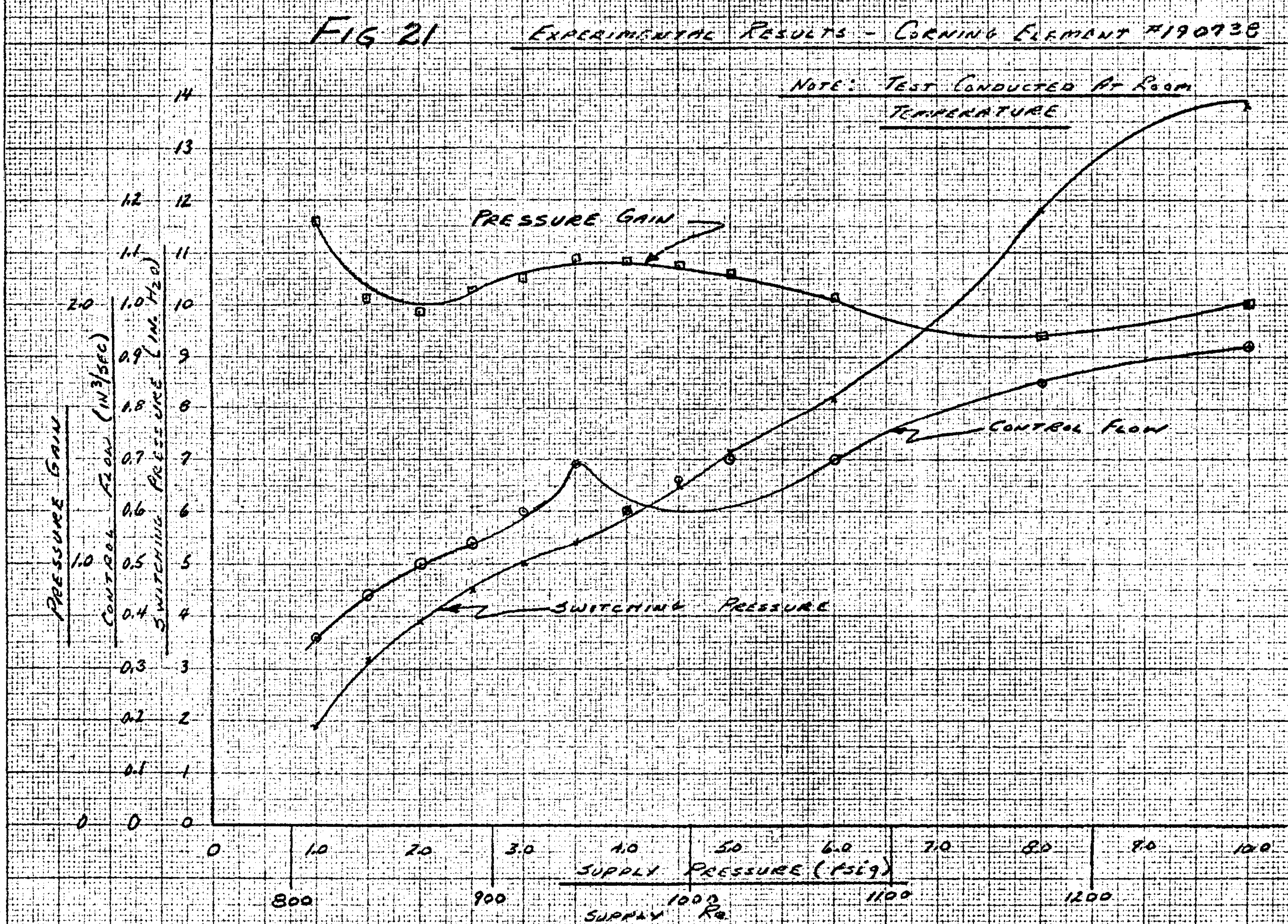
EXPERIMENTAL RESULTS - CORNING ELEMENT #190738
NOTE: TEST CONDUCTED AT ROOM TEMPERATURE
PRESSURE GAIN
CONTROL FLOW
SWITCHING PRESSURE
PRESSURE GAIN
CONTROL FLOW (IN³/SEC)
SWITCHING PRESSURE (IN. H2O)
SUPPLY PRESSURE (PSIG)
SUPPLY Re
0
1.0
2.0
3.0
4.0
5.0
6.0
7.0
8.0
9.0
10.0
800
900
1000
1100
1200
14
13
12
11
10
9
8
7
6
5
4
3
2
1
0
1.2
1.1
1.0
0.9
0.8
0.7
0.6
0.5
0.4
0.3
0.2
0.1
0
2.0
1.0
0

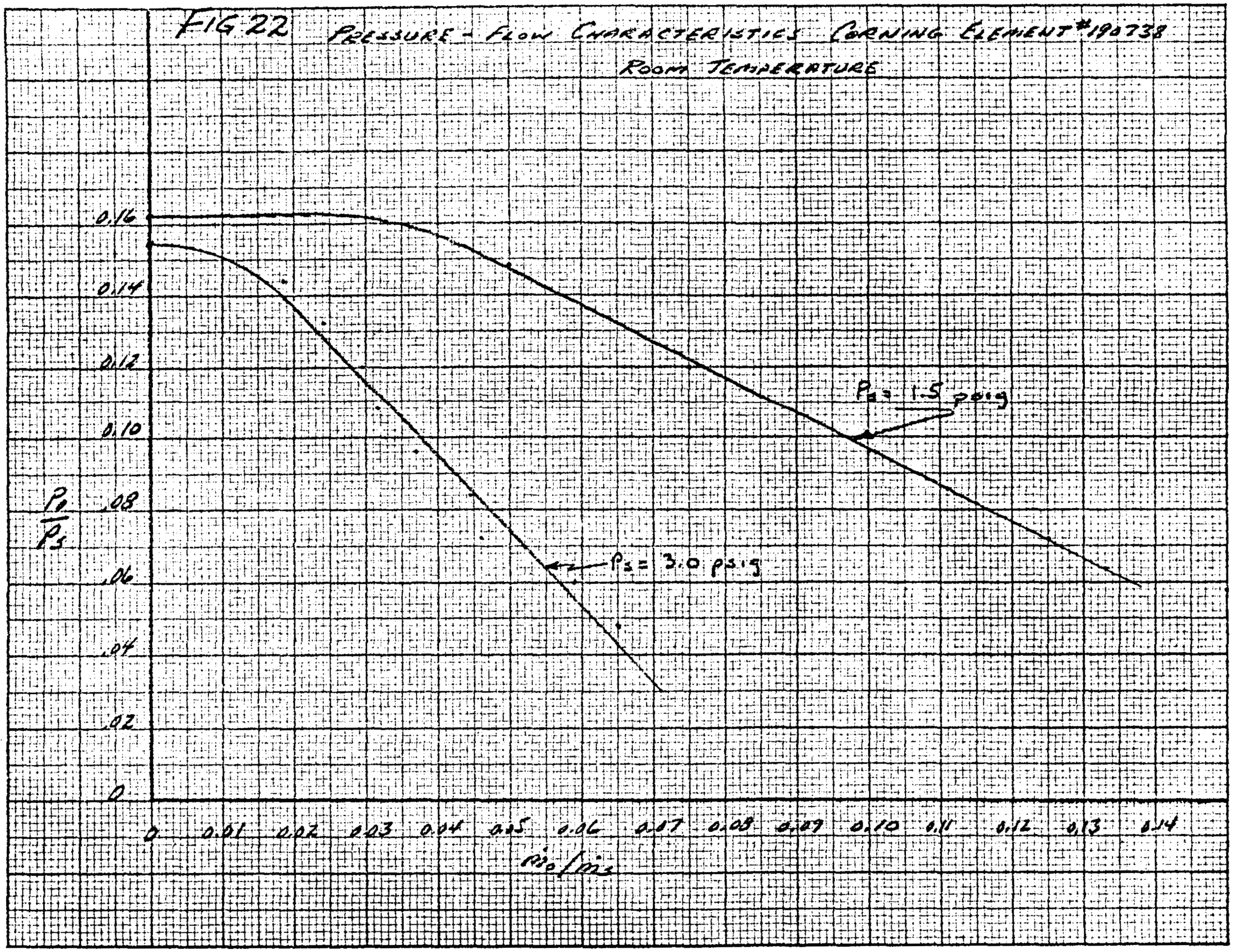
FIG 22
PRESSURE - FLOW CHARACTERISTICS CORNING ELEMENT #190738
ROOM TEMPERATURE
Po/Ps
0.16
0.14
0.12
0.10
.08
.06
.04
.02
0
0 0.01 0.02 0.03 0.04 0.05 0.06 0.07 0.08 0.09 0.10 0.11 0.12 0.13 0.14
ṁo/ṁs
Ps = 1.5 psig
Ps = 3.0 psig

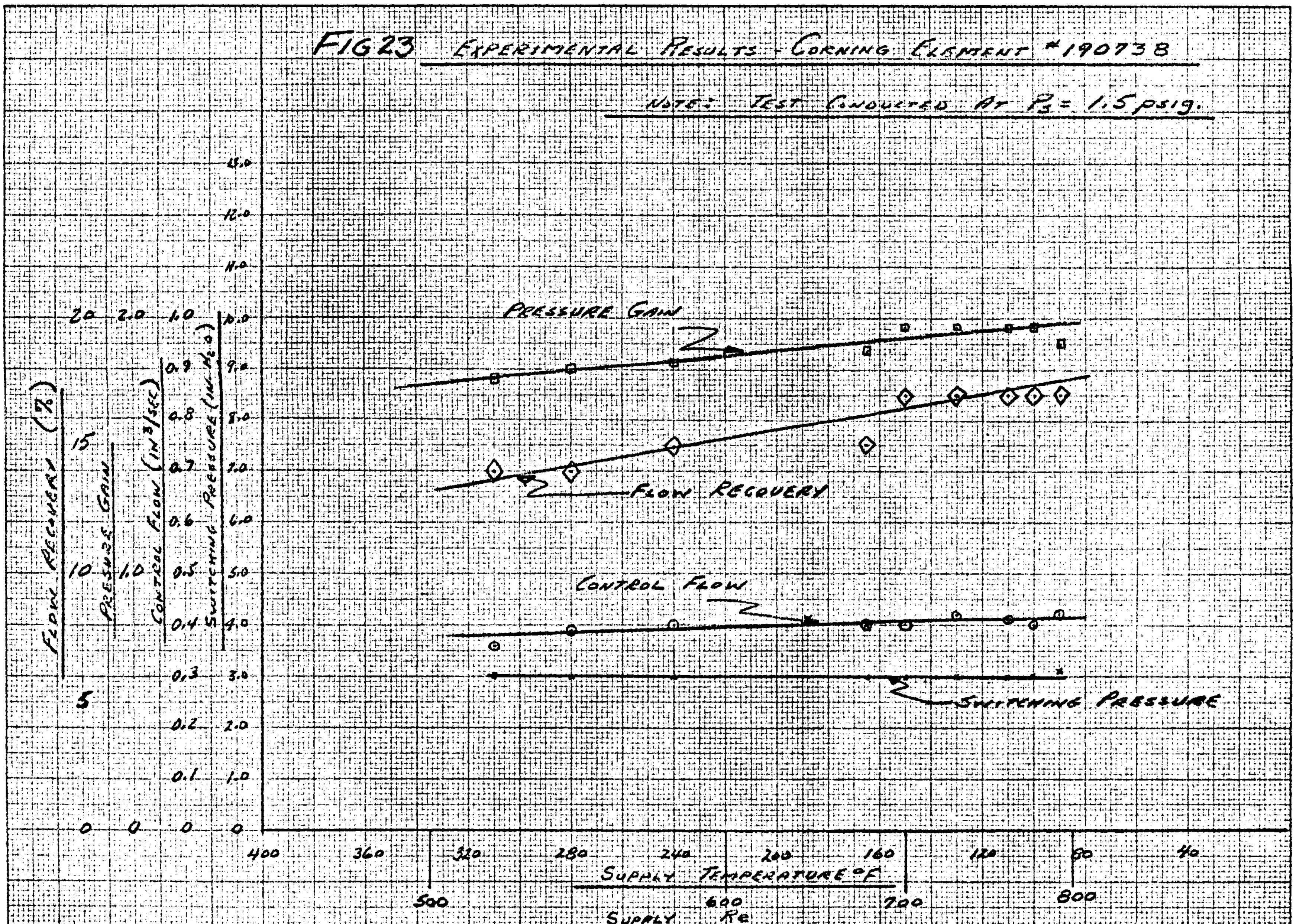

FIG 23 EXPERIMENTAL RESULTS - CORNING ELEMENT #190738

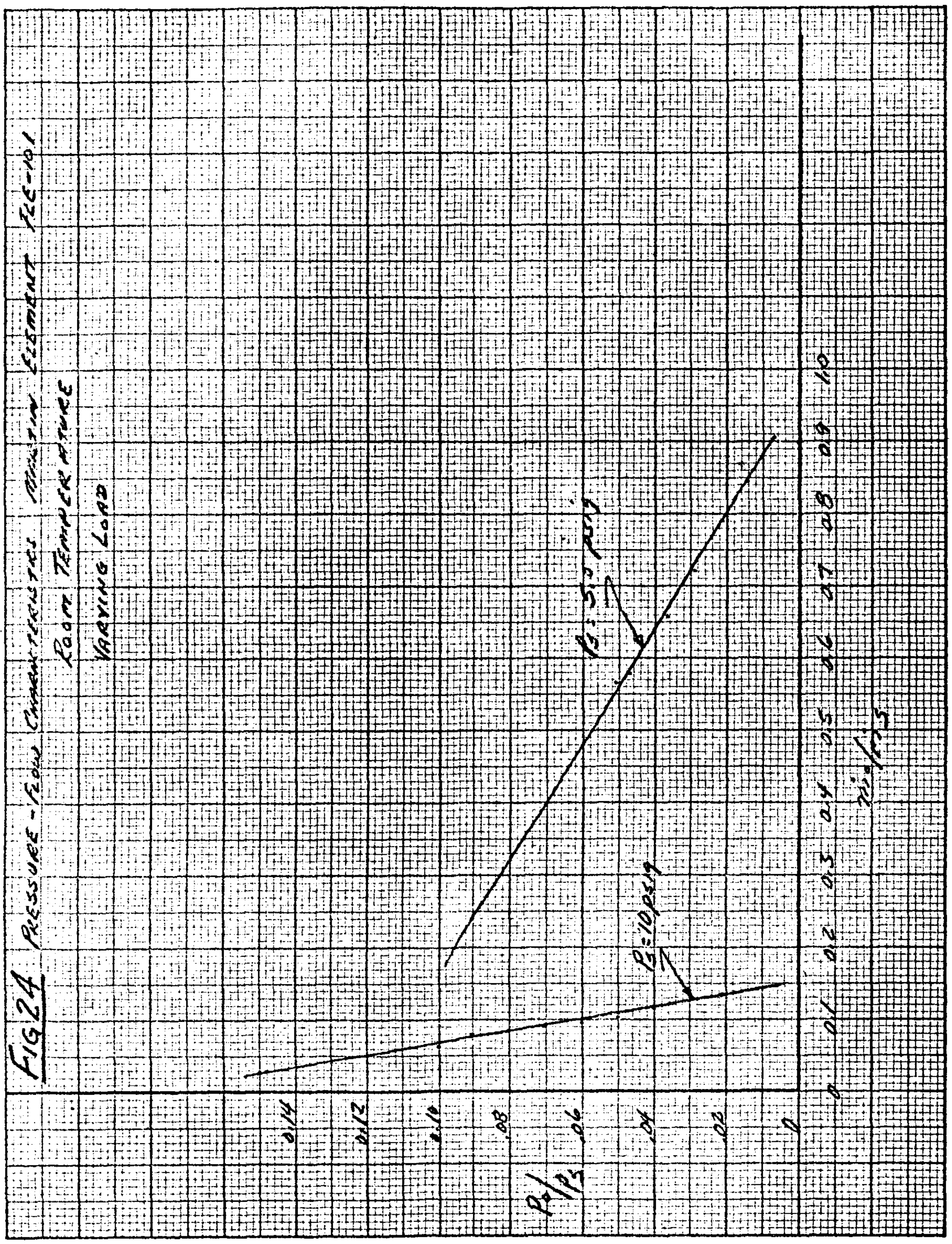
FIG 24 PRESSURE - FLOW CHARACTERISTICS MARTIN ELEMENT FLC-101
ROOM TEMPERATURE
VARYING LOAD
P3 = 5.5 psig
P3 = 10 psig
0.14
0.12
0.10
.08
.06
.04
.02
0
P0/P3
0 0.1 0.2 0.3 0.4 0.5 0.6 0.7 0.8 0.9 1.0

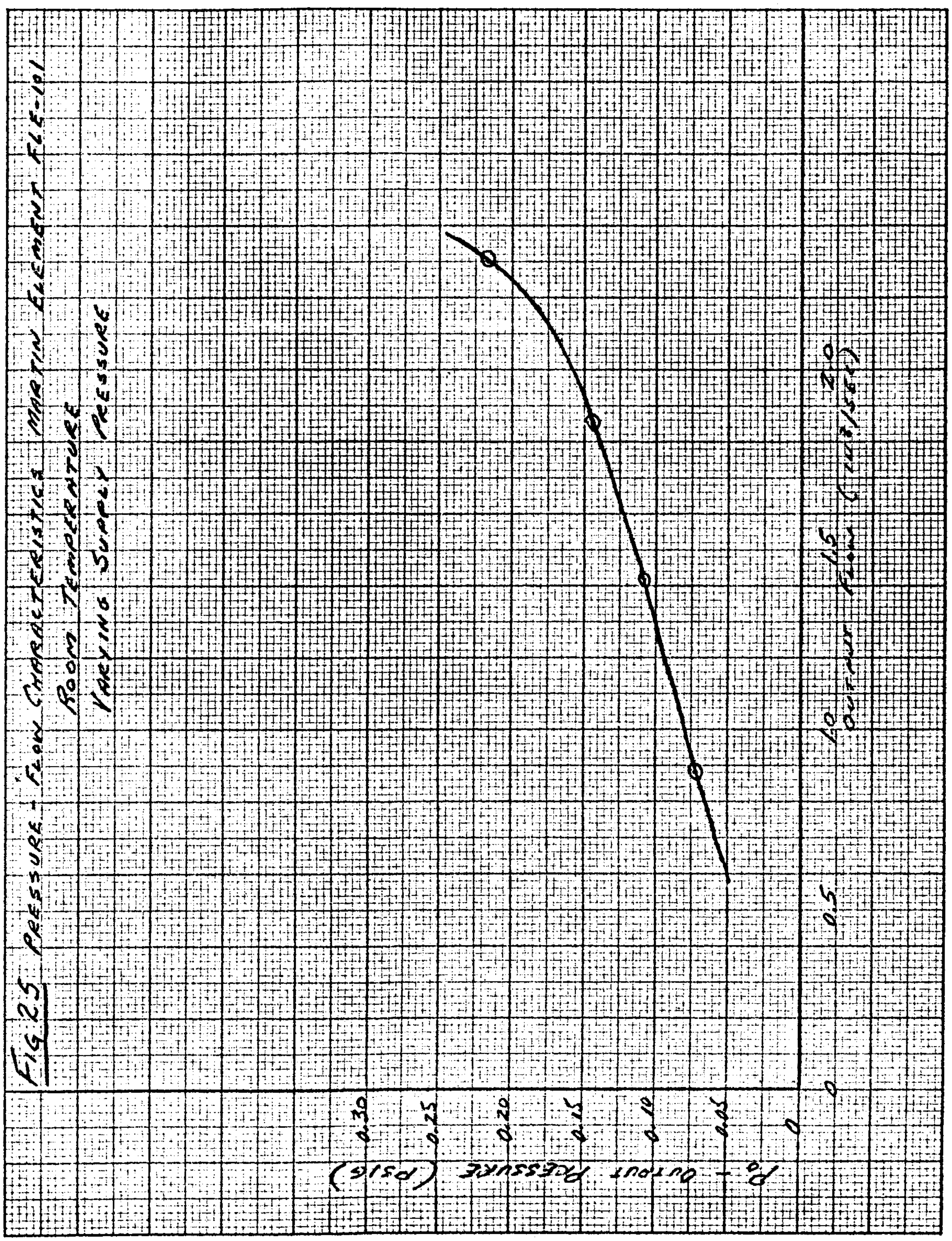

Fig. 25 Pressure - Flow Characteristics Martin Element FLE-101
Room Temperature
Varying Supply Pressure
Po - Output Pressure (psig)
0
0.05
0.10
0.15
0.20
0.25
0.30
0
0.5
1.0
1.5
2.0
Output Flow (in³/sec)

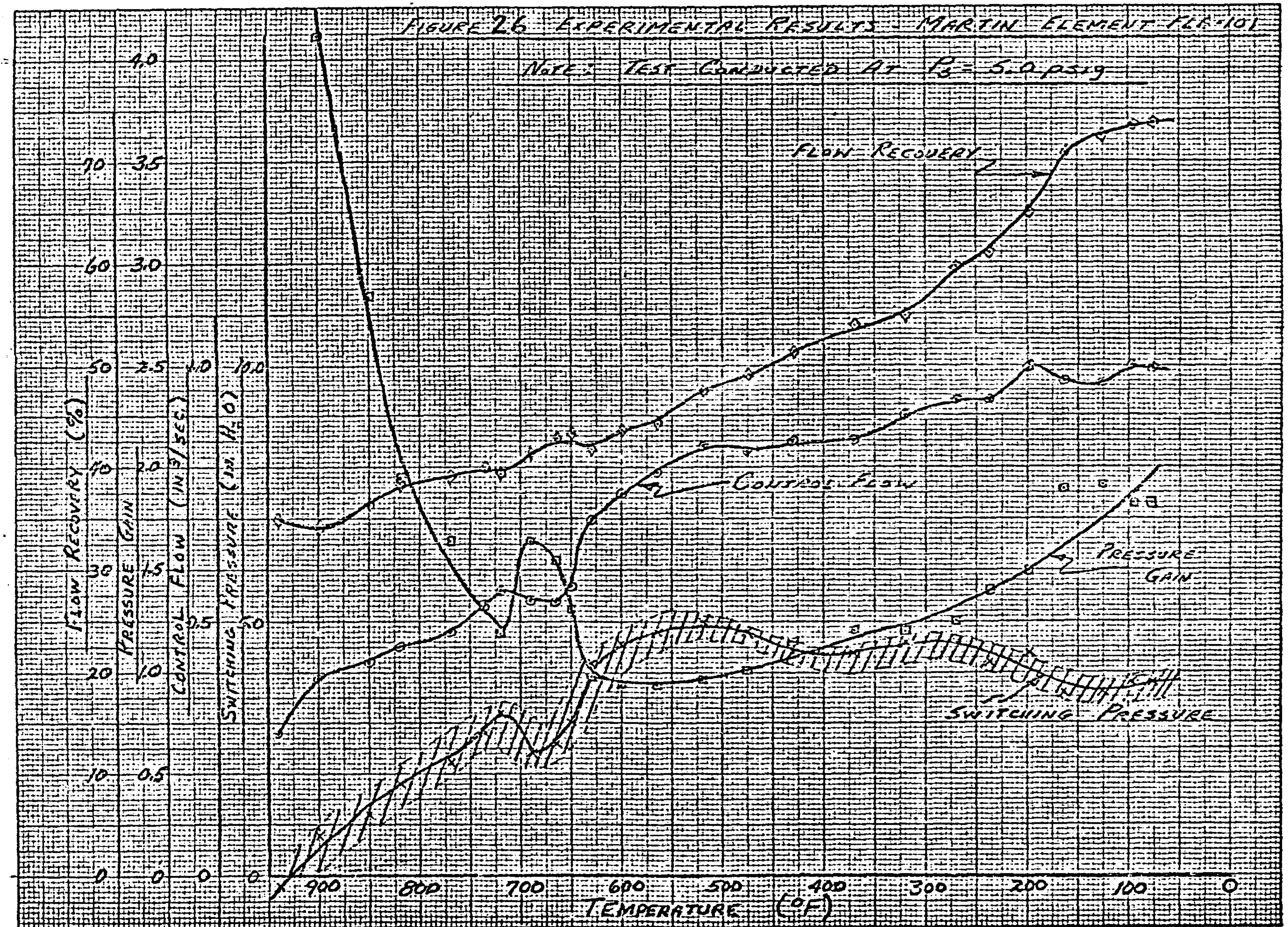

FIGURE 26 EXPERIMENTAL RESULTS - MARTIN ELEMENT FLF-101

NOTE: TEST CONDUCTED AT P_S = 5.0 psig

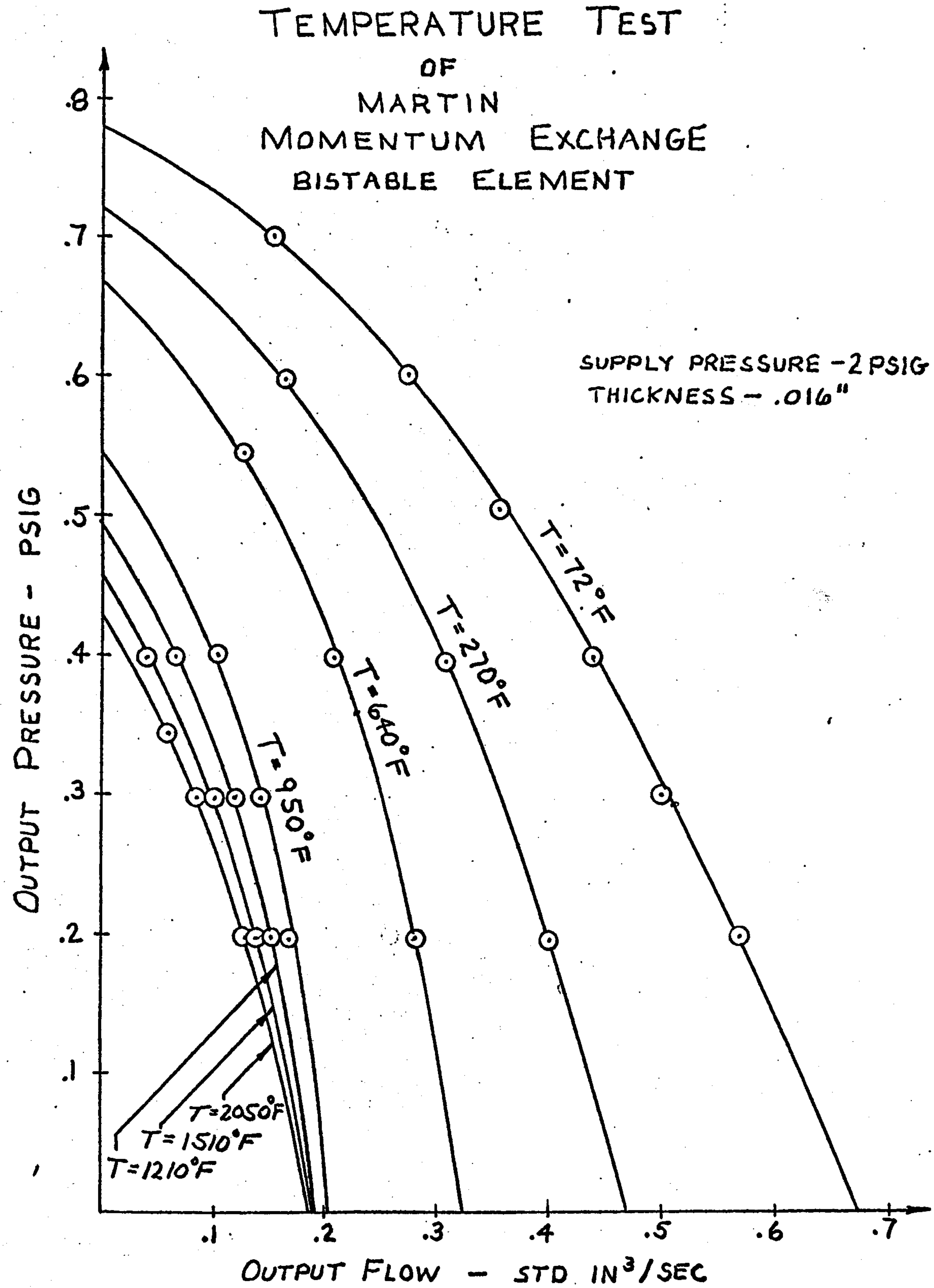
TEMPERATURE TEST
OF
MARTIN
MOMENTUM EXCHANGE
BISTABLE ELEMENT
SUPPLY PRESSURE - 2 PSIG
THICKNESS - .016"
OUTPUT PRESSURE - PSIG
.8
.7
.6
.5
.4
.3
.2
.1
T=72°F
T=270°F
T=640°F
T=950°F
T=2050°F
T=1510°F
T=1210°F
.1
.2
.3
.4
.5
.6
.7
OUTPUT FLOW - STD IN³/SEC

FIGURE 27

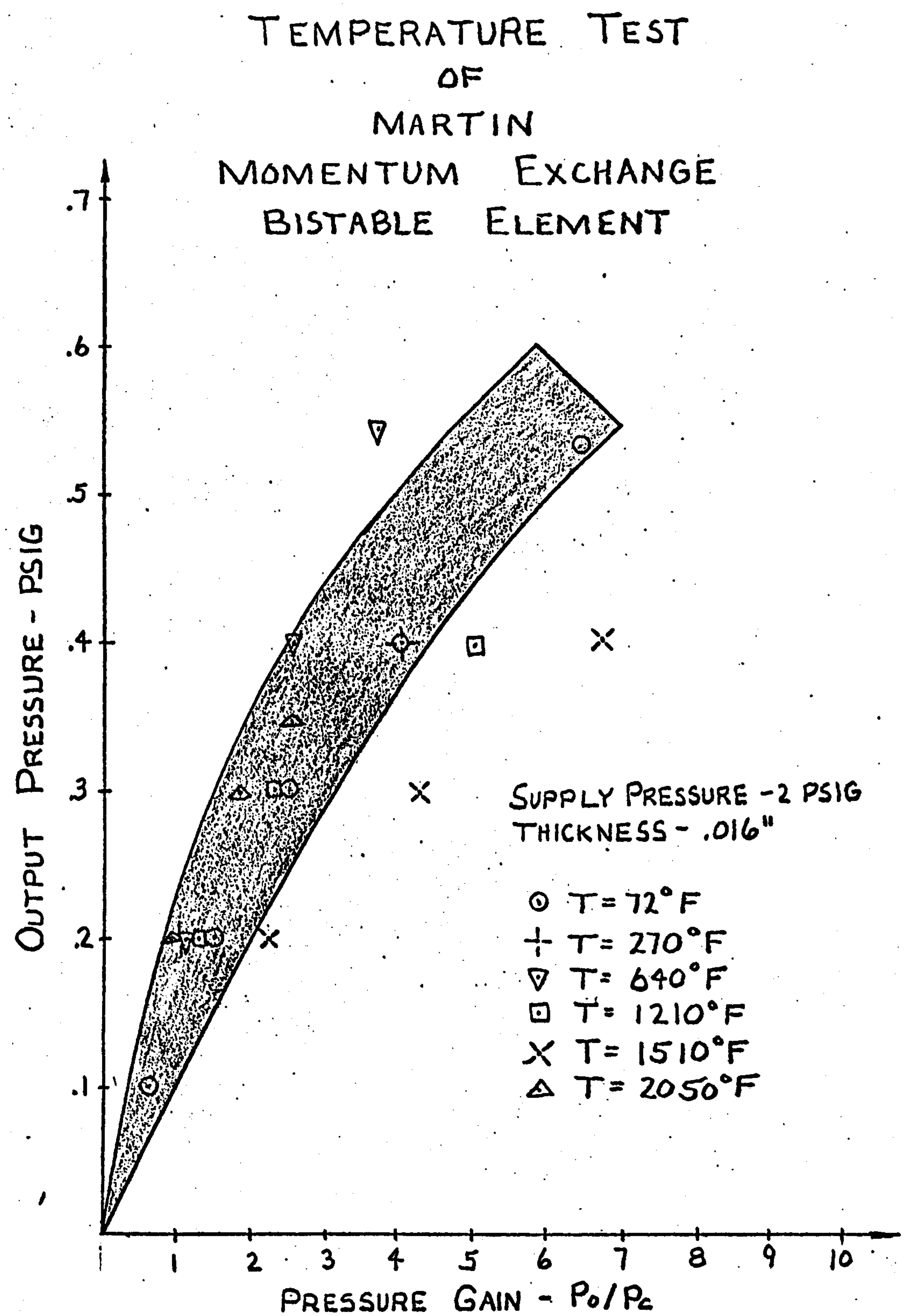
TEMPERATURE TEST
OF
MARTIN
MOMENTUM EXCHANGE
BISTABLE ELEMENT
OUTPUT PRESSURE - PSIG
.7
.6
.5
.4
.3
.2
.1
SUPPLY PRESSURE - 2 PSIG
THICKNESS - .016"
T = 72°F
T = 270°F
T = 640°F
T = 1210°F
T = 1510°F
T = 2050°F
1
2
3
4
5
6
7
8
9
10
PRESSURE GAIN - Po/Pc

FIGURE 28

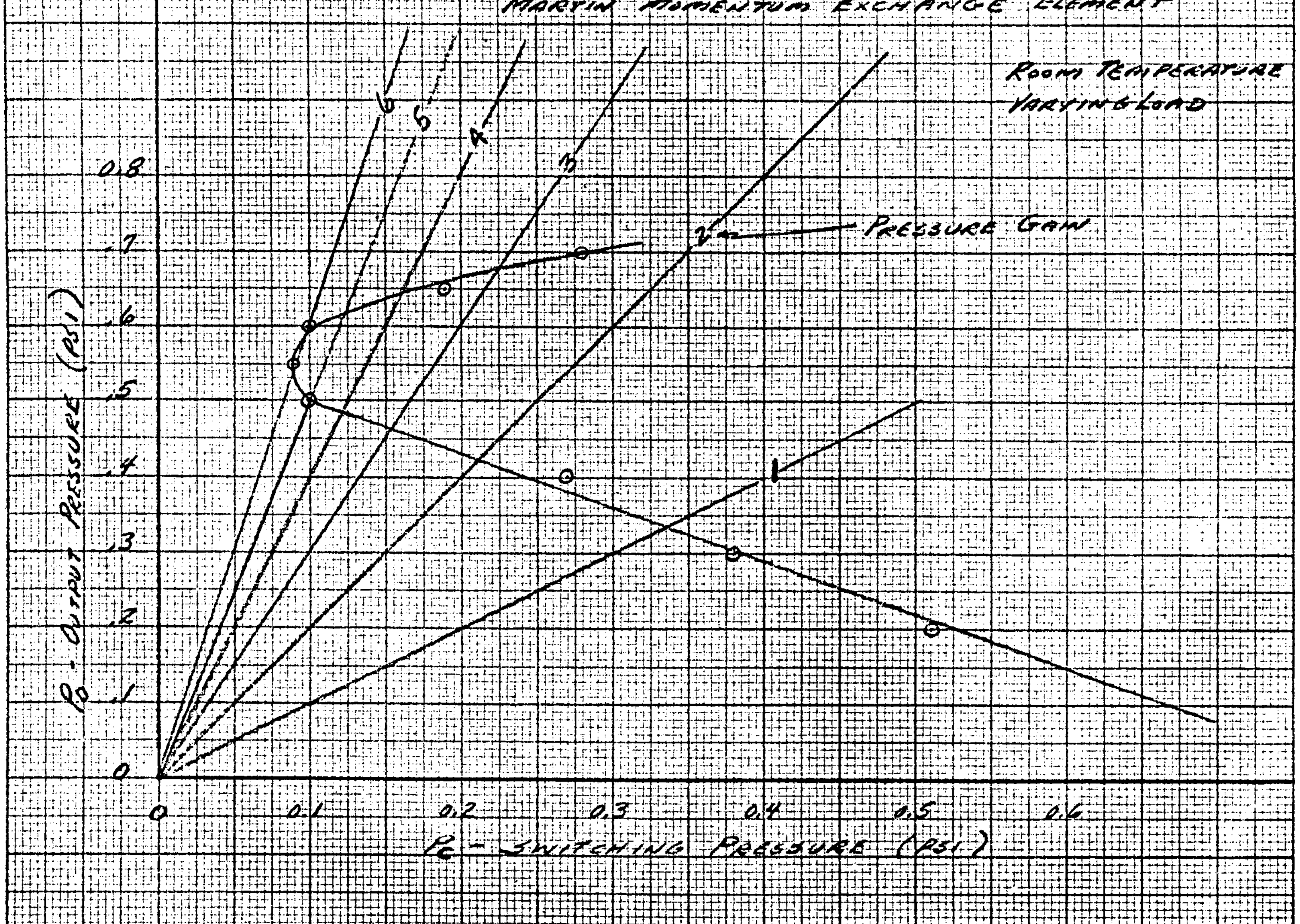

FIG 29 Control Pressure – Load Characteristics
Martin Momentum Exchange Element

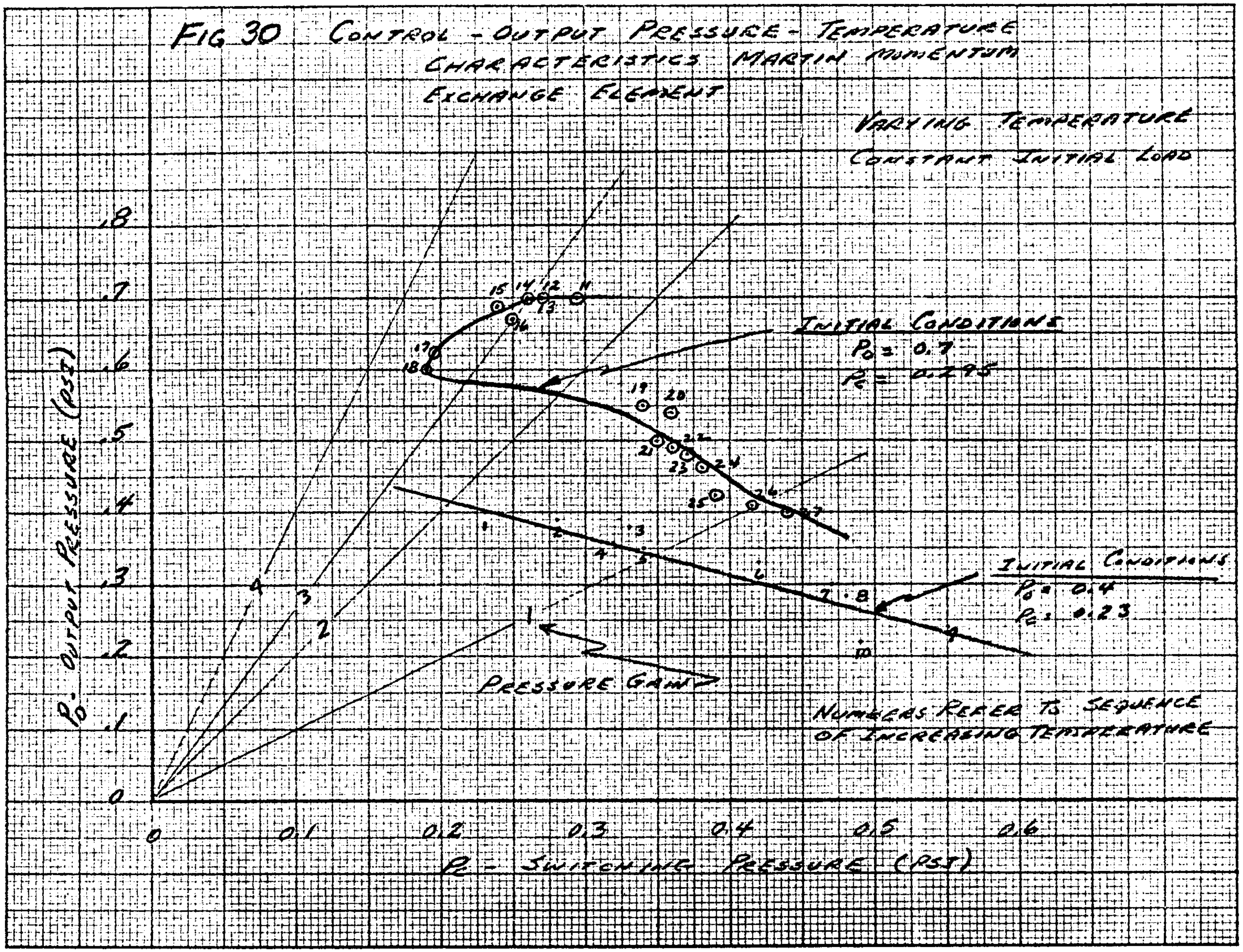

FIG 30 CONTROL - OUTPUT PRESSURE - TEMPERATURE CHARACTERISTICS MARTIN MOMENTUM EXCHANGE ELEMENT

FIGURE 31. EXPERIMENTAL RESULTS - MARTIN